Proteomic Study of the Ubiquitin E3 Ligase HUWE1 Interaction with Ubiquitin and ADP-ribose Modified Proteins

Nour Nader

A Thesis Submitted to the Faculty of Graduate Studies in Partial Fulfillment of the Requirements for the Degree of Master of Science

Graduate Program in Biology

York University

Toronto, Ontario

June 2025

Abstract

Ubiquitination and ADP-ribosylation are important post-translational modifications (PTMs), especially in cellular response to DNA damage. HECT, UBA, and WWE domain containing E3 ubiquitin protein ligase 1 (HUWE1) is an important ubiquitin E3 ligase involved in many cellular processes. HUWE1 contains regions involved in substrate interaction and domains for PTM recognition. Specifically, HUWE1 WWE and tandem ubiquitin-binding motif (tUBM) domains interact with ADPr/iso-ADPr and ubiquitin, respectively. However, the interaction between these domains and cellular ADP-ribose and ubiquitin and potentially substrate interactions are not well investigated. Thus, this project aimed to investigate the interactome of HUWE1 WWE and tUBM domain, focusing on their ability to bind proteins modified by mono-ADP-ribose (MAR)/poly-ADP-ribose (PAR) and ubiquitin using GST pulldown assay. First, using Western blot and confocal microscopy, distinct dynamics of ubiquitination and ADP-ribosylation were observed in response to different DNA damage treatments. Second, the study demonstrated that the WWE-tUBM domain interacts with both cellular ADP-ribose and ubiquitin. Moreover, through a proteomic approach using affinity mass spectrometry, this study identified novel proteins that interact with the WWE and tUBM domains following Ultraviolet (UV) induced DNA damage. Together, the findings of this project contribute to a better understanding of how HUWE1 engages with its substrates and highlight the role of WWE and tUBM domains and their ability to recognize PTMs in mediating these interactions.

Acknowledgments

First, I would like to thank Dr. Yi Sheng. Thank you for being the best supervisor I could have hoped for. You always supported and pushed me to give my best, and gave me the opportunity to work in your lab. I would like to extend my thanks to my advisor, Dr. Chun Peng, who helped me to improve my project through discussion, questions and valuable advice. I want to extend my thanks to Maxime Rossato, the Mass Spectrometry specialist at York University for his help and valuable advice throughout my Masters.

I would like to thank my lab members in the Sheng lab current and past for supporting me both academically and personally. Daniel, thank you for training me and sharing your knowledge with me. Angelo, I enjoyed our talks and spending time together, thank you for helping me during my Masters. Gaby, thank you for sharing your knowledge with me and being there when I needed advice about my project. Rufei, it was a great pleasure to get to know you and become friends while we navigated our way through our Masters. Vanessa, it was great having you around the lab, I enjoyed training and working alongside you. Erica, I enjoyed training you and the great time we spent performing the experiments. Joyce, I will forever be indebted to you for training me the way you did, for your patience and kindness that always encouraged me to speak my mind and ask questions whenever I felt lost.

I want to extend my thanks to the great people that I met at LSB who became my second family. Ivan, you were the best friend I could have ever wished for. Thank you for being there for me, believing in me and supporting me. I will forever cherish the times and memories we shared. Marjan, my fries' partner, thank you for listening to all my stories and providing wisdom and support. Su, thank you for your warm heart and understanding whenever I came to you for support. Sihat, thank you for all the memes you shared with me that lightened my day. Sahib, thank you for your support, it was great being friends with you as we navigate our journey through undergraduate and graduate studies and beyond. To the Saridakis lab members past and current, I want to say thank you for being there and making lab work fun and enjoyable. Kristina, thank you for the memories and laughs we shared together. To my singing partners Serena, Kanwar, and Jatin, it was great sharing these great moments with you. I also want to thank Sarah for the beautiful memories throughout my masters during our bus trips and the time we spent in

the confocal room imaging our samples. I would also like to thank Farnaz, Brittney, Connor, Nick, Tobi, Riddhi, Gagan, Mahtab, Relam, Sehaj, Alex and Christina.
Finally, to the people that I wouldn't have been able to make it without their support and love, my beloved family. My brothers Nader, Akram, Majd and George, you were and always will be my rocks. My mother Mayada, thank you for being there for me and supporting me. My sister-in-law Dina, thank you for the fun memories we shared. To my uncles, aunts, grandparents and cousins, I am grateful to all of you for supporting and motivating me. To the person who never fails to lighten up my day and bring so much happiness and joy into my life, my nephew Lucas, I would like to say thank you for being in my life. Finally, to my beloved late father Mufrej, Baba, thank you for the great values you planted in me, your teachings, sacrifices, and love taught me to never give up and made me the person I am today.

Table of Contents

List of Tables

List of Figures

Chapter 1: Introduction

1.1 An overview of protein post-translational modifications

Protein post-translation modifications (PTMs) refer to chemical changes that occur on proteins after synthesis. By acting as molecular signals, PTMs regulate critical aspects of protein behavior in the cell, including protein activity, stability, localization, and interactions, thereby, influencing diverse biological pathways (Komander & Rape, 2012; Walsh et al., 2005). The precise formation and regulation of these modifications are indispensable for maintaining cellular homeostasis (Karve & Cheema, 2011; H. Wang et al., 2023). When such PTMs are dysregulated, they can disrupt cellular functions, contributing to the development of many diseases, such as neurological disorders and cancer (Karve & Cheema, 2011; H. Wang et al., 2023).

Protein PTMs encompass diverse modifications, varying from simple chemical additions such as phosphorylation, methylation, and acetylation, to more complex structural and chemical changes including ubiquitination and ADP-ribosylation (Teloni & Altmeyer, 2016). Each PTM plays a distinct role and operates through unique mechanisms, impacting a wide range of cellular processes (H. Wang et al., 2023). Among them, ubiquitination and ADP-ribosylation are particularly noteworthy for their roles in DNA damage signaling and cell stress responses (Doil et al., 2009; H. C. Kang et al., 2011; Liu et al., 2013, 2017; Longarini et al., 2023; Luo & Kraus, 2012; Mandemaker et al., 2017; Panier et al., 2012; Sheng et al., 2024; Thorslund et al., 2015; Yan et al., 2013). This study specifically examines ubiquitination and ADP-ribosylation, focusing on their interplay in the context of DNA damage repair through a proteomic approach.

1.2 Ubiquitination

Ubiquitination is a special type of protein modification, in which the small, globular protein ubiquitin is covalently attached to a target protein, thereby altering its stability, activity or interactions (Ciechanover, 2009; Kelsall, 2022; Komander & Rape, 2012). Ubiquitin consists of 76 amino acids (Figure 1.1 A) and is highly conserved among eukaryotes (Ciechanover, 2009; Wiborg et al., 1985). In humans, four different genes encode for ubiquitin: UBA52, RPS27A, UBB, and UBC (Dubois et al., 2020). The UBB and UBC genes produce polyubiquitin precursors, while RPS27A and UBA52 encode ubiquitin fused to the ribosomal proteins S27A and L40, respectively (Baker & Board, 1987; Redman & Rechsteiner, 1989; Webb et al., 1994; Wiborg et al., 1985). To generate free ubiquitin for use in the cellular ubiquitination process, these precursor proteins must be further processed by deubiquitinating enzymes (DUBs) (Kirschner & Stratakis, 2000; Park & Ryu, 2014).

1.2.1 Types of ubiquitination

Ubiquitin can be conjugated to substrates in at least three distinct ways: as a single moiety (*i.e.* mono-ubiquitination), as multiple individual moieties (*i.e.* multi-mono ubiquitination), or as a chain (*i.e.* poly-ubiquitination) (Figure 1.1 B) (Komander & Rape, 2012). Each type plays a unique role in the regulation of cellular processes (Dikic et al., 2009). For instance, mono-ubiquitination of histones is involved in chromatin remodeling, and multi-mono ubiquitination is known to regulate endocytosis and lysosomal degradation (Haglund et al., 2003; Marsh et al., 2020).

Poly-ubiquitination, on the other hand, exhibits remarkable complexity in both structural assembly and functional roles (Dikic et al., 2009). Poly-ubiquitin chains can be formed by linking ubiquitin molecule through one of the seven lysine residues (K6, K11, K27, K29, K33,

K48 and K63), giving rise to various distinct chains (Dikic et al., 2009; Komander & Rape, 2012). Poly-ubiquitin chains can be homotypic when the same lysine residue is being modified, or heterotypic mixed or branched chains when linked with different lysine residues (Figure 1.1 B) (French et al., 2021; Komander & Rape, 2012). As different ubiquitin linkages can assume different conformations, the structural complexity of these chains contributes to their functional specificity (Varadan et al., 2005). For example, the K63-linked chain adopts a more extended conformation that facilitates roles in non-proteolytic functions, such as signaling in DNA damage repair (Dikic et al., 2009; Komander & Rape, 2012; Sato et al., 2009; Sims & Cohen, 2009) . In contrast, K48-linked chains assume a more compact structure, which is involved in predominantly targeted-protein degradation via 26s proteasome (Varadan et al., 2005)

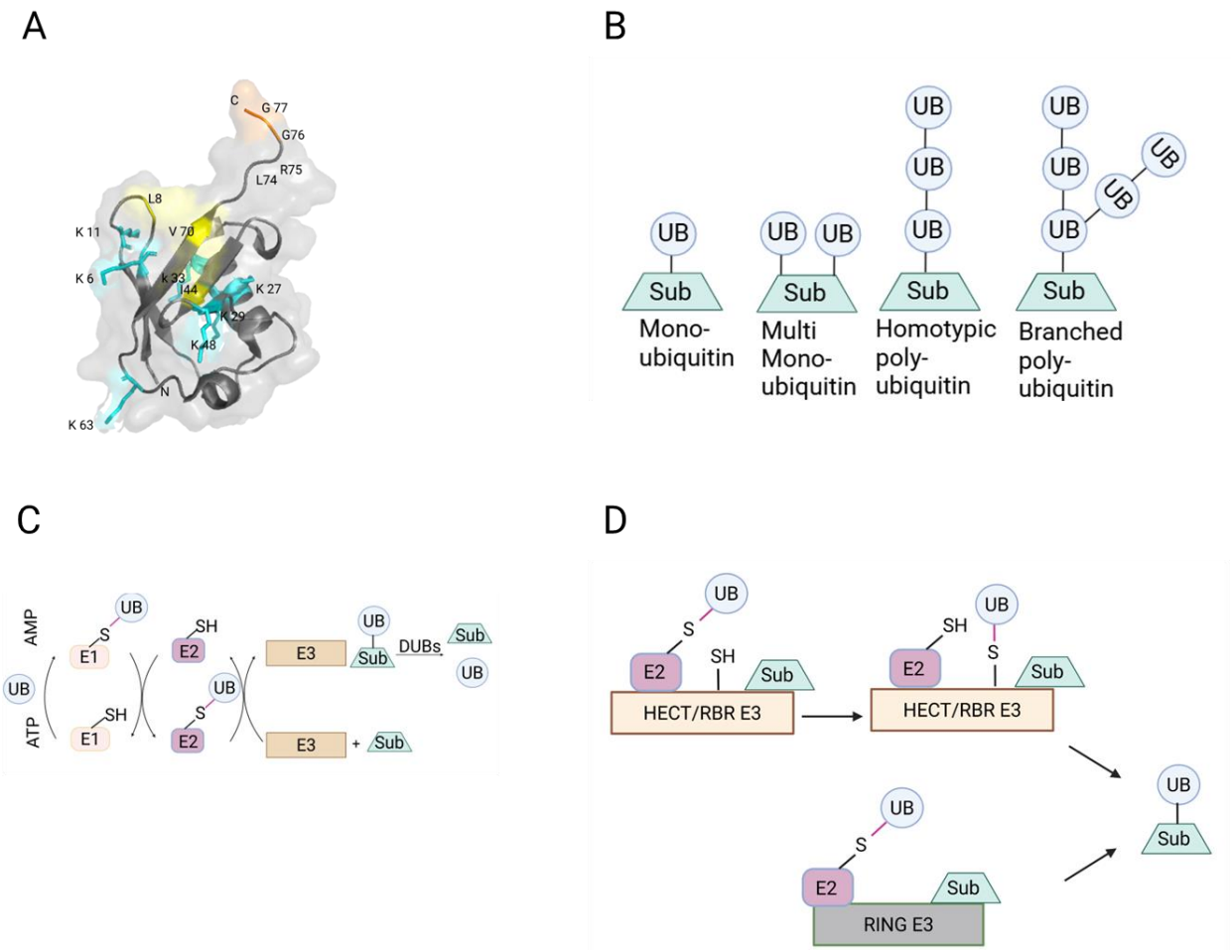

Figure 1.1. Type of ubiquitination and an overview of ubiquitination processes. ***A.*** *The ribbon diagram of human ubiquitin (Protein data bank (PDB): 1d3z) (Cornilescu et al., 1998). The seven Lysine residues that contribute to chain formation are highlighted in Cyan. The hydrophobic patch consisting of L8, I44 and V70 is depicted in yellow. The LRGG residues found at the C-terminus of ubiquitin are indicated with diglycine being highlighted in orange. Generated using the PyMOL Molecular Graphics System, Version 3.1.0 Schrödinger, LLC.* ***B.*** *Different types of ubiquitin (UB) modification including mono-ubiquitin and polyubiquitin (homotypic and branched). Adapted and modified from (Komander & Rape, 2012)* ***C.*** *Schematic depiction of the ubiquitination process. The enzymes E1, E2, and E3 are responsible for activating, conjugating and ligating ubiquitin to the target proteins, respectively. The purple line depicts the thioester-bond. Adapted and modified from (Husnjak & Dikic, 2012)* ***D.*** *The three major classes of E3 ligases which include the RING, HECT and RBR and their mode of action are depicted. Adapted and modified from (Berndsen & Wolberger, 2014). The figure 1.1 B, C, & D are created with BioRender.com.*

In addition to well-established Lysine-linked polyubiquitin, recent studies have revealed the presence of non-lysine linked atypical ubiquitin chains, which represent an emerging aspect

of ubiquitin signaling and function (Cadwell & Coscoy, 2005; Kirisako et al., 2006; X. Wang et al., 2007). One such example is the linear polyubiquitin chain, which is formed in a head to tail manner linked through N-terminal methionine (M1) of ubiquitin (Kirisako et al., 2006). M1-linked linear ubiquitin chain plays a critical role in nuclear factor (NF-κB) signaling (Rahighi et al., 2009). Furthermore, non-lysine receptor sites, such as Serine, Threonine, and Cysteine residues on target proteins have been reported as part of host-pathogen responses in virus infection (Cadwell & Coscoy, 2005; X. Wang et al., 2007). A herpesvirus E3 ligase mK3 ubiquitinates host protein Serine/Threonine residues via esterification, which modulates host signaling and immune responses (X. Wang et al., 2007). Despite the identification of non-lysine ubiquitination in the cell, the mechanism and function of these modifications are still not well understood.

1.2.2 The process of protein ubiquitination

Canonical protein ubiquitination is achieved by the sequential actions of three classes of enzymes: the activating enzyme E1, the conjugating enzyme E2, and the ligase E3 (Hershko & Ciechanover, 1998; Pickart & Eddins, 2004) (Figure 1.1 C). Briefly, the E1 enzyme activates ubiquitin in the presence of ATP forming a thioester bond between its Cysteine and ubiquitin (Hershko & Ciechanover, 1998; Pickart & Eddins, 2004). Then, the E2 enzyme transfers the activated ubiquitin from E1 to its catalytic Cysteine residue (Hershko & Ciechanover, 1998; Pickart & Eddins, 2004). Finally, E3 ligases facilitate the conjugation of ubiquitin to substrates by catalyzing the formation of an iso-peptide bond between the carboxyl group of a Glycine residue at the C-terminus of ubiquitin and the ε-amino group of a Lysine residue on the substrate proteins (Hershko & Ciechanover, 1998; Pickart & Eddins, 2004). Importantly, protein ubiquitination is a reversible process (Dikic et al., 2009; Husnjak & Dikic, 2012).

Deubiquitinating (DUB) enzymes catalyze the removal of ubiquitin from substrates and ubiquitin precursors, contributing to the maintenance of ubiquitin homeostasis within the cell (Park & Ryu, 2014).

In the human genome, there are two genes encoding for E1 enzymes, and approximately 40 genes encoding E2 enzymes (Kelsall, 2022b; Stewart et al., 2016; G. W. Xu et al., 2010). E3 ligases are the most diverse group of enzymes as they are responsible for determining substrate specificity, with an estimated 500 to 1000 members in the human genome (Yang et al., 2007). There are three main types of E3 ligases, Really Interesting New Gene (RING), homology to E6AP C terminus (HECT), and RING between RING E3 ligases (RBR) differing in their structures and mechanism of action (Figure 1.1 D) (Berndsen & Wolberger, 2014; Zheng & Shabek, 2017). RING E3 ligases facilitate a direct transfer of ubiquitin from the ubiquitin-loaded E2 to the substrates (Berndsen & Wolberger, 2014; Zheng & Shabek, 2017). In contrast, HECT and RBR E3 ligases follow a two-step mechanism: first, the E3 forms a thioester intermediate with ubiquitin (E3~Ub) via a catalytic Cysteine residue on either the HECT domain or one of the RBR RING domains; then, ubiquitin is transferred to the substrates (Berndsen & Wolberger, 2014). The structural and functional diversity of these E3 ligases allows for precise regulation of protein ubiquitination, ensuring the specificity of cellular signaling processes (Zheng & Shabek, 2017).

1.2.3 Ubiquitin signal recognition and transduction

Once ubiquitin is attached to target proteins, it serves as a molecular signal to regulate various cellular processes (Dikic et al., 2009; Hicke et al., 2005). However, for the ubiquitin signal to be effectively relayed in the cells, it must be recognized by effector proteins (Dikic et al., 2009; Husnjak & Dikic, 2012). The key mechanism for this recognition involves specialized

protein domains capable of binding ubiquitin molecules (Dikic et al., 2009; Hicke et al., 2005; Hurley et al., 2006; Husnjak & Dikic, 2012). The effector proteins containing these ubiquitin binding domains (UBDs) can detect and respond to ubiquitin modifications on substrates, thereby regulating ubiquitin mediated-processes such as DNA damage repair (Dikic et al., 2009; Doil et al., 2009; Hicke et al., 2005; Hurley et al., 2006; Husnjak & Dikic, 2012; Panier et al., 2012; Thorslund et al., 2015).

To date, at least twenty different UBDs have been identified, and categorized into five distinct structural classes: α-Helical structures, Zinc finger (ZnF), Plekstrin homology (PH) domain, Ubiquitin-conjugating (Ubc)-like domain, and a miscellaneous group for UBDs that do not fit into these categories (Table 1.1) (Dikic et al., 2009; Husnjak & Dikic, 2012).

Table 1.1. ***Classes of UBDs and representative proteins containing these domains.*** *The UBD contact residues on the ubiquitin surfaces are depicted. Adapted and modified from* (Dikic et al., 2009; Husnjak & Dikic, 2012)

UBDs	Ubiquitin Binding Surface	Protein Containing UBDs
α-Helix		
UBA	I44	hHR23A, NBR1
CUE	I44	Vps9
UIM	I44	Vps27, STAM, RAP80
MIU/IUIM	I44	Rabex-5
DUIM	I44	Hrs
VHS	I44	STAM
GAT	I44	GGA3, TOM1
UBAN	I44, F4, linker region	NEMO, optineurin, ABIN1-3
UBM	L8	Polymerase ι, polymeraseRev1
Zinc Finger		
NZF	I44	NPL4, Vps36, TAB2, TAB3
ZnF A20	D58	Rabex-5
ZnF UBP	L8, I36, tail	USP5
UBZ	I44	Polymerase-h, polymerase-k, Tax1BP1
PH Domain		
PRU	I44	Rpn13
GLUE	I44	EAP45
UBC Like Domain		
UBC	I44	UbcH5C
UEV	I44	VPS23, TSG 101
Others		
Jab1/MPN	I44	Prp8p
PFU	I44	Doa1
SH3	I44	Sla1, CIN85

Despite their structural diversity, most UBDs appear to interact with ubiquitin through a conserved hydrophobic patch on the surface of ubiquitin (Brzovic et al., 2006; Dikic et al., 2009; Lee et al., 2006). Structural studies reveal that the ubiquitin hydrophobic patch is located on its β-sheet, containing multiple hydrophobic residues L8, I44, and V70 (Figure 1.1 A & Table 1.1) (Dikic et al., 2009). Some UBDs, such as ubiquitin associated domain (UBA), ubiquitin interacting motif (UIM), GGA and TOM1 (GAT) and coupling of ubiquitin conjugation to endoplasmic reticulum degradation (CUE), interact with ubiquitin hydrophobic patch through their helical structures (R. S. Kang et al., 2003; Shiba et al., 2004; Swanson et al., 2003, 2006). Other UBDs such as Ubc-like domain of UbcH5C form a β-sheet that binds the ubiquitin hydrophobic patch (Figure 1.2 A) (Brzovic et al., 2006). Conversely, the UBDs, like zinc finger UBDs, could recognize different recognition sites on ubiquitin such as ZnF A20 domain of Rabex5 that recognizes D58 (Figure 1.2 B) and the ZnF UBP domain of USP5 which binds to the C-terminus of ubiquitin (Lee et al., 2006; Penengo et al., 2006; Reyes-Turcu et al., 2006).

In addition to binding mono-ubiquitin, many UBDs recognize linkage specific ubiquitin chains, showing a preference towards a distinct chain type (Sato et al., 2009; Sims & Cohen, 2009; Varadan et al., 2005). For example, receptor associated protein 80 (RAP 80) contains two ubiquitin-interacting motifs (UIMs), which specifically recognize and bind K63-linked polyubiquitin chains formed on histones at DNA double-strand break (DSB) sites (Al-Hakim et al., 2010; Hu et al., 2011; H. Kim et al., 2007). Upon DNA damage, this interaction facilitates the recruitment of a RAP80-binding protein BRCA1, a key DNA repair protein, to initiate DNA repair through homologous recombination (Hu et al., 2011; H. Kim et al., 2007). Notably, the two UIMs in RAP80 are separated by a seven amino acid linker which enables the UIMs to

engage with the extended conformation of K63-linked ubiquitin chains while excluding the more compact K48-linked chains (Figure 1.2 C) (Komander & Rape, 2012; Sato et al., 2009; Sims & Cohen, 2009).

In contrast, the ubiquitin receptor hHR23A which is associated with the 26s proteasome, preferentially binds K48-linked polyubiquitin through its UBA domain (Varadan et al., 2005). The structural studies of the UBA-Ub complex reveal that UBA adopts a three-helix fold that is sandwiched between the two K48-linked ubiquitin moieties (Varadan et al., 2005). The orientation of the two Ub-interacting helices of UBA aligns with the closed, compact conformation of K48-linked polyubiquitin moiety, enables its selective recognition of K48-specific ubiquitin chains (Varadan et al., 2005) (Figure 1.2 D)

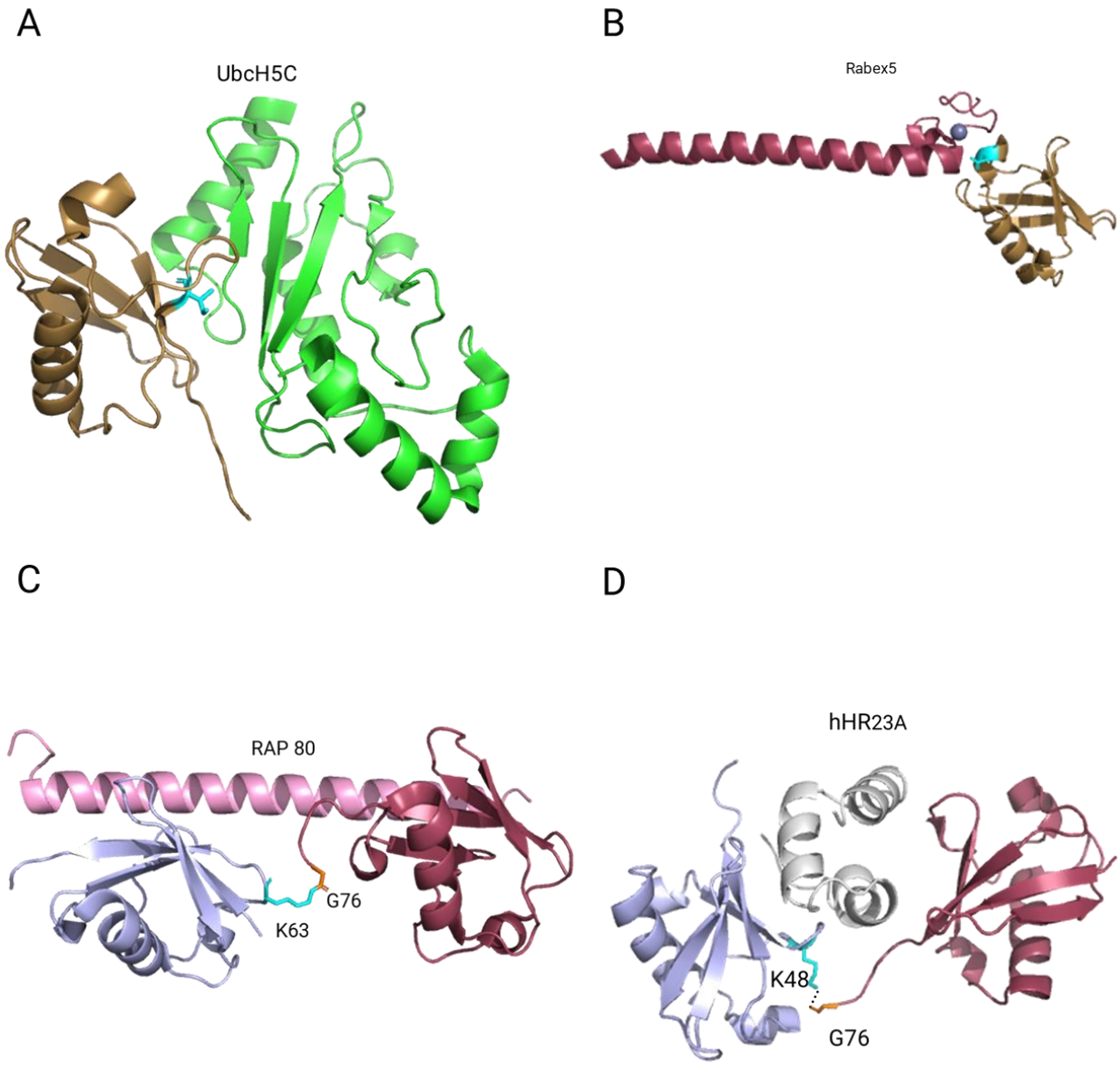

Figure 1.2. Different binding modes of UBDs to ubiquitin. *The figure depicts different UBD complexes with mono-ubiquitin (**A&B**) or di-ubiquitin (**C&D**). **A.** UBC domain (green) of UbcH5C in complex with ubiquitin (brown) (PDB: 2fuh) (Brzovic et al., 2006). I44 is highlighted in Cyan. **B.** ZnF A20 domain (dark pink) of Rabex5 in complex with ubiquitin (PDB: 2C7N) (Penengo et al., 2006). D58 is highlighted in Cyan. **C.** Tandem UIM domains of RAP 80 (pink) in complex with K63 linked di-ubiquitin (PDB: 3a1q) (Sato et al., 2009). **D.** UBA domains (grey) of hHRAD23A in complex with K48 di-ubiquitin (PDB:1ZO6) (Varadan et al., 2005). Generated using the PyMOL Molecular Graphics System, Version 3.1.0 Schrödinger, LLC.*

Over the past decades, more than 150 effector proteins have been identified to contain one or more UBDs (Dikic et al., 2009). The structural diversity of these UBDs enables the effector

proteins to recognize and decode distinct ubiquitin modifications, in turn, to achieve ubiquitin-mediated signal transduction (Dikic et al., 2009). Despite these advances, many aspects of ubiquitin-mediated cellular signaling remain poorly understood. Given the critical role of ubiquitin in processes such as DNA damage and protein degradation, further research is needed to elucidate the complexity of the ubiquitin-UBD network, in particular, how it influences downstream pathway activation and how UBD-containing proteins integrate ubiquitin signals to regulate different cellular processes.

1.3 ADP-ribosylation

1.3.1 Types of ADP-ribosylation

Unlike ubiquitination, which involves the attachment of a protein modifier, ADP-ribosylation modifies protein structure by covalently attaching one or more ADP-ribose (ADPr) units to target substrates (Lüscher et al., 2022). This modification varies in both structure and size (Li & Yu, 2015; Liu et al., 2017). When a single ADPr, composed of an adenosine moiety, two phosphates, and a ribose sugar, is added to a substrate, it is termed mono-ADPr (MAR) (Liu et al., 2017; Lüscher et al., 2022). Conversely, the attachment of multiple ADPr units is referred to as Poly-ADP-ribose (PAR) (Lüscher et al., 2022). PAR can form either linear or branched chains, with ADPr polymer lengths ranging from 2 to approximately 200 units (Li & Yu, 2015; Liu et al., 2017). The highly negatively charged ADPr, due to its two phosphates, alters both the structure and charge of target substrates, thereby impacting various cellular pathways regulated by ADP-ribosylation (Liu et al., 2017).

1.3.2 The process of ADP-ribosylation

The ADP-ribosylation reaction is catalyzed by a class of enzymes known as the ADP-ribosyl transferases (ARTs) (Lüscher et al., 2022). The general mechanism involves the transfer of an ADPr from NAD^+ to the acceptor amino acid of the substrate protein forming a glycosidic bond (Lüscher et al., 2022). During ADP-ribosylation, the nucleophilic acceptor amino acid attacks the C1'' carbon of the non-adenosine ribose in NAD+ (Figure 1.3 A) (Suskiewicz et al., 2023). This ribose, also known as adenine-distal ribose as it is not directly attached to the adenine ring, undergoes covalent bond formation with the acceptor amino acid, resulting in a glycosidic linkage between ADPr and the target protein (Lüscher et al., 2022; Suskiewicz et al., 2023; K. Zhu et al., 2022). This reaction leads to mono-ADP-ribosylation (MARylation) of the protein (Suskiewicz et al., 2023). Notably, there are many acceptors amino acid residues that could be modified by ADP-ribosylation including Arginine, Cysteine, and Serine, which give rise to N- glycosidic, S- glycosidic, and O-glycosidic bonds, respectively (Lüscher et al., 2022).

Poly-ADP-ribose (PAR) chains are formed through a mechanism similar to MARylation, in which the nucleophilic hydroxyl moiety (OH) of the pre-existing ADPr performs the attack on the C1'' of NAD^+ leading to a sequential elongation of the ADP-ribose chain on the substrates (Suskiewicz et al., 2023). A linear PAR chain will be formed when ADPr units are linked to the adenosine group of the preceding units (Figure 1.3 B) (Suskiewicz et al., 2023). Conversely, the PAR chain branches when ADPr units are added to the non-adenosine ribose of a pre-existing unit (Suskiewicz et al., 2023). As a result, it will generate highly heterogeneous signals with variable lengths and structures (Li & Yu, 2015; Liu et al., 2017). The influence of the structural diversity of ADP-ribosylation on the biological outcomes is less understood (Reber & Mangerich, 2021). However, evidence supports that heterogeneity of the ADP-ribose structures is important in determining their distinct biological functions (Reber & Mangerich, 2021). To

avoid confusion, from this point forward throughout the thesis, ADPr will be used to describe the ADPr moiety consisting of Adenosine diphosphate and ribose sugar, whereas ADP-ribose is used to describe mono-ADP-ribose and poly-ADP-ribose (MAR/PAR) signal on proteins collectively unless otherwise indicated.

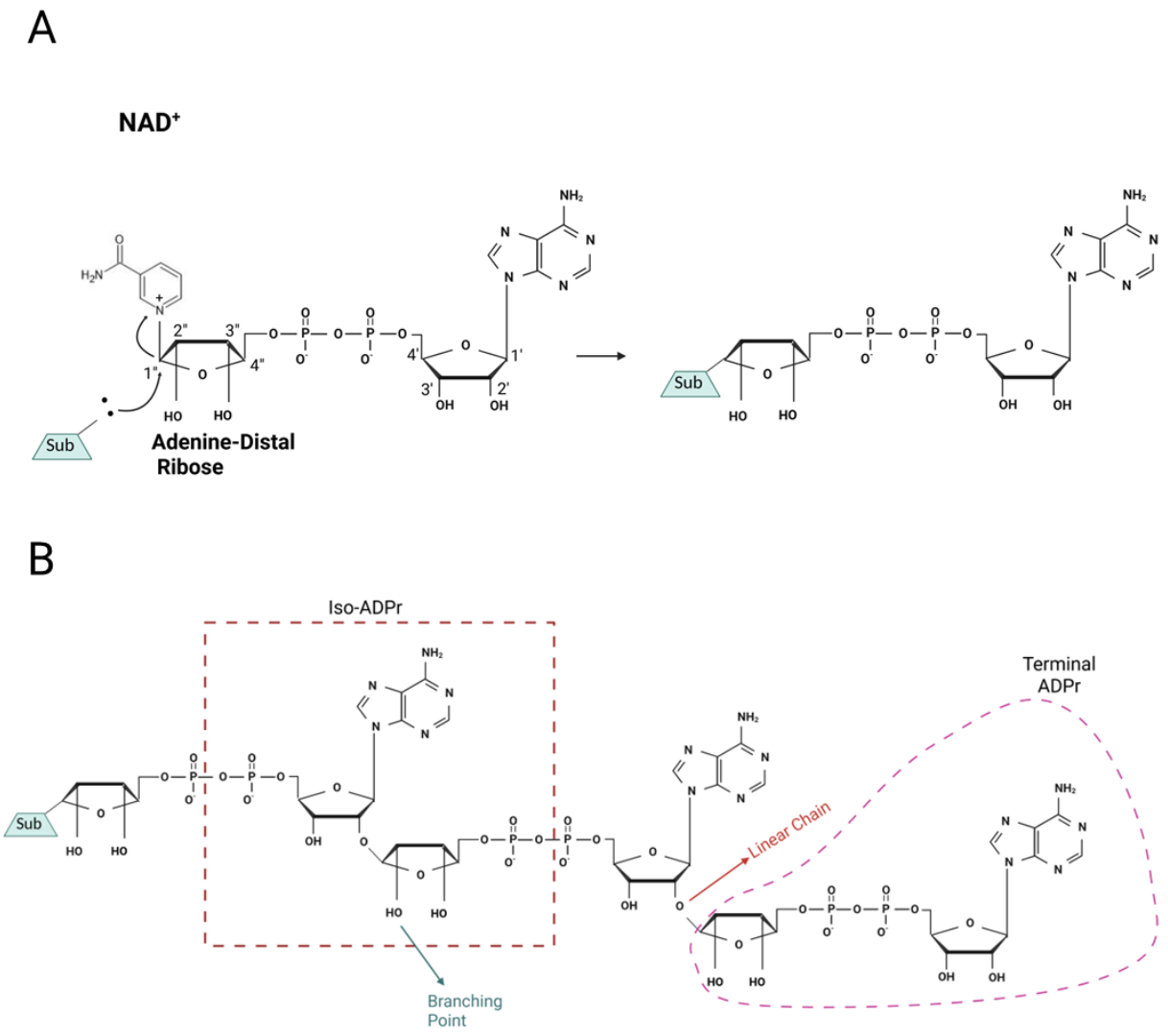

Figure 1.3. The mechanism of ADP-ribosylation and ADP-ribose chain structure. *The mechanism of ADP-ribosylation. The nucleophile of the substrate attacks the C1˝of Adenine-distal ribose of NAD^+ which results in the covalent attachment of ADPr to the substrate. Adapted and modified from (Suskiewicz et al., 2023).* ***B.*** *ADP-ribose chain structure where iso-ADPr and the terminal ADPr units are depicted. The OH-linkage sites where linear and branched chains are formed are also depicted. Adapted and modified from (Teloni & Altmeyer, 2016). Created with Biorender.com.*

1.3.3 Enzymes involved in ADP-ribosylation

Unlike ubiquitination which is only found in eukaryotes, ADP-ribosylation appears to be an ancient PTM found in bacteria, archaea, and eukaryotes (Lüscher et al., 2018, 2022; Wiborg et al., 1985). ADP-ribosylation was originally discovered as the pathogenic mechanism for diphtheria toxin, a secreted bacterial ART enzyme encoded by *Corynebacterium diphtheriae* that blocks host cell protein synthesis by catalyzing ADP-ribosylation on the key host translation elongation factor eEF2 (Collier, 2001). Therefore, the diphtheria toxin-like ARTs are known as ADP-ribosyl transferase diphtheria-toxin like (ARTDs) or H-Y-E ARTs, named after their catalytic Histidine, Tyrosine and Glutamate residues critical for NAD^+ binding (Cohen & Chang, 2018; Lüscher et al., 2018). In contrast, another class of ARTs contains Arginine, Serine and Glutamate in their catalytic domains (Cohen & Chang, 2018; Lüscher et al., 2018). These are designated as ADP-ribosyl transferase cholera-toxin like (ARTCs) or R-S-E ARTs, with cholera toxin being the primary example of this group (Cohen & Chang, 2018; Lüscher et al., 2018).

In humans, more than 20 ARTs have been identified, most of which belong to ARTDs or ARTCs, based on their structural homologies to the bacterial toxin ARTs (Cohen & Chang, 2018; Lüscher et al., 2018). Of these, more than 17 enzymes belong to ARTDs, while four are classified as ARTCs (Cohen & Chang, 2018). ARTDs were also known as poly-ADP-ribose polymerases (PARPs) as many members of this class synthesize ADP-ribose polymers, with PARP1 being the first and most well-characterized member of the family (Cohen & Chang, 2018; Lüscher et al., 2018). However, human ARTCs have only been shown to catalyze the addition of MAR to their substrates (Lüscher et al., 2018).

Intriguingly, the mode of ADP-ribosylation can be further modulated by the presence of auxiliary proteins, such as PARP1-Requires-Histone-PARylation-Factor 1 (HPF1) (Bonfiglio,

Fontana, et al., 2017; Longarini et al., 2023; Suskiewicz et al., 2023). PARP1 is known to add PAR to Aspartate and Glutamate residues of acceptor substrates (Suskiewicz et al., 2020). However, when PARP1 binds to HPF1, the cooperative action shifts PARP1 activity, leading to the attachment of MAR to Serine residues on the target substrates, thereby changing the structure of the modification (Longarini et al., 2023; Suskiewicz et al., 2020). This alteration in the ADP-ribosylation mode could have significant implications on the biological outcome of the modification, influencing pathways such as DNA repair and cellular stress responses (Longarini et al., 2023).

Similar to ubiquitination, ADP-ribosylation is also a reversible modification (O'Sullivan et al., 2019). Many enzymes act as "erasers" of the ADP-ribose signal, such as Poly ADP-ribose glycohydrolase (PARG) and ADP-ribosyl-hydrolase (ARH) (O'Sullivan et al., 2019; Suskiewicz et al., 2023). PARG is the main enzyme for PAR hydrolysis (O'Sullivan et al., 2019). Specifically, PARG cleaves glycosidic bonds between two ADPr units, leaving only the last ADPr unit attached to the substrate (O'Sullivan et al., 2019; Suskiewicz et al., 2023). In contrast, the enzymes that remove the amino acid attached ADPr act in receptor specific manner (Suskiewicz et al., 2023). For example, Terminal ADP-ribose glycohydrolase 1 (TARG1), MacroD1, and MacroD2 remove ADPr units attached to acidic residues like Glutamate and Aspartate, while ARH1 and ARH3 hydrolyze ADPr units attached to Arginine and Serine residues, respectively (Abplanalp et al., 2017; O'Sullivan et al., 2019; Rosenthal et al., 2013).

1.3.4 ADP-ribose signal recognition and transduction by ADP-ribose-reading domains

Beyond the enzymes that regulate ADP-ribosylation by adding or removing ADP-ribose signal, a distinct class of proteins contains specialized ADP-ribose-recognition domains that bind to ADP-ribose modification and mediate downstream cellular effects (H. C. Kang et al., 2011;

Liu et al., 2013; Teloni & Altmeyer, 2016). In humans, these ADP-ribose reading domains are found in large numbers of proteins (~800 proteins), which belong to diverse classes of effectors involved in different cellular processes such as DNA damage repair, RNA metabolism, and gene expression (Cohen & Chang, 2018; Gagné et al., 2008; H. C. Kang et al., 2011; M. Li et al., 2013; Liu et al., 2013; Malanga et al., 2008; Teloni & Altmeyer, 2016).

To this day, at least nine different classes of ADP-ribose-reading domains have been identified (Teloni & Altmeyer, 2016). Among these, the best-studied reading domains are macrodomains, PAR-binding zinc finger (PBZ), and WWE domains (Kalisch et al., 2012; Karras et al., 2005; Münzker et al., 2024; Oberoi et al., 2010; Teloni & Altmeyer, 2016; Timinszky et al., 2009; Z. Wang et al., 2012). Additionally, other protein modules, such as BRCA1 C-terminal (BRCT) and Forkhead-associated (FHA) domains, have been reported to recognize ADP-ribose (M. Li et al., 2013). Notably, some of these domains were previously known for their ability to bind RNA and DNA (Teloni & Altmeyer, 2016).

The mode of interaction between some of these domains and ADP-ribose can be diverse (Teloni & Altmeyer, 2016). For example, some ADP-ribose reading domains, such as BRCT and FHA domains, interact with ADP-ribose through electrostatic interactions by binding to it phosphate groups (M. Li et al., 2013). Similarly, many DNA/RNA binding domains, also recognize ADP-ribose potentially through electrostatic interaction (Teloni & Altmeyer, 2016).

In addition to these general electrostatic attractions, some ADP-ribose-reading domains form stable structural complexes with ADP-ribose, enabling selective recognition, as exemplified by a macrodomain protein Af1521 from the thermophilic archaea *Archaeoglobus fulgidus* (Figure 1.4 A) (Karras et al., 2005). The crystal structure studies of the Af1521-ADPr complex showed that Af1521 primarily interacts with the adenine ring through aromatic stacking and also

forms hydrogen bonds with the non-adenosine ribose (adenine-distal ribose), giving rise to high binding affinity of Af1521 to ADPr (K_D=0.13 μM) (Karras et al., 2005). Further studies revealed that macrodomains generally bind to MAR or the terminal PAR unit (Figure 1.3 B) as its access to the internal units was restricted, exemplified in the interaction between the macrodomain protein macroH2A1.1 and ADPr (Kalisch et al., 2012; Timinszky et al., 2009). In contrast, a PAR-Binding-Zinc-finger (PBZ) domain was found to contain two adenine binding sites, which enable it to interact with two consecutive ADPr units and thereby recognizing internal PAR moieties (Figure 1.4 B) (Oberoi et al., 2010).

Among the ADP-ribose readers, the WWE domains are unique in their interactions with ADP-ribose. While WWE domains share a conserved three-dimensional fold, the WWE domain of E3 ligase RNF146 demonstrates a distinct PAR-binding by recognizing the internal iso-ADPr moiety (*i.e.* the adenosine-monophosphate of one ADPr unit connected to the ribose and monophosphate of a consecutive ADPr unit) (Münzker et al., 2024; Z. Wang et al., 2012) (Figure 1.3 B & Figure 1.4 C). However, the WWE domain of the E3 ligase HUWE1 shows a preference towards ADPr compared to iso-ADPr, potentiating it to bind to MAR and PAR (Figure 1.4 D) (Münzker et al., 2024).

Although the molecular mechanisms of ADP-ribose signal recognition are less understood, it is generally believed that once these distinct ADP-ribose modifications, such as MAR or PAR, are recognized by their respective reader domains, they initiate a cascade of signaling events. This leads to the recruitment of effector proteins that regulate different cellular responses such as DNA repair and stress responses (H. C. Kang et al., 2011; Liu et al., 2013).

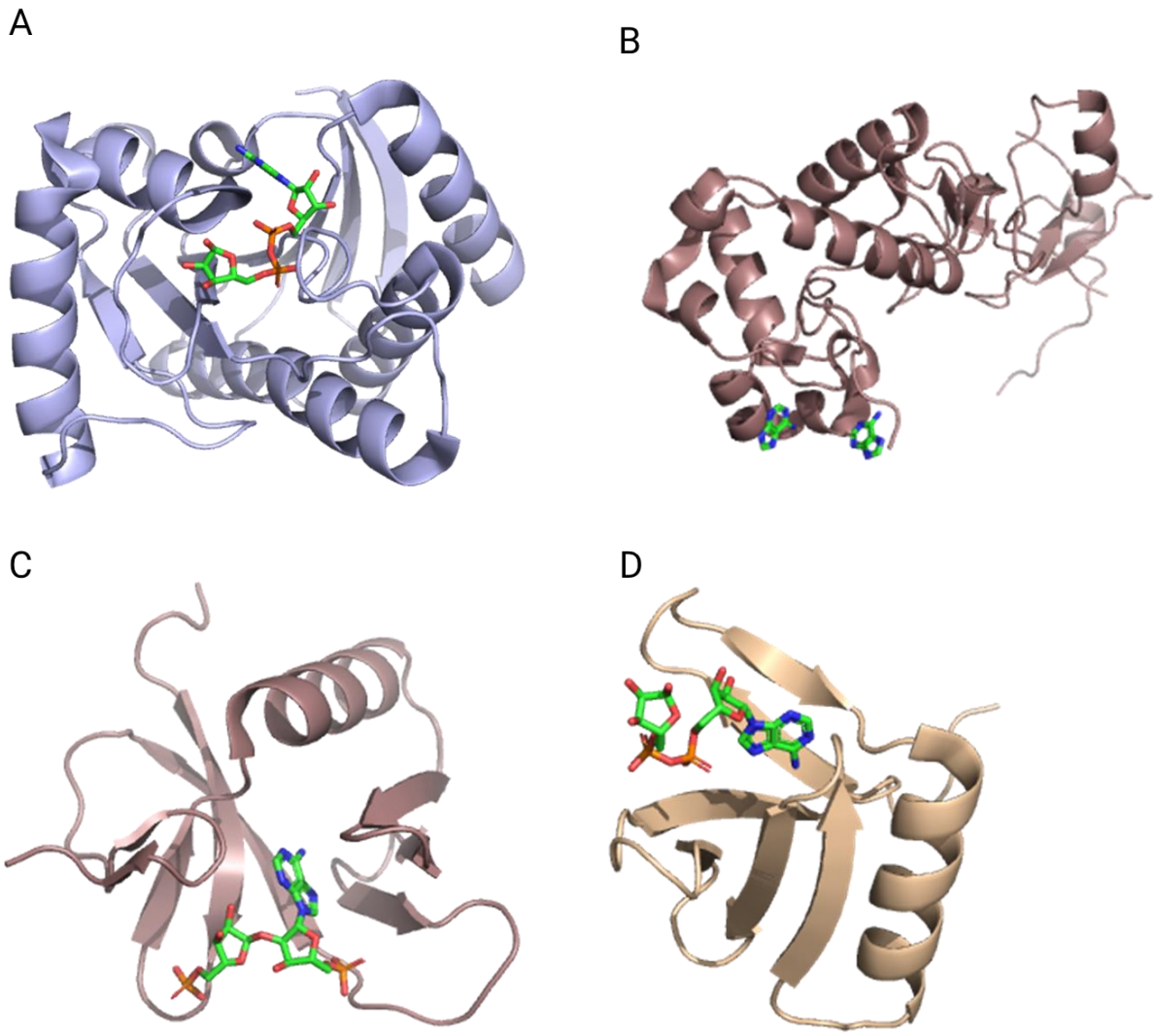

Figure 1.4. Different modes of ADP-ribose binding. *Ribbon structures of four ADP-ribose binding domains in complex with different ADP-ribose derived species.* ***A.*** *The macro domain of AF1521 in complex with ADPr (PDB: 2bfq) (Karras et al., 2005).* ***B.*** *The PBZ domain of CHFR protein in complex with two adenine moieties (PDB: 2XOC) (Oberoi et al., 2010).* ***C.*** *The WWE domain of RNF146 in complex with iso-ADPr (PDB: 3V3L) (Z. Wang et al., 2012).* ***D.*** *The WWE domain of HUWE1 in complex with ADPr (PDB: 8rd7) (Münzker et al., 2024). Images generated using the PyMOL Molecular Graphics System, Version 3.1.0 Schrödinger, LLC.*

1.4 Proteomic study of ubiquitination and ADP-ribosylation

Traditional approaches for PTM research often targeted specific modifications on a single protein (G. Xu & Jaffrey, 2013). PTM-specific antibodies enable techniques such as Western blotting and immunoprecipitation to detect these PTMs (Gagné et al., 2008; G. Xu & Jaffrey, 2013). However, mass spectrometry (MS) has emerged as a more comprehensive method, capable of identifying a wide range of PTMs with high sensitivity and accuracy (Daniels et al., 2015; Jeram et al., 2009; Vertegaal, 2011). In particular, MS has been applied for proteomic studies of cellular ubiquitination and ADP-ribosylation (Elia et al., 2015; Gagné et al., 2008; Mandemaker et al., 2017; Martello et al., 2016; Peng et al., 2003; Shi et al., 2011). This section will discuss the MS techniques used in studying ubiquitination and ADP-ribosylation as well as some of the challenges that face the field.

1.4.1 Proteomic study of ubiquitination

The proteomic study of ubiquitination is challenging for various reasons, including the low abundance of conjugated ubiquitin in the cell and the rapid turnover of this modification (Peng et al., 2003; G. Xu & Jaffrey, 2013). The advancement in the MS instrument enabled the global study of ubiquitination and the identification of ubiquitination sites (Kirkpatrick et al., 2005). A routine step in MS proteomic analysis involves the digestion of the proteins in the sample into peptides (Kirkpatrick et al., 2005). The digested peptides are then pass through tandem mass spectrometers (MS/MS), where they are further fragmented and sequenced (Kirkpatrick et al., 2005).

Despite the availability of many proteases for MS studies, trypsin is commonly used in studying ubiquitination, as it enables the identification of ubiquitinated peptides (Xu & Jaffrey, 2013). Trypsin specifically cleaves proteins at the amino acid residues Arginine and Lysine

(Kirkpatrick et al., 2005; Šlechtová et al., 2015). When ubiquitin is digested by trypsin, it leaves a diglycine remnant covalently attached to the modified Lysine residue (K-GG) of the ubiquitinated protein (Figure 1.5 A) (Shi et al., 2011; P. Xu & Peng, 2006). This diglycine remnant results in a mass shift of +114.043 Da, which allows for the identification of the site of the modification (Shi et al., 2011). Additionally, it enables the study of ubiquitin linkage by identifying the specific modified Lysine on the ubiquitin peptides (Figure 1.5 B) (Kirkpatrick et al., 2005; P. Xu & Peng, 2006).

To enhance detection sensitivity, mass spectrometry-based proteomic studies of ubiquitination typically involve the enrichment of ubiquitinated proteins followed by MS/MS analysis (Figure 1.5 C) (Peng et al., 2003; Shi et al., 2011; Tan et al., 2008). In one of the first global proteomic studies of ubiquitination, Peng et al. (2003) expressed exogenous HIS_6-tagged ubiquitin in yeast cells so that the HIS_6-tagged ubiquitin could be incorporated during the ubiquitination process in the cell. Ubiquitinated proteins were then purified using metal affinity chromatography and analyzed by MS/MS (Figure 1.5 C) (Peng et al., 2003). This study identified 110 ubiquitination sites from 72 modified proteins (Peng et al., 2003). However, a caveat of using epitope-tagged ubiquitin in an overexpression system is that it may alter ubiquitination dynamics and disrupt protein homeostasis in the cell due to induced stress response (Tan et al., 2008).

As UBDs are specific ubiquitin-binding domains, they have been used to enrich endogenous ubiquitinated proteins in mass spectrometry studies of the cellular ubiquitome (Figure 1.5 C) (Shi et al., 2011; Tan et al., 2008; Vertegaal, 2011). To address the general low affinity of most UBDs for ubiquitin in MS-based proteomic studies, multiple UBDs were fused together to create tandem ubiquitin-binding entities (TUBES), which increases the binding

affinity by up to a 1000-fold (Hjerpe et al., 2009; Vertegaal, 2011). One study utilized an engineered GST-fusion proteins containing four tandem UBA domains of ubiquilin-1 in a GST pulldown assay to capture ubiquitinated proteins from 293T cells under endogenous conditions and identified 294 ubiquitination sites (Shi et al., 2011).

In recent years, the detection of ubiquitin modification has improved significantly with the use of the K-GG antibody, which effectively enriches low-abundance ubiquitinated peptides for MS studies (Figure 1.5 C) (Bustos et al., 2012). This approach has enabled the identification of more than 10, 000 ubiquitination sites from over 4000 human proteins from whole-cell lysates in different studies (Bustos et al., 2012). However, challenges remain in detecting non-lysine ubiquitin modifications, such as ubiquitin conjugation through thioester or ester linkage, as they are often overlooked by current enrichment methods due to their labile nature (Cadwell & Coscoy, 2005; Longarini & Matić, 2024).

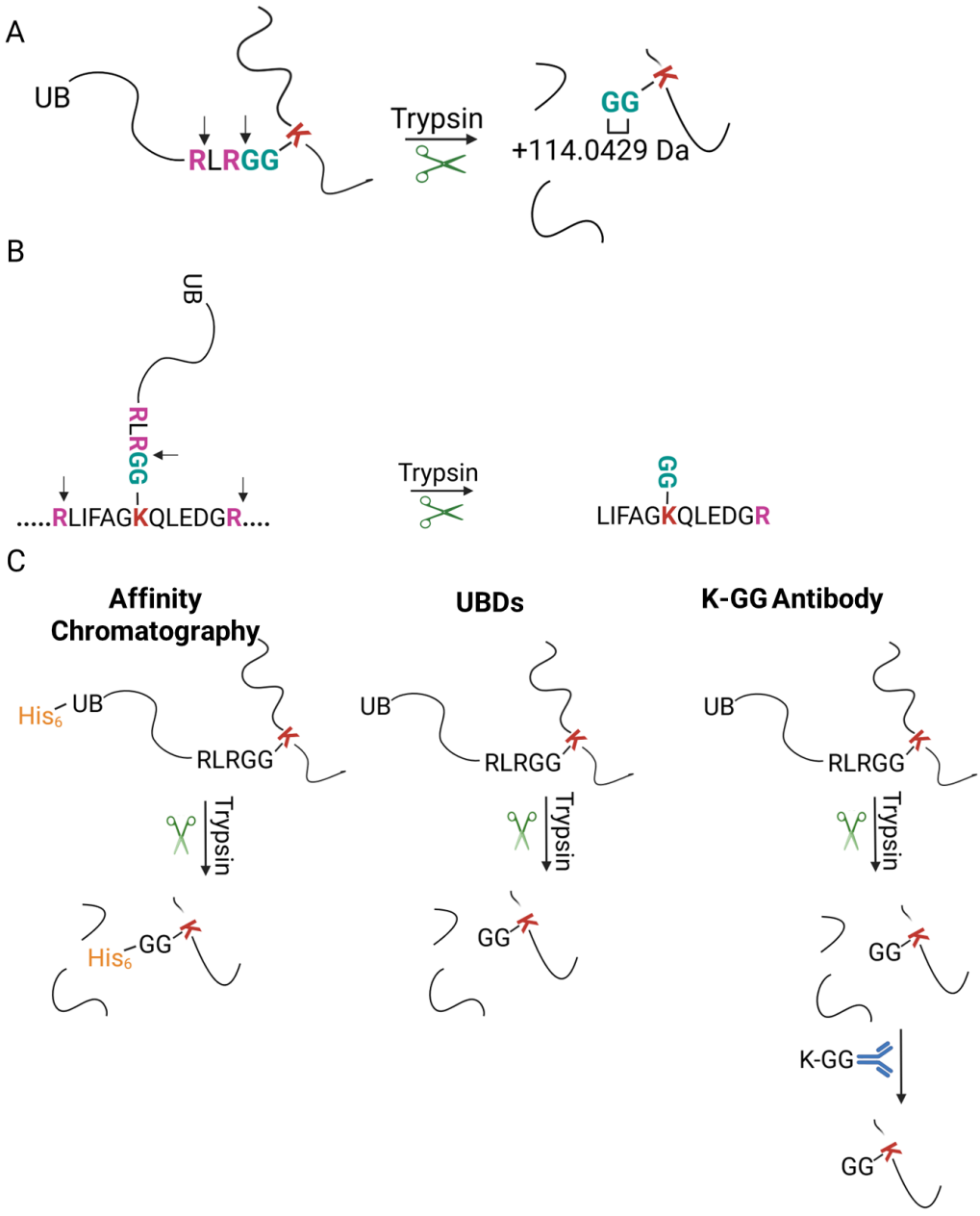

Figure 1.5. MS study of ubiquitination. A. *Tryptic digestion of ubiquitin leaves diglycine ubiquitin remnant on the modified Lysine residue which results in +114.0429* ***B.*** *K48 ubiquitin linkage is depicted. Following tryptic digestion, the diglycine remnant on k48 of ubiquitin would allow the identification of the type of ubiquitin linkage. A&B are adapted and modified from (Kirkpatrick et al., 2005; P. Xu & Peng, 2006)* ***C.*** *Three different techniques in studying ubiquitination are depicted which include affinity purification of His_6 tagged ubiquitin, using UBDs as baits to purify ubiquitinated proteins, and using the K-GG antibody to capture ubiquitinated peptides following trypsin digestion. Adapted and modified from (Vertegaal, 2011). Created with BioRender.com.*

1.4.2 Proteomic study of ADP-ribosylation

While MS has been instrumental in identifying the ubiquitination events in the cell, it has also played a crucial role in uncovering other PTMs, including ADP-ribosylation (Daniels et al., 2015; Gagné et al., 2008; Jungmichel et al., 2013; Kirkpatrick et al., 2005; Martello et al., 2016; Vivelo & Leung, 2015). Like ubiquitination, ADP-ribosylation is a transient, low-abundance and dynamic modification in the cell, and thus requires enrichment strategies for reliable MS-based detection (Vivelo & Leung, 2015). One of the earliest mass spectrometry studies by Gagne et al. (2008) used a PAR antibody 10 H to enrich the cellular PAR in a neuroblastoma cell line and identified 334 proteins associated with PAR (Gagné et al., 2008). In recent years, the detection of ADP-ribose modifications has improved with the use of a MAR-PAR reader domain Af1521 to enrich the modified peptides (Jungmichel et al., 2013). However, a later discovery revealed that Af1521 has hydrolysis activity towards acidic amino acids (Rosenthal et al., 2013). As a result, using Af1521 for enrichment might create biases toward non-acidic amino acids (Vivelo & Leung, 2015).

Furthermore, many techniques have been implemented to overcome the challenge of detecting heterogenous PAR structures by MS (Vivelo & Leung, 2015). One approach involves the addition of PARG, which will hydrolyze the PAR chains into MAR, converting PARylated proteins into MARylated proteins (Martello et al., 2016). Thus, both MARylation and PARylation can be detected by a distinct mass shift of +541.0611 Da to the acceptor amino acid, corresponding to one unit of ADP-ribose (Figure 1.6) (Martello et al., 2016; Vivelo & Leung, 2015).

Another challenge of ADP-ribosylation detection using MS is the inherent lability of the modification (Gehrig et al., 2021; Polasky et al., 2023). Because ADP-ribose is labile,

fragmentation methods used in tandem mass spectrometry, such as collision-induced dissociation (CID) and high energy collision dissociation (HCD), often cause ADPr to break apart in the process (Bonfiglio, Colby, et al., 2017; Gehrig et al., 2021). This complicates the identification of ADP-ribosylated peptides (Gehrig et al., 2021). However, the collision results in the production of diagnostic ions including 136.06232, 250.09401, 348.07036, 428.03669, and 584.09018 Da which correspond to Adenine, Adenosine with water loss, Adenosine monophosphate, Adenosine diphosphate and ADPr-carobodiimide (when Arginine residue is being modified), respectively (Figure 1.6) (Gehrig et al., 2021; Polasky et al., 2023). These ions are useful markers for ADP-ribosylation detection (Gehrig et al., 2021).

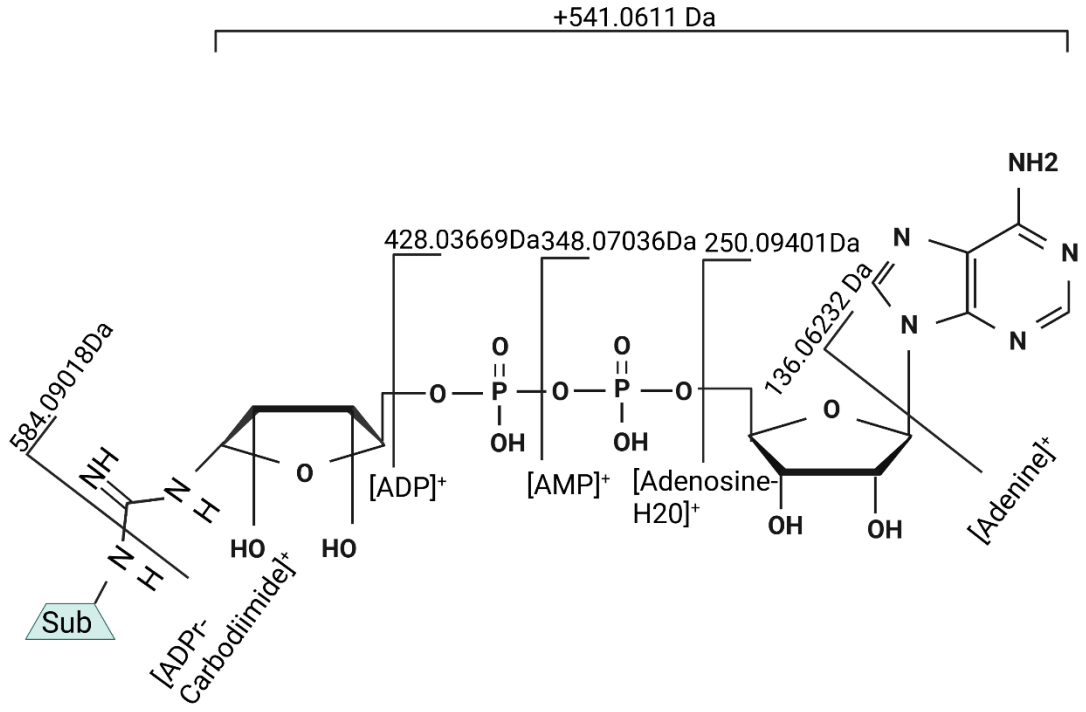

Figure 1.6. MS study of ADP-ribosylation. *The mass shift and diagnostic ions produced by ADPr following LC-MS/MS analysis. The figure depicts a substrate Arginine residue modified by MAR which will result in a mass shift of +541.0611Da. The diagnostic ions resulting from the fragmentation of the modification along with their m/z are also depicted. Adapted and modified from (Gehrig et al., 2021). Created with BioRender.com.*

1.5 Ubiquitination and ADP-ribosylation in DNA damage

MS has enabled the identification of cellular ubiquitination and ADP-ribosylation with great depth (Gagné et al., 2008; Jungmichel et al., 2013; Mandemaker et al., 2017; Martello et al., 2016; Peng et al., 2003; Shi et al., 2011). However, the biological significance of these modifications requires further functional characterization. Both ubiquitination and ADP-ribosylation are crucial for cellular response to stress including oxidative stress and DNA damage (Doil et al., 2009; Jungmichel et al., 2013; H. C. Kang et al., 2011; Liu et al., 2013, 2017; Longarini et al., 2023; Panier et al., 2012; Thorslund et al., 2015). Although ubiquitination and ADP-ribosylation have distinct mechanisms and functions, they often coordinate to regulate complex cellular pathways (H. C. Kang et al., 2011; Liu et al., 2013; Yan et al., 2013).

Understanding how these modifications contribute to cellular function requires not only mapping their sites but also deciphering their dynamic interactions and regulatory roles.

This interplay of ubiquitination and ADP-ribosylation is especially evident in the cell's response to DNA damage, where both ubiquitination and ADP-ribosylation play critical roles in detecting, signaling, and repairing DNA lesions (H. C. Kang et al., 2011; Liu et al., 2013, 2017; Longarini et al., 2023; Yan et al., 2013). PARylation is one of the first events triggered by DNA damage, such as double-strand breaks (DSBs), which is primarily catalyzed by PARP1 (Liu et al., 2017). Due to its nuclear abundance and its DNA binding ability, PARP1 functions as a sensor of DSBs, rapidly detecting the DNA lesions and catalyzing the addition of PAR chains to itself and other proteins (M. Y. Kim et al., 2005; Li & Yu, 2015; Liu et al., 2017). These PAR chains serve as recruitment signals for effector repair proteins containing ADP-ribose-binding domains, facilitating the assembly of the repair machinery (M. Li et al., 2013). For example, the MRE11-RAD50-NBS1 (MRN) complex, a critical early response signaling factor, is recruited to DBS through the interaction between the BRCT domain of NSB1 and PAR chains at the damage site (M. Li et al., 2013). MRN then activates a key DNA damage kinase ataxia telangiectasia mutated (ATM), which subsequently phosphorylates the histone variant H2AX, generating γH2AX, a hallmark of DNA damage signaling (Burma et al., 2001; M. Li et al., 2013).

Beyond ADP-ribosylation and phosphorylation, ubiquitination represents another crucial PTM in DNA damage signaling (Doil et al., 2009; Mandemaker et al., 2017; Panier et al., 2012; Thorslund et al., 2015). At the site of DNA damage, multiple E3 ligases are recruited including RNF8, RNF168 and BRCA1, to generate non-proteolytic ubiquitin modification that serves as docking sites for downstream repair factors (Al-Hakim et al., 2010). Importantly, growing evidence suggests extensive crosstalk between ADP-ribosylation and ubiquitination at DSBs

(Liu et al., 2013; Yan et al., 2013). This crosstalk leads to the propagation of the DNA damage signal, as seen in the recruitment of the PARP9-BBAP complex to the site of DNA damage (Yan et al., 2013). Specifically, B-lymphoma and BAL associated protein (BBAP) is an E3 ligase and its interacting partner, PARP9 is an ART that contains the macrodomain (Yan et al., 2013). The PARP9/BBAP complex gets recruited to the site of DNA damage through interaction between the macrodomain of PARP9 and PAR moiety (Yan et al., 2013). Once at the DNA lesion, BBAP ubiquitinates histones leading to the recruitment of effector proteins such as 53BP1 (Yan et al., 2013). On the other hand, PARylation-ubiquitination crosstalk could lead to protein degradation and signal turnover (H. C. Kang et al., 2011; Liu et al., 2013). The E3 ligases, CHFR and RNF146 are recruited to the site of DNA damage through their ADP-ribose reading domains, recognizing PAR modification at DNA lesion (H. C. Kang et al., 2011; Liu et al., 2013). Once recruited, these E3 ligases mediate PARP1 ubiquitination, promoting its degradation and turnover (Kang et al., 2011; Liu et al., 2013).

Recent research has revealed more E3 ligases with ADP-ribose reading domains implicated in DNA damage regulation (Gatti et al., 2020; H. C. Kang et al., 2011; Liu et al., 2013). These ligases may contribute to various aspects of the DNA damage response including protein recruitment, signal amplification, and protein degradation (H. C. Kang et al., 2011; Liu et al., 2013; Yan et al., 2013). One such E3 ligase is HUWE1, which has been reported to play a role in DNA damage repair and protein degradation (Kao et al., 2018; Mandemaker et al., 2017). The following section explores the structure and function of HUWE1 in DNA damage regulation and discusses its potential involvement in PARylation-ubiquitination crosstalk.

1.6 E3 ligase HUWE1

HECT, UBA, and WWE domain containing E3 ubiquitin protein ligase 1 (HUWE1) is a HECT domain ubiquitin E3 ligase (Hunkeler et al., 2021; Kao et al., 2018). It is encoded by the HUWE1 gene found on the X chromosome short arm (Xp11.22) (Moortgat et al., 2018). HUWE1 is a large protein that consists of 4374 amino acids with the size of 482 KDa (Figure 1.7 A) (Kao et al., 2018; Moortgat et al., 2018). Through the ligation of ubiquitin to its substrates, HUWE1 is involved in many important processes in the cell such as DNA damage response and apoptosis (Kao et al., 2018; Mandemaker et al., 2017; Zhong et al., 2005). The dysregulation of HUWE1 has been implicated in many disorders such as cancer and neurodevelopmental disorders, including X-linked intellectual disability (Hunkeler et al., 2021; Kao et al., 2018; Moortgat et al., 2018).

1.6.1. The functional domains of HUWE1

The cryo-electron microscopy (Cryo-EM) studies revealed that HUWE1 has a donut-shaped structure, with its ring-like core composed of four armadillo domains (ARLD) that serve as a scaffold (Figure 1.7 B) (Hunkeler et al., 2021). Other functional domains are distributed throughout the structure, including the UBA-UIM (residues 1317-1390), WWE (residues 1600-1700), Bcl-2 homology region 3 (BH3) (residues 1972-1994) domain, tandem ubiquitin binding motif (tUBM) (residues 2951-3123), and proliferating cell nuclear antigen (PCNA) interacting peptide (PIP) box (residues 3880-3887) (Figure 1.7 A & B) (Choe et al., 2016; Hunkeler et al., 2021; Khatun, 2017; Zhong et al., 2005). However, due to the intrinsic flexibility of these domains, only the WWE was visible in the Cryo-EM structure of HUWE1 (Figure 1.7 B) (Hunkeler et al., 2021). Notably, mutations in these functional domains impair HUWE1 substrate recognition and disrupt its cellular function (Choe et al., 2016; Ohtake et al., 2016; Zhong et al., 2005).

The catalytic HECT domain is positioned at the C-terminus above the plane of the ring-like core (Figure 1.7 B) (Hunkeler et al., 2021). Like other HECT domains, the HUWE1 HECT domain consists of an N lobe, which binds to the Ub-E2 enzyme, and a C lobe, which harbors the catalytic Cysteine (Hunkeler et al., 2021). The two lobes are connected by a flexible linker, to accommodate the conformation change and chain elongation during the ubiquitination process (Pandya et al., 2010; Takeda et al., 2023).

Uniquely, HUWE1 contains multiple PTM reading domains including UBA-UIM, WWE and tUBM (Hunkeler et al., 2021). Among these, the HUWE1 WWE domain demonstrates a stronger affinity towards ADPr (Figure 1.4 D) rather than iso-ADPr thus expected to bind to both MAR and PAR chains (Münzker et al., 2024). This is different from the WWE domain of the E3 ligase RNF146, which specifically recognizes PAR through its interaction with iso-ADPr (Z. Wang et al., 2012) (Figure 1.4 C).

Additionally, two ubiquitin-binding modules were found in HUWE1: UBA-UIM and tandem UBM (Hunkeler et al., 2021). The UBA-UIM domain of HUWE1 was shown to interact with K63 ubiquitinated E3 ligase TRAF6, involved in NF-kB signaling (Ohtake et al., 2016). After being recruited through its UBA-UIM domain, HUWE1 catalyzes the addition of K48 chains to TRAF6 leading to the formation of a branched ubiquitin chain (Ohtake et al., 2016). The K48 branching protects the K63 chain on TRAF6 from deubiquitylation which enhances the NF-kB signal (Ohtake et al., 2016).

The second ubiquitin binding module is located N-terminal to the HECT domain, spanning amino acids from 2951 to 3123 (Khatun, 2017). This region contains three UBMs, UBM1, UBM 2 and UBM3 arranged in an array and collectively called tandem UBM (tUBM) (Khatun, 2017). Although HUWE1 tUBM shows sequence homology to the UBM domains of

Pol ι and Rev1, its function is not well characterized (Khatun, 2017). Moreover, the ability of the HUWE1 tUBM to bind to ubiquitin was previously investigated by a previous lab member through biochemical assays (Khatun, 2017). It was found that the tUBM was able to bind to mono-ubiquitin and showed a higher affinity towards polyubiquitin (Khatun, 2017).

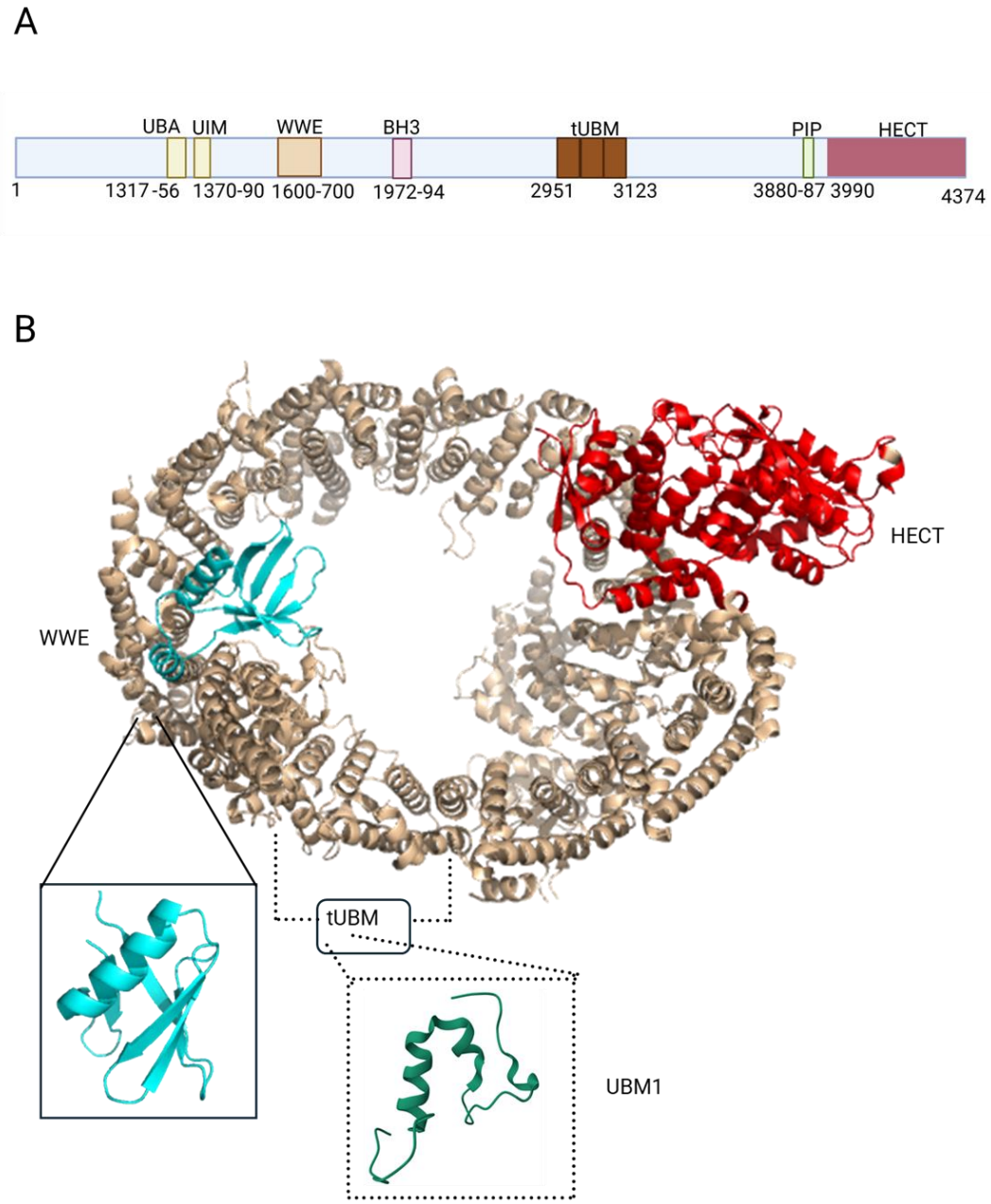

Figure 1.7. The protein structure of HUWE1. A. *HUWE1 domain structure. Depicted are the UBD UBA-UIM, the ADP-ribose reading domain WWE, the Mcl1 interacting domain BH3, the UBD tUBM, the PCNA interacting domain PIP, and the HECT catalytic domain. Created with BioRender.com.* ***B.*** *The Cyro-EM structure of HUWE1 (PDB:7jq9) (Hunkeler et al., 2021). The HECT catalytic domain is highlighted in red. The WWE domain along with its ribbon structure are shown in cyan (PDB:8rd7) (Münzker et al., 2024). Images generated using the PyMOL Molecular Graphics System, Version 3.1.0 Schrödinger, LLC. The tUBM is not visible in the structure but its location is indicated by dashed lines. The ribbon structure of UBM1 is shown in green (PDB: 2MUL).*

1.6.2. HUWE1 substrate recognition and its role in cellular functions

By targeting a diverse array of substrates, HUWE1 regulates a variety of processes in the cell such as DNA damage repair and apoptosis (Kao et al., 2018; Mandemaker et al., 2017; Zhong et al., 2005). The BH3 domain of HUWE1 is important for targeting and ubiquitinating the antiapoptotic protein Mcl-1 leading to its degradation (Zhong et al., 2005). Specifically, knocking down HUWE1 resulted in the stabilization of Mcl1, and attenuated DNA damage-induced apoptosis (Zhong et al., 2005). Moreover, HUWE1 contains a PIP box, which is a conserved motif involved in the interaction with PCNA (Choe et al., 2016). PCNA functions not only as a processivity factor for DNA replication but also as a key regulator of the replication stress response (Choe et al., 2016). It promotes DNA damage tolerance by facilitating the restart of stalled replication forks through lesion bypass (Choe et al., 2016). The interaction between the HUWE1 PIP box and PCNA is crucial for the replication fork progression under replication stress, as mutation of the conserved PIP residues impairs the process (Choe et al., 2016).

Despite having domains that enable HUWE1 to interact with its substrate, HUWE1 regulates a large number of targets (Hunkeler et al., 2021; Kao et al., 2018). The number of substrates regulated by HUWE1 exceeds that of the domains involved in target recruitment (Hunkeler et al., 2021). Thus, it is of great importance to investigate the mechanism of HUWE1 substrate recruitment, which will provide a better understanding of HUWE1's function.

1.7 Rationale

HUWE1 is an important E3 ligase that is known to be involved in many cellular processes such as DNA damage repair through the ubiquitination of its substrates (Kao et al., 2018). The dysregulation/mutation of HUWE1 is associated with various disorders such as

neurodevelopmental disorders and cancers (Kao et al., 2018; Moortgat et al., 2018). Despite being involved in many cellular processes, the mechanism by which it interacts with many of its substrates is not well understood.

In addition to its ubiquitin ligase activity, HUWE1 also is a reader protein for ADP-ribose and ubiquitin (Münzker et al., 2024; Ohtake et al., 2016; Z. Wang et al., 2012). This capacity enables HUWE1 to be recruited to ADP-ribosylated or ubiquitinated sites for coordinated regulation of protein stability, activity, and functional responses (Martinho, 2023; Ohtake et al., 2016). For example, the recruitment of HUWE1 by its UBA-UIM to K63-ubiquitinated TRAF6 promotes the formation of branched ubiquitin chains, thus, protecting the K63 chain from deubiquitination (Ohtake et al., 2016). Moreover, previous lab members established PARP1 as a substrate of HUWE1 and that HUWE1 targets PARP1 through the interaction between WWE and PAR (Huang, 2021; Martinho, 2023). Thus, using its ADP-ribose and ubiquitin reading domains could be a general mechanism by which HUWE1 interacts with its substrates.

Based on previously accumulated evidence, I propose that HUWE1 functions as an ADP-ribose or ubiquitin-dependent E3 ligase. I hypothesize that HUWE1 recognizes proteins pre-modified with ADP-ribose and/or ubiquitin through its WWE and tUBM domains. This interaction would enable HUWE1 to further ubiquitinate these pre-modified proteins, thereby regulating their stability and function. To test this hypothesis, the research will be divided into two parts, 1- focusing on identifying the subset of ADP-ribosylated and/or ubiquitinated proteins that HUWE1 can recognize and physically interact with; 2- examining whether HUWE1 directly ubiquitinates these candidate substrates.

This investigation is particularly relevant in the context of the DNA damage response. Prior studies have shown that HUWE1 is required for maintaining genome stability and participating in multiple DNA damage pathways (Kao et al., 2018; Mandemaker et al., 2017). Furthermore, ADP-ribosylation (both mono- and poly-ADP-ribose) and ubiquitination are two key post-translational modifications that coordinate the cellular response to DNA damage (Doil et al., 2009; Liu et al., 2013, 2017; Longarini et al., 2023; Mandemaker et al., 2017). Thus, my MSc project centers on addressing the first part of this hypothesis, to investigate HUWE1 recognition of ADP-ribose (mono- or poly-ADP-ribose) and ubiquitin modified proteins during DNA damage repair through WWE and tUBM domain. While the biochemical and structural features of HUWE1 WWE and tUBM have been previously studied individually (Huang, 2021; Khatun, 2017; Martinho, 2023; Münzker et al., 2024; Z. Wang et al., 2012), the current study examines their combined function in the context of HUWE1. Specifically, I aim to examine how a WWE-tUBM fusion protein recognizes ADP-ribose (mono- or poly-ADP-ribose) and ubiquitin modified proteins, as these two domains coincide together in HUWE1. This study has the following objectives:

Objective 1- Characterizing the dynamic changes of ubiquitination and ADP-ribosylation signal in response to different DNA damaging agents

Ubiquitination and ADP-ribosylation are well-known cellular responses to DNA damage (Doil et al., 2009; H. C. Kang et al., 2011; Liu et al., 2013, 2017; Longarini et al., 2023; Mandemaker et al., 2017; Panier et al., 2012; Thorslund et al., 2015; Yan et al., 2013). Thus, this research aims to profile the dynamics of these modifications in response to different DNA-damaging conditions. To achieve this goal, Western blot using both total cell lysate and nuclear fraction was performed. The levels of ubiquitination and ADP-ribosylation were investigated in

response to different types of DNA damage-inducing treatments. Moreover, confocal microscopy was used to examine the levels and subcellular localization of these modifications inside the cells.

Objective 2- Investigating the interaction between WWE-tUBM and cellular ADP-ribosylation and ubiquitination

Previously, the WWE domain of HUWE1 was shown to interact with iso-ADPr; however, a recent report biochemically illustrated the ability of the WWE to interact with higher affinity to ADPr which potentiates it to bind to both MAR and terminal PAR (Münzker et al., 2024; Z. Wang et al., 2012). However, no reports have investigated the ability of HUWE1 to interact with ADP-ribosylated proteins. Additionally, while the ability of tUBM to bind to ubiquitin has been illustrated through biochemical binding assays (Khatun, 2017), its role in cellular ubiquitin binding has not been investigated. Thus, this project aims to investigate the ability of WWE-tUBM fusion protein in MAR/PAR and ubiquitin binding. To achieve this goal, a GST-WWE-tUBM fusion protein was generated. GST pulldown assays were performed followed by Western blotting to investigate the interaction between GST-WWE-tUBM and cellular ubiquitin and ADP-ribose.

Objectives 3- Identifying the WWE-tUBM interactome using LC MS/MS

It is hypothesized that WWE-tUBM potentiates HUWE1 to interact with pre-modified targets. Thus, I sought to investigate the proteins being pulled down by WWE-tUBM. To achieve this goal, I performed GST pulldown assays using WWE-tUBM followed by LC-MS/MS to identify the interacting proteins. The MS study would give insights into different aspects of the WWE-tUBM interactome. First, it would enable the characterization of interaction between WWE-tUBM and ubiquitin/ADP-ribose, and allow profiling these recognized modifications in

terms of type (mono versus poly), sites, and linkage. Second, the MS study would also enable the identification of the proteins interacting with WWE-tUBM, which could be potential HUWE1 substrates.

Overall, this study not only provides insight into how the WWE-tUBM region of HUWE1 mediates interactions with specific PTMs but also aids in the identification of potential HUWE1 substrates. Understanding mechanism by which HUWE1 recognizes PTM signals is critical for elucidating how HUWE1 contributes to key cellular processes such as DNA damage response, particularly through its ability to selectively engage substrates pre-modified by ADP-ribose and ubiquitin.

Chapter 2: Materials and Methods

2.1 Cloning

2.1.1. Generation of WWE-tUBM fusion

To create the WWE-tUBM (1600-1700; 2951-3123) fusion, Gibson assembly (Gibson et al., 2009) was performed sequentially. First, HUWE1 WWE was amplified using PCR primers that were designed to add BamHI and EcoRI cut sites and the nuclear localization signal (NLS) (Creative Biogene, 2022) to the PCR product (Table 2.1). Second, the plasmid vector (mCherry pcDNA 3.1) was cut with the following restriction enzymes BamHI (Biolabs #R0136) and EcoRI (Biolabs #R0101). Then, Gibson assembly was performed between the cut plasmid and PCR product (NLS-WWE) (Gibson et al., 2009). Last, the generated plasmid was transformed into NEB 5α *E.Coli*. Single colonies were checked with colony PCR to ensure the presence of the insert, and then sent for sequencing. To insert tUBM into the plasmid, the same steps were repeated. tUBM was amplified using primers that insert NotI and XbaI cutting sites (Table 2.1). The plasmid generated from the previous step (pcDNA 3.1-NLSWWE) was digested with NotI (Biolabs # R0189) and XbaI (Biolabs #R0145) and Gibson assembly was performed to insert tUBM downstream of the WWE. WWE and tUBM are separated by 12 amino acids which represent the amino acid from the cut site of EcoRI and NotI and part of the plasmid backbone.

2.1.2. Generation of GST fused WWE and WWE-tUBM using restriction enzyme cloning

WWE and WWE-tUBM were cloned into the plasmid pGEX-2tk (Provided by Dr. Sheng). Briefly, the WWE (1600-1700) and WWE-tUBM domains of HUWE1 generated from step 2.1.1 (Figure S.2 C&D) (1600-1700; 2951-3123) were amplified using the PCR primers in table 2.1. The PCR primers were designed to contain the cutting sites for NdEI and BamHI. The amplified PCR products were purified using the gel purification kit (Monarch #T1020). After being purified, the PCR products were cut using 1 μL of each of the following restriction enzymes:

BamHI (Biolabs #R0136) and NdeI (Biolabs #R0111). The cut product was purified again with gel extraction kit. Then, a ligation reaction with 0.5-1µl of T4 ligase (Biolabs #M0202S) was performed between the digested PCR product and the pGex-2tk plasmid (digested with the same restriction enzymes). The ligation products were then transformed into NEB 5α bacteria and plated on Ampicillin (Bioshop #AMP201.25, 100 µg/ml), agar plates and incubated overnight at 37C^{o}. Single colonies were selected and grown overnight in 5ml of LB broth with Ampicillin (100 µg/ml). Colony PCR was performed to confirm that the domains were cloned into the plasmids. The plasmids were purified with a mini-prep kit following the manufacturer instructions and sent for sequencing.

Table 2.1. Forward (F) and reverse (R) cloning primers. *Primers used for amplifying the WWE and WWE-tUBM to enable their cloning into pcDNA3.1 and pGex-2tk plasmids*

Primer	Sequence
HUWE1-NLS1600F-BAMHI	GGCGCGCCATTAAATAAGGATCCACCTG CTGCCAAGAGGGTCAAGTTGGACTCAAA AAGGAGAGCC CAG
HUWE1-1700RNSC-ECORI	GTGTGATGGATATCTGCAGAATTCTAGTT CCTGTCC ATTGCT
HUWE1-2951F-NOT1	TGCAGATATCCATCACACTGGCGGCCGC TCACA AGCAGTGAAGAAGAA
HUWE1-3123R-xba1	ACTATAGAATAGGGCCCTCTAGATCAAG CAGAGAG TGCGGAGGT
HUWE1-1600F-NdeI-Conv	AGATTGATTCATATGTCAAAAAGGAGAG CCCAG
HUWE1-1700R-BAMH-I-Conv	GATTAAGGATCC TCATAGTTCCTGTCC ATTGCT
HUWE1-3123R-BAMHI-Conv	GATTAAGGATCCTCAAGCAGAGAGTGCG GA

2.2 GST-tagged protein purification

The pGex-2tk plasmids coding for GST-WWE and GST-WWE-tUBM cloned in 2.1.2 as well as pGEX-2tk empty vector coding for GST alone were transformed into BL21 *E. coli* to express GST-WWE, GST-WWE-tUBM and GST proteins, respectively. To express the proteins, the bacteria were grown with LB Broth supplemented with Ampicillin (100µg/mL) at 37C ^{0} until the Optical Density reached 0.5-0.7. Then, protein expression was induced using 1mM Isopropyl ß-D-1-thiogalactopyranoside (IPTG) (Bioshop # IPT001.50) and left to incubate overnight at 18C^{o}.

The bacteria then were harvested by centrifugation and the pellets were mixed with the lysis buffer (~10mL/1g of pellet) (Table 2.2). The bacteria were sonicated on ice using thermofisher scientific Sonic Dismembrator Model 500 sonicator (20% Amplitude, 2s pulse on, 10s pulse off, 30s). The lysate was then cleared with centrifugation. The clear lysate was incubated with the pre-washed glutathione beads (GE healthcare #17075604) for 1h at 4C^{0} with rotation. The beads were then washed extensively with the wash buffer which was the same as the lysis buffer. The proteins were then eluted using 0.5-1mL of the elution buffer (Table 2.3). The purified proteins are then dialyzed to the immunoprecipitation (IP) buffer to perform the pulldown assays (Table 2.4) which was supplemented with protease inhibitors (Benzamidine Hydrochloride (1mM) and PMSF (0.5mM)).

***Table 2.2**. Lysis/wash buffer for protein purification*

Reagent	Final Concentration
Tris-HCL pH 7.4/7.5	20mM
NaCl	500mM
Glycerol	10%
Triton x-100	0.1%
Protease Inhibitors	
Benzamidine Hydrochloride (Bioshop BEN# 601.100)	1mM
PhenylmethaneSulfonyl Fluoride (PMSF) (Bioshop #PMS 123.100)	1mM

Table 2.3. *Elution buffer for protein purification*

Reagent	Final Concentration
Tris-HCL pH 8/8.8	50mM
Reduced Glutathione (Bioshop#GTH001.100)	30mM
Glycerol	10%
NaCl	300mM
Dithiothreitol (DTT)	5mM

Table 2.4*. IP buffer recipe*

Reagent	Final Concentration
Tris-HCL pH 7.4/7.5	25mM
NaCl	150mM
Glycerol	5%
Nonidet P-40 (NP-40)	1%

2.3 Cell culture

Human 293T (embryonic kidney cells) and U2OS (osteosarcoma) cells were cultured in Dulbecco's Modified Eagle Medium (DMEM) supplemented with 10% Fetal bovine serum

(FBS) and 1% Penicillin/Streptomycin. The cells were grown in an incubator with 5% CO_2 and 37C^o.

2.4 Cell treatment

UV treatment. The cells were washed with ice-cold phosphate buffered saline (PBS) and then placed on ice with the dish led open. The crosslinker XL-1500 (Spectolinker) is used for UV exposure with energy set to 40J/m^2. Then, media was added back to the treated cells and incubated for the indicated times. For most experiments in this study, unless otherwise specified, cells were treated with UV and recovered for 2 hours.

Etoposide treatment. The etoposide (Sigma #E1383) powder was dissolved in DMSO to make a 5mM stock. To perform the experiment, etoposide stock was diluted with media to a final working concentration of 10μM to treat the cells for the indicated times. For most experiments in this study, unless otherwise specified, cells were treated with etoposide for 2 hours.

H_2O_2 treatment. H_2O_2 (Sigma # H1009-500ML) was diluted in PBS to a 1mM working concentration and the cells were treated for 10min or 30min.

PARP inhibitor treatment. PARP inhibitors Pj34 (Sigma #528150) and Olaparib (Toronto Research Chemical # O514500) were used to inhibit cellular ADP-ribosylation. Pj34 stock solution was prepared by dissolving the chemical in DMSO to a concentration of 50mM, and for experimental dilution, the stocks were diluted with media to the desired working concentration of 10 μM. Similarly, Olaparib stock solution was prepared by dissolving the chemical in DMSO to a concentration of 15mM and further diluted with media to the working concentration of 50 μM for cell treatment. To inhibit ADP-ribosylation, cells were incubated with PJ34 or Olaparib overnight.

Ubiquitin activating enzyme E1 inhibitor treatment. The E1 inhibitor PYR 41 (Sigma #N2915-5MG) was prepared by dissolving it in DMSO to a concentration of 27mM. To treat the cells, Pyr41 was further diluted in media to a working concentration of 15 μM. To inhibit both ADP-ribosylation and ubiquitination, cells were incubated with PJ34 and PYR41 which were diluted in media to final working concentrations of 10 μM and 15 μM, respectively. The cells were incubated with the inhibitors overnight, followed by UV treatment to induce DNA damage as indicated above.

2.5 Nuclear Extraction

To perform nuclear extraction, the protocol from Khan et al. (2020) was followed with slight variation. After treating the cells as mentioned above in section 2.4, cells were collected by trypsinization. The collected cells were then washed with PBS. After centrifugation, PBS was discarded, and cells were washed with buffer A (Table 2.5). Cells were then centrifuged at 300g for 5min. After discarding the supernatant, the cells were resuspended again in 1 mL buffer A with Triton X-100 added to a final concentration of 0.2% and the cells were incubated for 5 min on ice. The cells were then centrifuged at 600g for 5 min. The supernatant containing the cytoplasmic fraction was stored and nuclei were lysed using 2x SDS buffer (Table 2.6) by resuspending the nuclei with 250 μL of the buffer. The samples were then vortexed at maximum speed for 10 seconds and sonicated with the manual sonicator (Fisher Scientific) (10% amplitude, 10s pulse on, 10s pulse off). The nuclei were vortexed again at maximum speed to ensure proper lysis. The nuclei were then centrifuged at 16000g for 15 min and transferred to new tubes. BCA assay was used to determine the protein concentration. The samples were prepared to a final concentration of proteins of 1μg/μL using 4X SDS sample buffer and water and were boiled for 10 min and analyzed with Western blot as described in section 2.6.2.

Table 2.5. *Buffer A for nuclear extraction*

Reagent	**Final Concentration**
HEPES pH 7.35	10 mM
KCl	10 mM
MgCl2	1.5 mM
Sucrose	340 mM
Glycerol	10%
DTT	1 mM
Inhibitors	
N-Ethylmaleimide (NEM) (Sigma #E3876)	10mM
ADP-HPD (Sigma #118415)	1μM
50x Protease inhibitor cocktail (Roche #05056489001)	1x
PMSF	200μM

***Table 2.6**. 2x SDS lysis buffer*

Reagent	Final Concentration
Tris pH 7.4	20 mM
Ethylenediaminetetraacetic acid (EDTA)	20 mM
SDS	2%
Glycerol	20%

2.6 Western blot

2.6.1. Mammalian cell lysis and sample preparation

After treating the cells as mentioned above in section 2.4, cells were washed with PBS. 2X SDS lysis buffer (Table 2.6) was added to the plates containing the cells and the cells were scraped to be harvested. The samples were boiled for 5 min and then were handled similar to nuclei lysis in section 2.5 where they were vortexed, sonicated, vortexed, centrifuged, and followed by protein quantification and sample preparation.

2.6.2. Signal detection by Western blot

The prepared samples were run on a gradient gel (4-12%) (Invitrogen #XP04120BOX) until the dye front reached the bottom of the gel. The gel was transferred to a PVDF membrane (GE Healthcare Life Science # 10600021) at 30V for 18-19.5 hrs. The membrane was stained using Ponceau S staining to ensure proper transfer which was then washed with water. 5% milk in Tris Buffered Saline Tween-20 (TBS-T) was used to block the membrane for 2h at room temperature followed by blocking with 5% Bovine Serum Albumin (BSA) for 1h. The

membranes were then incubated with primary antibody (Table 2.7) at 4C^{o} overnight with gentle agitation. The membrane was washed with TBS-T three times. Following the washing, the membrane was incubated with the secondary antibody for 1h at room temperature with gentle agitation. Then, the membrane was washed TBS-T another 3 times followed by incubation with ECL (Perkin Elmer #NEL10500) for 5 min and then imaged using either using the MicroChemi (DNR Bioimaging) or the azure biosystems 280.

Table 2.7. *Primary and secondary antibiotics used for Western blotting (WB) and Immunofluorescence (IF)*

Antibodies	Cat #	Dilution
GAPDH	Proteintech #60004-1	1:1000 (WB)
Ubiquitin (P4D1)	Santa Cruz #sc-8017	1:1000 (WB)
Multi-ubiquitin (FK2)	Cayman Chemistry #14220	1:1000 (WB)
Anti-ubiquitin (FK2)	EMD Millipore # St-1200-100UG	1:100 (IF); 1:1000 (WB)
PAR	R&D Systems #4335-MC-100	1:1000 (WB)
Anti-PAR (10H)	EMD Millipore #AM80-100UG	1:100 (IF); 1:1000 (WB)
Anti Mono-ADP Ribose	Sigma # MABE 1076	1:2000 (WB)
Poly/Mono-ADP Ribose (E6F6A)	Cell Signaling Technology #83732	1:1000 (WB)
H2AX	Cell Signaling Technology #2595	1:1000 (WB)
P-Histone H2AX (D7T2V)	Cell Signaling Technology #80312	1:100 (IF);1:1000(WB)
Lamin B2 (E1S1Q)	Cell Signaling Technology #13823	1:1000 (WB)
XRCC 5 (C48E7)	Cell Signaling Technology #2180	1:1000 (WB)
Anti-Mouse HRP-Linked	Cell Signalling Technology #7076P2	1:10000 (WB)
Anti-Mouse HRP-Linked	Thermofisher Scientific #G21040	1:5000 (WB)
Anti-Rabbit HRP-linked	Cell Signalling Technology #7074P2	1:10000 (WB)

Anti-Mouse Alexa Fluor Plus 488	Invitrogen #A32723	1:1000 (IF)
Anti-Rabbit Alexa Fluor Plus 555	Invitrogen #A32732	1:1000 (IF)

2.7 Immunofluorescence

Cells were seeded in well plates (Lab-Tek #177437) and then treated with either etoposide (10 μM) or UV (40 J/m^2) as described previously in section 2.4. After the treatment, cells were fixed with 2% Paraformaldehyde for 15 min then they were washed with PBS. The cells were then permeabilized using 0.5% Triton X-100 for 15 min. The cells were then washed again with PBS and blocked for 1h using 3% BSA. The cells were then stained overnight with primary antibodies at $4C^0$ (Table 2.7). After antibody incubation, cells were washed with PBS and then stained with secondary antibodies for 1h at room temperature. After washing the cells, coverslips were mounted on the slides using anti-fade mountant with NucBlue (Thermofisher #P36981). The slides were imaged with Zeiss LSM 700 using the 63x lens. The images were visualized and captured using the Zen software.

2.8 GST pulldown assay

2.8.1. Mammalian cell lysis for GST pulldown assay

After treatments, cells were harvested with trypsinization and washed with PBS. IP buffer (Table 2.4) was used to resuspend the cells supplemented with protease inhibitors, NEM, ADP-HPD and when indicated in the results section, PARP inhibitor PJ34 was also added to the IP buffer (Table 2.8). The cells are then vortexed at maximum speed for 10 seconds and sonicated on ice with the manual sonicator (Fisher Scientific) (10% Amplitude, 10s pulse on, 10s pulse off). The cells were then vortexed again at maximum speed. The lysate was then cleared by

centrifugation at 16000g for 15 min. The cleared lysate was then collected to a new tube. BCA assay was used to determine protein concentration.

2.8.2. GST pulldown

The GST-tagged proteins were immobilized to the pre-washed Glutathione Sepharose beads by adding an equimolar amount of proteins to them and incubating for 1h at $4C^0$ with rotation. To perform GST pulldown assays, cleared cell lysates from 2.8.1 were added in equal amounts to the immobilized GST and GST-tagged proteins (1-2mg for Western blot and 8-11 mg for mass spectrometry). They were then incubated for 2h at $4C^o$ with rotation. The beads were then washed extensively to remove nonspecific binding with IP buffer (Table 2.4); however, for the samples that were sent for MS analysis the wash buffer did not contain NP-40. For Western blot detection, 4X SDS loading buffer was added to the samples and they were boiled for 10 min to elute the proteins. The beads were then centrifuged, and the supernatants were subject to detection by Western blot similar to section 2.6.2. Section 2.9 explains mass spectrometry sample preparation.

Table 2.8. *Additives to IP buffer for GST pulldown assay*

Reagent	Final Concentration
PMSF	1mM
Benzamidine Hydrochloride	1mM
Protease inhibitor cocktail	1x
ADP-HPD	1μM
NEM	20mM
PJ34	10 μM

2.9 Mass spectrometry

To prepare samples for mass spectrometry, following the washing steps for the GST pulldown, as described in section 2.8.2, the beads were resuspended with 106.5μL water. Then, 15 μL of 25mM of ammonium bicarbonate was added to the sample followed by 15 μL of 1% of the detergent RapiGest (Waters #186001861). Then, 3 μL of 0.5M Tris (2-carboxyethyl) phosphine (TCEP) was added to the samples. The samples were then vortexed and incubated at 60C^{o} for 15 min with shaking at 700RPM then were left to cool down and collected with a quick spin. The samples were then alkylated, where 3 μL of 1M iodoacetamide (IAA) was added to the samples, and they were incubated at 25C^{o} for 1h with shaking at 700RPM in the dark. After alkylation, the samples were digested with trypsin (Thermo scientific #90057) where 5μL of 1μg/μL trypsin was added to each sample and it was incubated overnight at 37 C^{o} and shaking at 700RPM. After the 16h overnight incubation, an additional 2.5μL of trypsin was added to each

sample, and they were incubated for additional 2h at 37 C^o and shaking at 700RPM. Then, the samples were cooled down at room temperature and collected through quick centrifugation. The digestion reaction was then quenched using Trifluoroacetic acid (TFA) where 6µL of 50% TFA was added to each sample, then they were vortexed to mix and incubated for 30 min at $37C^0$ with shaking at 300RPM.

To isolate the samples from the beads, the following steps were followed: 1. the samples were centrifuged at 400g for 2 min and transferred to a new tube. 2. The beads were then rinsed with 150 µL of water and they were centrifuged again, and the supernatant was combined with the supernatant from step 1. 3. The rinsing step was repeated again like in step 2, and the collected supernatant from steps 1-3 were combined and centrifuged at 16100 g for 10 min and the samples were transferred to a new 1.5 mL tubes and lyophilized using speed-vac.

The GST pulldown MS experiments were performed twice. In the first experiment, samples were prepared as previously described. Lyophilized samples were resuspended with 156 µl of 1% formic acid and submitted to the mass spectrometry facility at York University (YSCi Core mass spectrometry facility at York University) for analysis using a timsTOF Pro2 (trapped ion mobility spectrometry time-of-flight) mass spectrometer. Two separate LC-MS/MS runs were performed on this sample: one run with two injection replicates, and the other with four injection replicates.

For the second GST pulldown MS experiment, sample preparation followed the same general procedures as the first, with one modification: Lyophilized samples were resuspended with 300 µL of PARG buffer (Table 2.9) and incubated overnight at 25°C to enrich more short-chain ADP-ribosylated and MARylated proteins prior to MS analysis. MS run was performed with four injection replicates.

Table 2.9. *PARG buffer recipe*

Reagent	Final Concentration
PARG (Sigma-Aldrich #SRP8023)	6 nM
Tris-HCL pH 8	50mM
NaCl	50mM
MgCl2	1mM
DDT	250 µM

2.10. Mass spectroscopy data processing

To perform MS data searching and analysis, the Fragpipe software was used (da Veiga Leprevost et al., 2020; Käll et al., 2007; Kong et al., 2017; K. Li et al., 2019; MacLean et al., 2010; Nesvizhskii et al., 2003; Polasky et al., 2023; Teo et al., 2021; K. L. Yang et al., 2023; Yu et al., 2021; Yu, Haynes, et al., 2020; Yu, Teo, et al., 2020). The data was searched against the reference proteome UP000005640 from UniProt *Homo sapiens*. The fragmentation mode was CID. Precursor tolerance was 20 ppm, minimum peptide length 7. Cysteine alkylation has been searched as a fixed modification along with methionine oxidation and acetylation of protein N-termini as variable modifications. GG (114.0429Da) on K, S, T and C were searched as variable modifications (Chua et al., 2019). Since ADP-ribosylation is a labile modification that could be fragmented during mass spectrometry analysis, mono-ADP-ribosylation (541.0611Da), di-ADP-ribosylation (1082.1222Da) and tri-ADP-ribosylation (1623.1833Da) on S, K, R, E, D, T and Y were searched as a variable modification (non-labile mode) and mass offset (labile mode) which

would allow the identification of the peptides that mostly retained the intact modification or mostly lost it, respectively (Larsen et al., 2018; Polasky et al., 2023). In addition, the following ADPr diagnostic ions, which are fragment ions of the fragmented modification, and are indicators of the presence of the modification, were searched at 136.06232, 250.09401, 348.07036, 428.03669, and 584.09018Da (Figure 1.6) (Bonfiglio, Colby, et al., 2017; Gehrig et al., 2021; Polasky et al., 2023). The peptide remainder ions, which refer to partially fragmented modification attached to an intact peptide, were also searched at masses 114.03169, 193.99802, 291.97492 and 406.00661Da (Polasky et al., 2023). Concerning protein inference from the digested peptides, the False Discovery Rate (FDR) was kept at 5 % and while trypsin cleaves proteins with high fidelity, miscleavages could occur (Šlechtová et al., 2015), thus, trypsin missed cleavages were set to 2. When Searching for the LRGG (ubiquitin miscleavage remnant), the 114.0429 and 383.2281Da were searched as a variable modification and mass offset and fragment remainder ions was searched at m/z −42.0205 Da (Denis et al., 2007; Polasky et al., 2023; Warren et al., 2005). Since GST tag is a protein originated from the blood fluke worm *Schistosoma japonicum* (Smith & Johnson, 1988) the data was searched against the human proteome but also the *Schistosoma japonicum* proteome. This enabled the identification of the GST protein found in the samples which would be used for normalization between the samples.

2.11 GO analysis

In order to get to the modified peptides and thereby proteins, the data was searched for peptides that are modified by K-GG and/or ADP-ribose. For the modified proteins to be included they have to follow specific criteria. First, the protein should have at least two assigned peptides. Second, the log2 fold difference (FD) of the protein in WWE-tUBM compared to GST should be ≥ 2. Specifically, the FD of a protein was calculated by first averaging the intensity of the

protein in the WWE-tUBM sample across the different injection replicates and averaging the intensity of GST across the injection replicates. Then, the FD was calculated by dividing the average of the protein intensity in GST-WWE-tUBM over the average for the GST. The log2 FD was then calculated, and the proteins that had a fold change less the 2 were removed. The gene names for the protein list were entered into Maayan lab enrichr tool at http://amp.pharm.mssm.edu/Enrichr (Chen et al., 2013; Kuleshov et al., 2016; Xie et al., 2021). The list of significantly enriched biological processes, cellular components and molecular function was reported.

2.12 Overall Experimental Design and Replicates

To ensure data reproducibility, key experiments described in this study have been repeated. A summary of the number of biological replicates used for each assay is provided below.

To profile cellular ubiquitination and ADP-ribosylation in total cell lysate in response to DNA damage, two independent experiments were performed and data in Figure 3.1 is representative of these biological replicates.

The GST pulldown assay investigating the interaction between WWE-tUBM and cellular ubiquitin and ADP-ribose (MAR/PAR) was performed three independent times. Unless otherwise mentioned, other experiment data presented by the Western Blot was performed once.

Chapter 3: Results

3.1. Profiling cellular ADP-ribosylation and ubiquitination

3.1.1 Profiling cellular ubiquitination and ADP-ribosylation in response to different DNA damaging agents

Ubiquitination and ADP-ribosylation are critical players in DNA damage signaling (Doil et al., 2009; H. C. Kang et al., 2011; Liu et al., 2013, 2017; Longarini et al., 2023; Mandemaker et al., 2017; Panier et al., 2012; Thorslund et al., 2015; Yan et al., 2013). They can act as signals to recruit DNA damage response factors to the site of DNA damage (Doil et al., 2009; M. Li et al., 2013; Longarini et al., 2023; Mandemaker et al., 2017; Thorslund et al., 2015; Yan et al., 2013). Thus, I sought to profile cellular ubiquitination and ADP-ribosylation in response to different DNA-damaging agents. For example, UV creates different types of DNA lesions such as single or double-strand breaks as well as Pyrimidine photoproducts (Rastogi et al., 2010). Conversely, the topoisomerase II poison etoposide is known to cause double-strand breaks (Z. Li et al., 2014). Hydrogen peroxide (H_2O_2) is an oxidizing agent which causes oxidative stress leading to single-strand breaks (Fairbairn & O'Neill, 1994). Thus, the cellular response to these different DNA-damaging agents was tested.

I first treated 293T cells with UV ($40J/m^2$) and recovered for 2 hours or with etoposide (10 μM) for 2 hours (Figure 3.1 A). The DMSO (0.2%) and media were used as the vehicle and no treatment controls, respectively. Following these treatments, cells were harvested, lysed and the levels of ubiquitination and ADP-ribosylation in total cell lysate (TCL) were investigated with Western blotting using ubiquitin and MAR/PAR specific antibodies. Because ubiquitin and ADP-ribose are conjugated to a wide range of proteins in heterogenous ways, both appear as smears rather than distinct bands in Western blots.

As shown in Figure 3.1, both etoposide and UV treatments resulted in an overall increase in ubiquitination levels compared to controls, with a more pronounced effect observed at ~16KDa and protein bands below 100 KDa (Figure 3.1 B). In parallel, both etoposide and UV treatments also led to an increase in ADP-ribosylation level compared to the control, with etoposide inducing a higher increase in ADP-ribosylation level than UV (Figure 3.1 C).

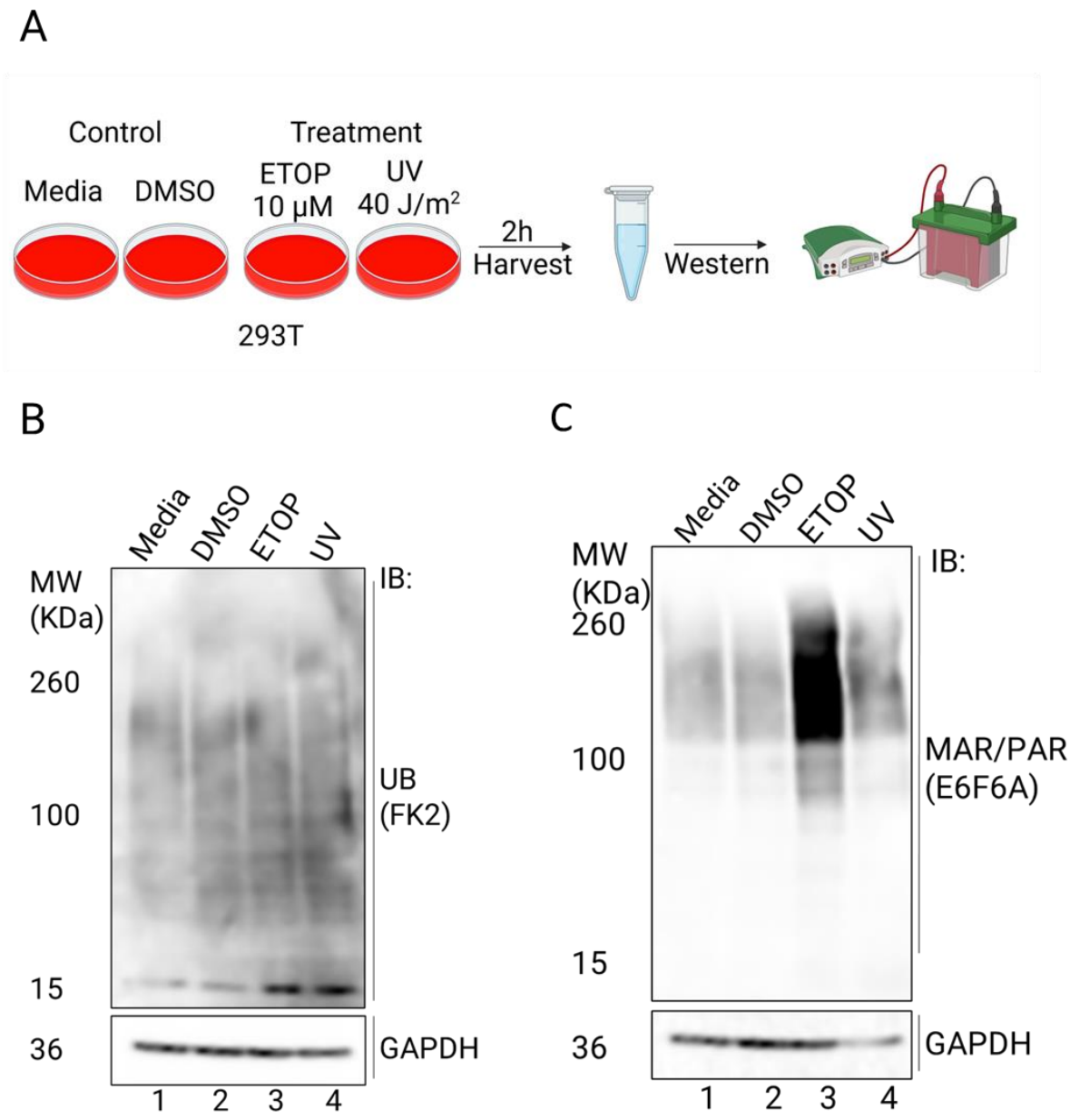

Figure 3.1. DNA damage treatments increase the levels of ubiquitin and ADP-ribose. A. *Schematic overview of the experimental design. 293 T cells were treated with either etoposide (Etop) (10 μM) or UV (40 J/m^2) for 2h. Media and DMSO were used as a control. Cells were collected, and the TCL was used for Western blotting. Created with BioRender.com* ***B-C*** *The level of ubiquitin (B) was detected by ubiquitin antibody (EMD Millipore# St-1200-100UG) and the level of MAR/PAR (C) was detected by MAR/PAR antibody (Cell Signaling Technology #83732). GAPDH was used as a loading control with a GAPDH antibody (Proteintech #60004-1).*

Since the DNA damage response occurs at the site of the DNA damage in the nucleus (Longarini et al., 2023), I sought to profile nuclear ubiquitination and ADP-ribosylation. As it was well established that ADP-ribosylation following DNA damage was largely due to the activity of PARP1, which primarily catalyzes poly-ADP-ribosylation (Liu et al., 2017). To specifically detect poly-ADP-ribosylation, I used the 10H antibody in the following experiments. Furthermore, three different DNA-damaging treatments, UV (40 J/m^2), etoposide (10 μM), and H_2O_2 (1mM) were applied for varying durations to track the dynamic changes of these two PTM events following DNA damage (Figure 3.2 A). Specifically, cells were treated with UV or etoposide for 30min, 1h or 2h, or treated with H_2O_2 for 10 or 30min. The cells were then collected, and I extracted the nuclei to perform a Western blot on the nuclear fraction.

Originally, Lamin B2 was blotted for as a loading control; however, its levels seem to be affected by DNA damage (Figure 3.2 B&C). Thus, H2AX was used as a loading control instead.

In response to DNA damage, H2AX gets phosphorylated (Burma et al., 2001), thus, as expected the levels of γH2AX increased in response to UV, etoposide, and H_2O_2 treatments (Figure 3.2 B). The increase in γH2AX in H_2O_2 treatment was less pronounced which could be explained by the lower levels of proteins in that treatment as evident from the Ponceau S staining and the loading control (Figure 3.2 B). Both ubiquitination and PARylation increase in response to UV and etoposide treatments (Figure 3.2 B&C), which is consistent with the previous observation (Figure 3.1 B&C). While H_2O_2 didn't show pronounced effect on ubiquitination (Figure 3.2 B), it increased the levels of PARylation (Figure 3.2 C). When comparing different time points or across UV and etoposide treatments, no pronounced difference on the level of ubiquitination was observed (Figure 3.2 B). However, comparing results for PARylation at different time points, UV-induced PARylation peaks after the 1h treatment and declines at the 2h

treatment (Figure 3.2 C). In contrast, the level of PARylation in response to etoposide treatment seems to be sustained after the 2h treatment (Figure 3.2 C).

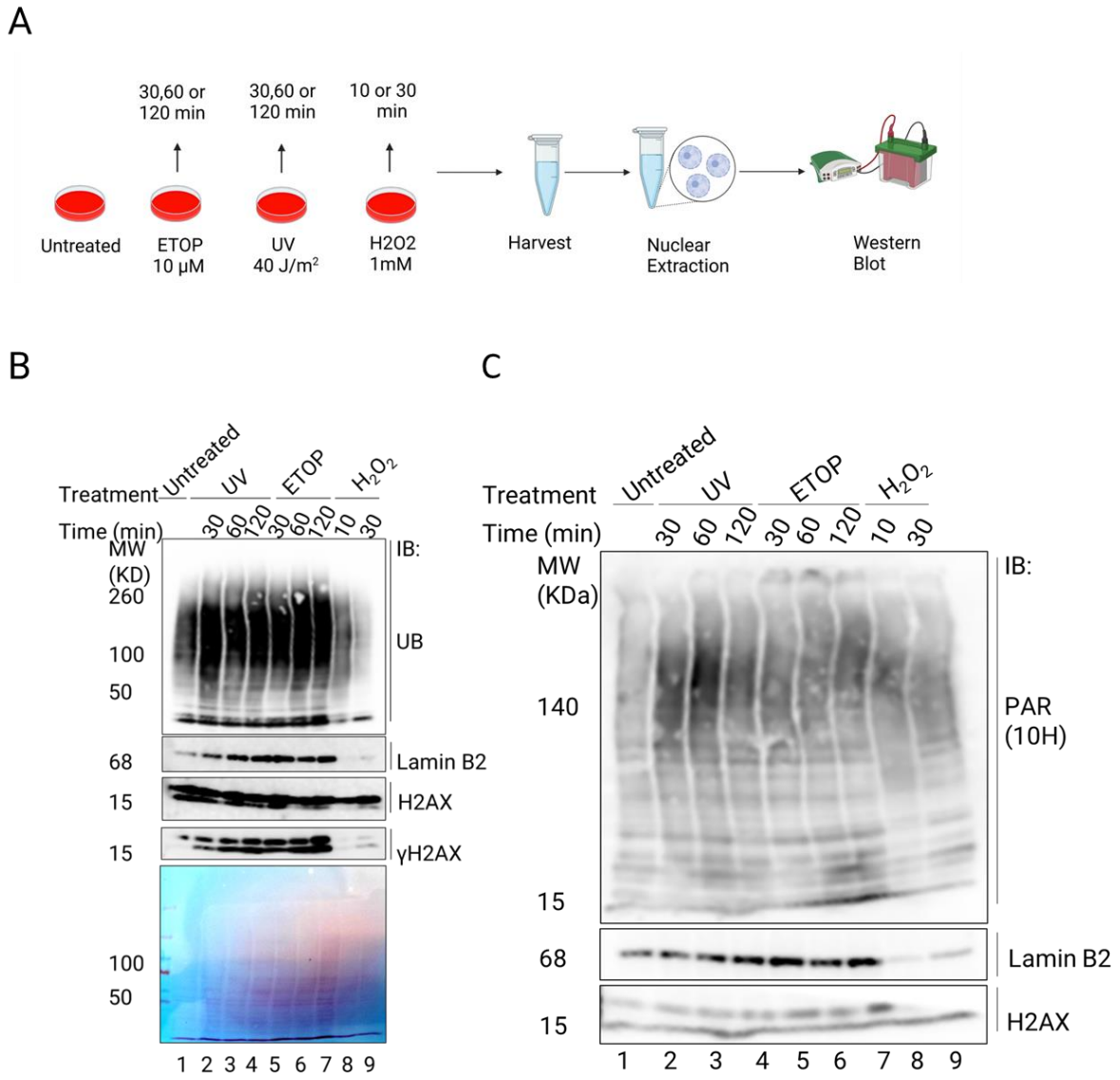

Figure 3.2. The effect of different DNA damaging agents on the levels of nuclear ubiquitin and PAR. A. *Schematic overview of the experimental procedure where 293T cells were treated with Etop (10μM), UV (40J/m^2) for 30, 60, or 120 min or H2O2 (1mM) for 10 or 30 min. Created with BioRender.com* ***B-C*** *Cells were collected, and the nuclei were extracted and blotted for ubiquitin (B) and PAR (C) in the nuclei using the antibodies for ubiquitin (Santa Cruz sc-8017) and PAR (EMD Millipore #AM80-100UG). γH2AX was blotted for using γH2AX (Cell Signaling Technology #80312) antibody. Lamin B2 and H2AX were used as a loading control and were blotted for using antibodies for Lamin B2 antibody (Cell Signaling Technology #13823) and H2AX (Cell Signaling Technology#2595). Ponceau S staining of the ubiquitin membrane is depicted.*

To complement the Western blot analysis that reflects the levels of ubiquitination and PARylation across the total cell population in the culture, confocal Immunofluorescence imaging (IF) was performed to investigate the cellular effects of etoposide and UV treatment on these PTMs. To achieve this goal, U2OS cells were treated with either UV (40 J/m^2) or etoposide (10 μM) for 2h. The cells were then fixed and incubated with primary and fluorescent secondary antibodies to stain for PAR, ubiquitin, and γH2AX (Table 2.7) which is the marker for DNA damage (Sharma et al., 2012). The nuclei were stained with Hoechst stain.

Figure 3.3 illustrates PAR, ubiquitin, and γH2AX signals in the untreated control cells and cells treated with UV or etoposide. As expected, compared to untreated cells, both etoposide and UV treatments induced strong γH2AX signals (Figure 3.3 right panel), which appeared as punctate nuclear staining, consistent with its role in marking DNA damage foci at sites of DNA lesions (Burma et al., 2001).

For PARylation in the untreated cells, the PAR signals were primarily localized in the cytoplasm (Figure 3.3 left panel). However, upon treatment with etoposide and UV, PAR signals were observed predominantly in the nucleus. In contrast, the distribution of ubiquitination detected by ubiquitin antibody FK2 (Figure 3.3 middle panel), appears to be in both cytoplasmic and nucleus. Following UV-induced damage, the nuclear staining of ubiquitination became slightly more prominent. In the etoposide treated cells, the ubiquitination signals showed punctate staining, similar to what was observed for γH2AX marked DNA damage foci.

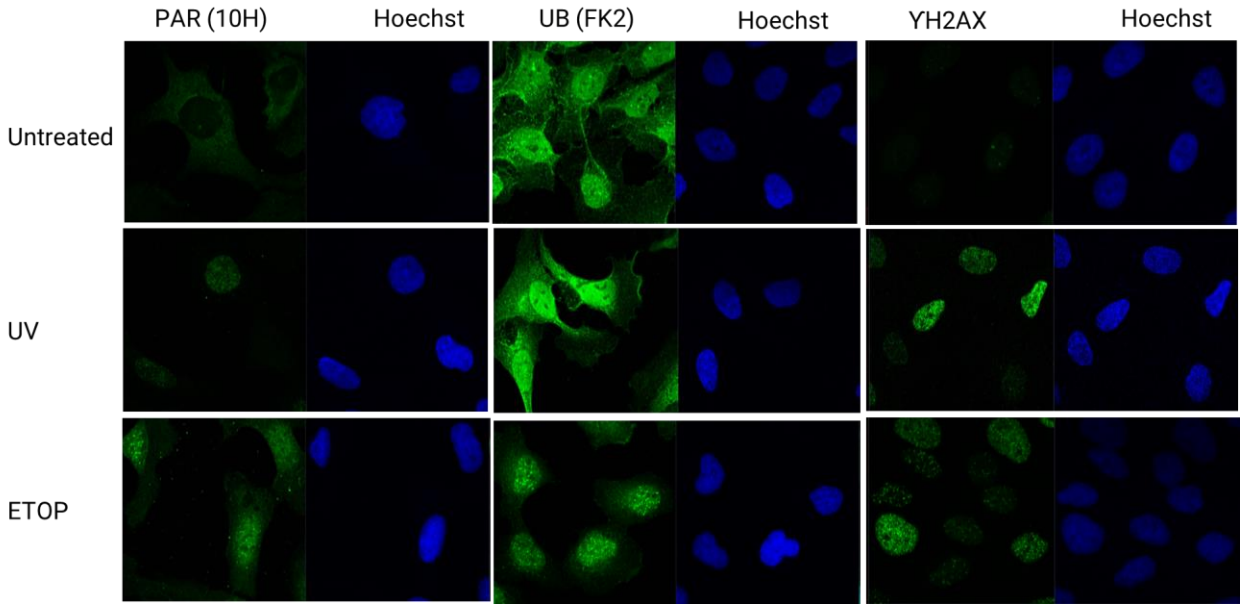

Figure 3.3. The effect of different DNA damaging agents on cellular PAR and ubiquitin. *Immunofluorescence (IF) was used to investigate cellular PAR and UB in U20S cells under etoposide (ETOP) (10 μM) and UV (40 J/m^2) treatments. PAR and UB were stained with PAR (EMD Millipore #AM80-100UG) and Ubiquitin (EMD Millipore # St-1200-100UG) antibodies. The nuclei were stained with Hoechst stain. γH2AX was stained using γH2AX (Cell Signaling Technology #80312) antibodies.*

3.1.2 Profiling cellular ubiquitination and ADP-ribosylation under E1 and PARP Inhibitors

There is growing evidence suggests a functional crosstalk between ubiquitination and ADP-ribosylation (H. C. Kang et al., 2011; Liu et al., 2013; Z. Wang et al., 2012; Yan et al., 2013). This prompted me to test whether inhibiting one pathway (ubiquitin or ADP-ribose) would affect the levels of the other PTM. To inhibit ubiquitination, the Ub-activating enzyme E1 inhibitor PYR41 (15 μM) was used (Figure 3.4 A). Two different PARP inhibitors (PARPi) were used to inhibit PARylation, PJ34 (10μM) or Olaparib (50μM). I performed Western blot analysis for ubiquitination and ADP-ribose (MAR/PAR) of the TCL. Surprisingly, the use of 15 μM PYR41 increased the levels of ubiquitination (Figure 3.4 B, lane 3-4 and lane 7-8) instead of reducing its levels. When testing higher concentrations of the PYR41, namely, 35 μM and 50 μM, it led to cell death (Data not shown). This suggests that the compound PYR41 might be toxic to the 293T cells used in this study and the reason for the increased ubiquitination is not clear. However, PYR41 at 15 μM greatly increased the levels of ADP-ribose in UV-untreated cells, and a similar observation was found with UV treatment alone (Figure 3.4 C lanes 3&5). Interestingly, combining PYR41 with UV treatment did not further enhance ADP-ribose levels (Figure 3.4 C Lane 7). This suggests PYR41 and UV treatment converge on the same cellular ADP-ribose response.

As shown in Figure 3.4 C, the use of PJ34 or Olaparib led to a decrease in the levels of ADP-ribosylation in the cells with Olaparib showing a better effect, consistent with their roles in inhibiting PARP1 activity. Using PARPi did not affect the levels of ubiquitination in UV-untreated or treated cells (Figure 3.4 B). Collectively, this set of experiments did not provide clear evidence of functional crosstalk between ubiquitination and ADP-ribosylation.

Together, the results from the total cell profiling and individual cell imaging revealed the dynamic and differential response of ubiquitination and ADP-ribosylation to DNA damage. Further research was performed to investigate the role WWE-tUBM plays in the recognition of these signals.

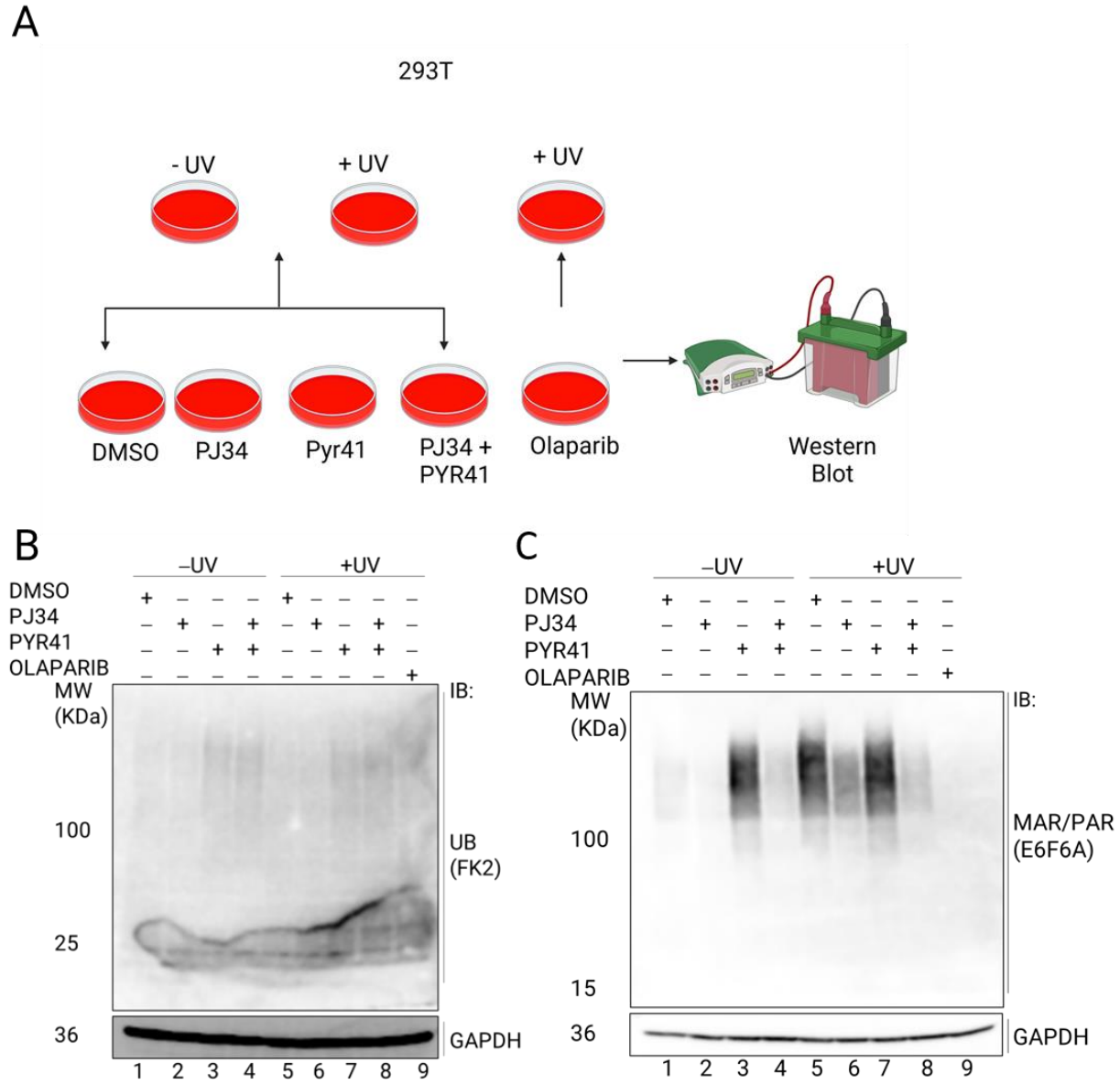

Figure 3.4. Inhibition of ADP-ribosylation using inhibitors. A. *Schematic overview of the experiment on 293T cells. Cells were treated with either PJ34 (10μM), Olaparib (50μM), PYR41(15μM) or PJ34 and PYR41 overnight. Then, cells were either treated with UV (40J/m^2) for 2h or were untreated except for Olaparib which was only UV treated. Created with BioRender.com* ***B-C*** *Western blot for ubiquitin (B) and MAR/PAR (C) using ubiquitin (EMD Millipore # St-1200-100UG) and MAR/PAR (Cell Signaling Technology #83732), respectively. GAPDH was used as a loading control and was blotted for using antibody (Proteintech 60004-1).*

3.2. GST-WWE-tUBM pulls down ubiquitinated and ADP-ribosylated proteins

The HUWE1 WWE and tUBM were previously shown to interact with iso-ADPr/ADPr and ubiquitin biochemically (Khatun, 2017; Münzker et al., 2024; Z. Wang et al., 2012). However, their interactions with cellular ubiquitin and ADP-ribose (MAR/PAR) have not been well investigated. Particularly, since HUWE1 contains both WWE and tUBM domains, can HUWE1 recognize ubiquitin and MAR/PAR simultaneously? To answer these questions, I performed GST pulldown assays using a recombinant GST-tagged WWE-tUBM fusion protein (GST-WWE-tUBM) against 293 T cell lysates. Figure 3.5 illustrates the workflow of this approach. This includes the following main steps: 1) creation of GST-WWE-tUBM plasmid construct encoding for a recombinant GST-tagged WWE-tUBM domains fusion protein; 2) purification of GST-WWE-tUBM fusion protein; 3) GST pulldown assays to investigate cellular proteins that interact with HUWE1 WWE and tUBM; and 4) detection of cellular proteins that interact with HUWE1 WWE and tUBM using Western blot or MS.

To create the GST-WWE-tUBM construct, restriction enzyme cloning was used to subclone the WWE-tUBM fusion from a previously generated mCherry pcDNA3.1- NLS-WWE-tUBM plasmid into the pGEX-2tk vector to create GST fusion protein of WWE-tUBM (Figure 3.5). Specifically, WWE-tUBM was amplified by adaptor PCR where cut sites for NdeI and BamHI were added to the PCR products. Then, pGEX-2tk plasmid and the PCR products of WWE and WWE-tUBM were digested with NdeI and BamHI followed by a ligation reaction. The resulting plasmids were transformed into bacteria, single colonies were selected and screened for the inserts through colony PCR. The positive colonies were sent for sequencing to confirm the insertion of the right sequence. A similar approach was used to generate GST-WWE fusion. Figure 3.6 (A&B) illustrates the sequencing results for WWE and WWE-tUBM that were

inserted into pGEX-2tk which confirms the successful insertion of WWE and WWE-tUBM into the vector plasmids.

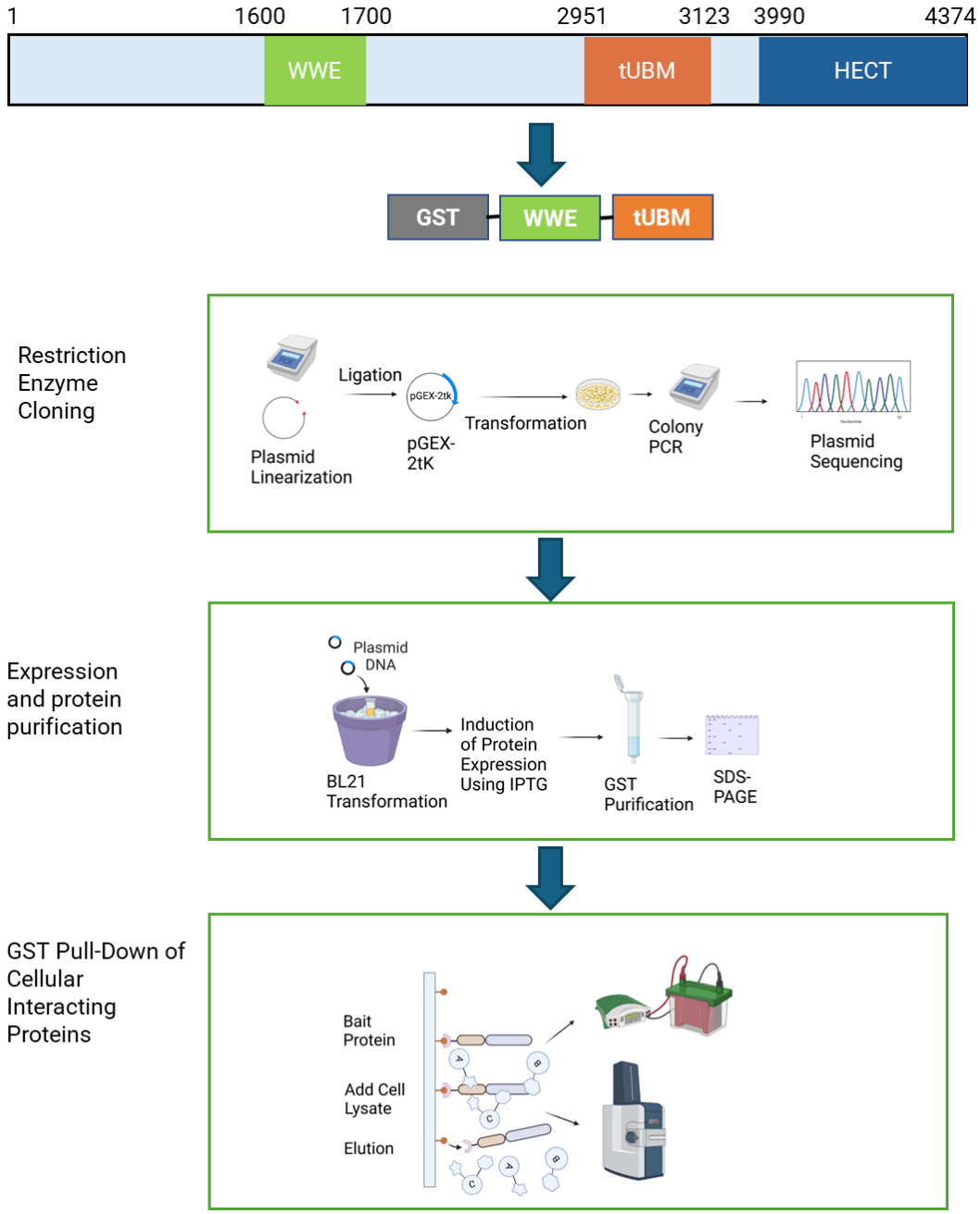

Figure 3.5. Overview of the GST pulldown approach. *To perform a GST pulldown, the WWE-tUBM domains were first cloned into the pGEX 2tk plasmid to generate GST-WWE-tUBM. The plasmid pGEX 2tk -WWE-tUBM was transformed into E.coli to express GST-WWE-tUBM fusion protein. The protein was then purified, and dialyzed. A pulldown assay was performed where the 293T cell lysate was added to the immobilized proteins and it was then followed by either running the eluted proteins for Western blot or sending for LC-MS/MS analysis. Bottom part of the graph is adpated and modified from "Protein interaction workflow", by biorender.com (2025). Created with BioRender.com.*

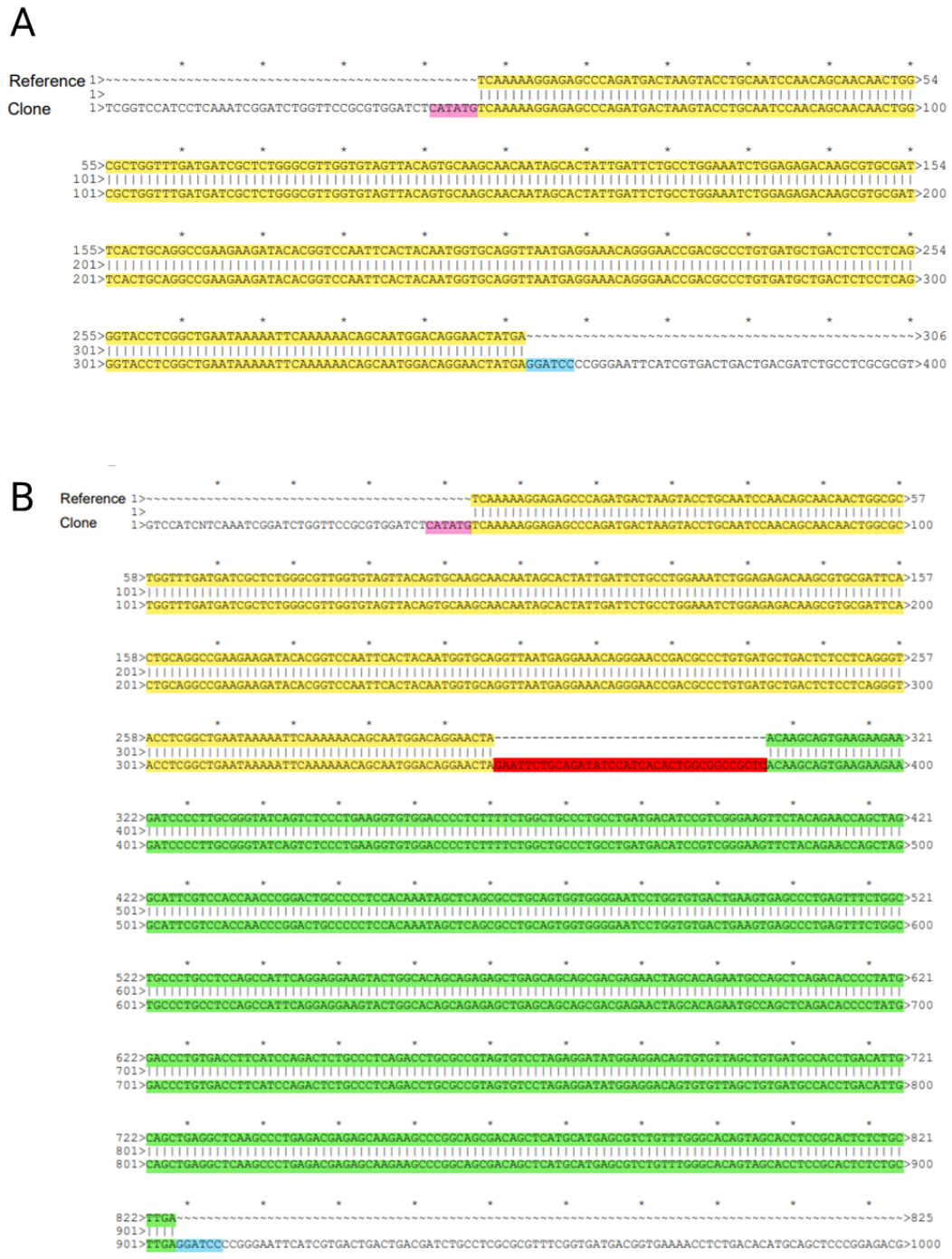

Figure 3.6. Cloning of WWE and WWE-tUBM into pGEX-2tk. ***A****. sequence alignment between reference HUWE1 WWE sequence and the cloned sequence for WWE.* ***B.*** *Sequence alignment between the WWE-tUBM HUWE1 reference sequence and the cloned sequence for WWE-tUBM where the WWE is colored in yellow and the tUBM colored in green. Pink and blue highlights indicate the cut sites of restriction enzymes NdeI and BamHI, respectively. The ApE software was used for sequence alignment (Davis & Jorgensen, 2022).*

To purify recombinant fusion proteins, the newly created GST-WWE and GST-WWE-tUBM plasmid were transformed into *E. coli* BL21 strain. Protein expression was induced with IPTG 1mM overnight at 18 degrees. The recombinant proteins were purified using standard GST-affinity chromatography (Figure 3.7 A&B).

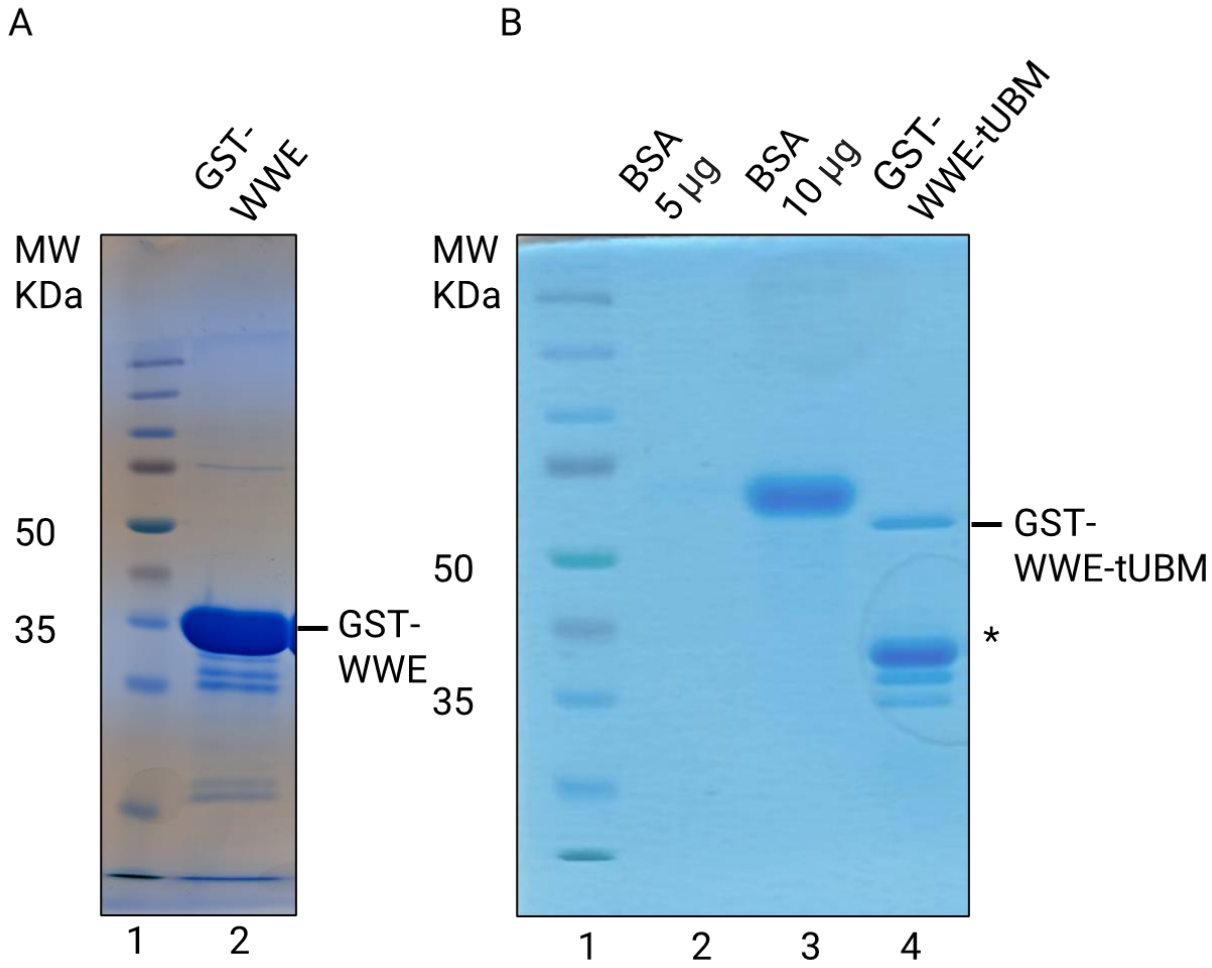

Figure 3.7. Purification of WWE and WWE-tUBM domains of HUWE1. A-B*. GST-WWE (A) and GST-WWE-tUBM (B) were expressed in and purified from BL21 E-coli. The purified proteins were run on SDS-PAGE gel to confirm proper purification. * Indicates degradation band corresponding to GST-WWE.*

Next, a GST pulldown assay was performed using GST-WWE-tUBM against TCL of 293T cells with or without UV ($40J/m^2$) treatment (Figure 3.8 A). GST was used as a negative control. As shown in Figure 3.8 (B&C), GST-WWE-tUBM interacts with both cellular ubiquitin and ADP-ribose. Ubiquitin was readily pulled down by GST-WWE-tUBM in the untreated and UV treated samples, whereas the negative control GST did not pulldown ubiquitin (Figure 3.8 B). As for ADP-ribosylation, I used an antibody that recognizes both MAR and PAR. Figure 3.8 C showed that GST-WWE-tUBM pulled down MARylated/PARylated proteins, but not GST alone.

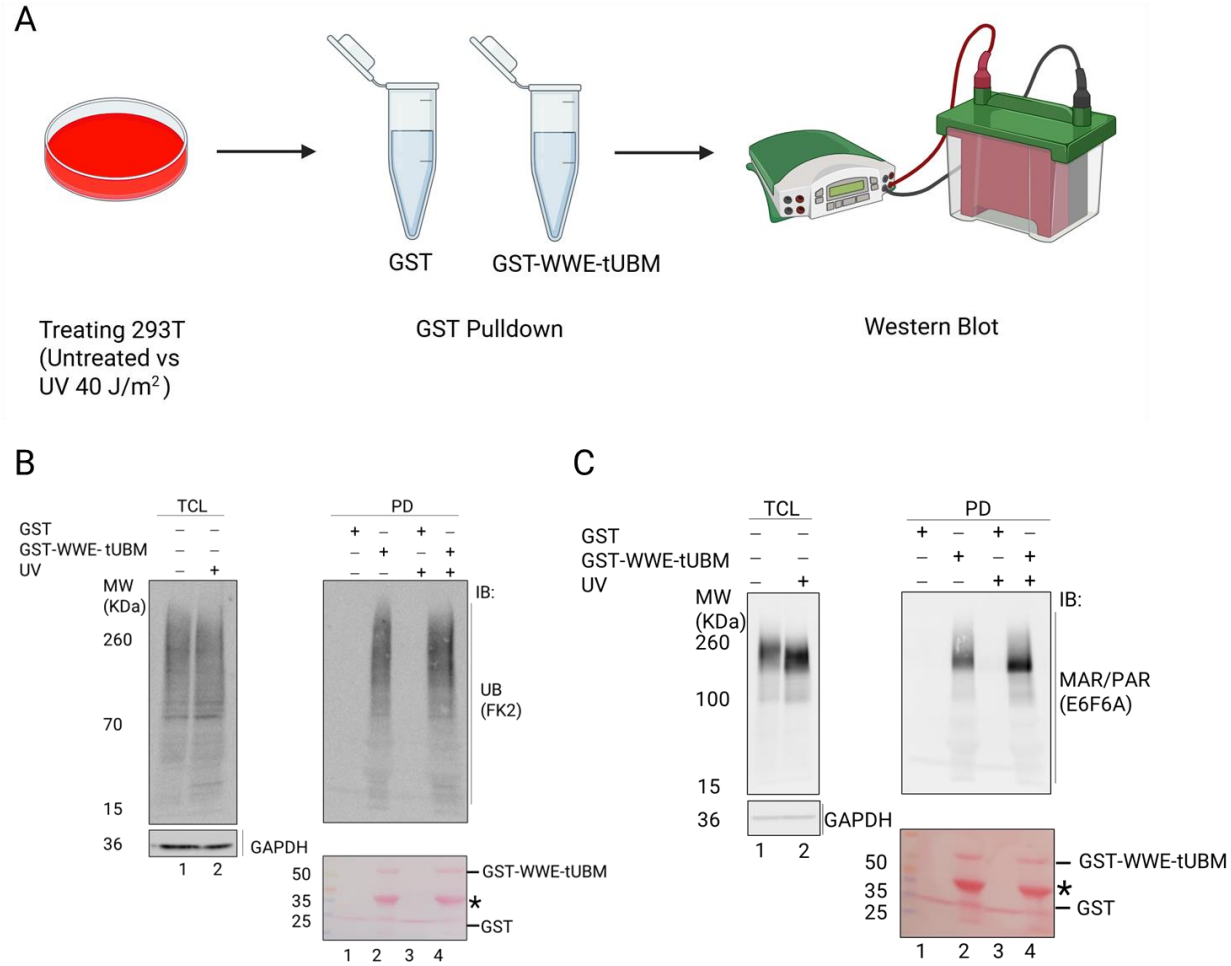

***Figure 3.8. GST-WWE-tUBM pulls down ubiquitinated and ADP-ribosylated proteins**. **A.** Schematic of the GST pulldown assay. 293T cells were treated with 40 J/m² UV or left untreated. TCL was used to perform GST pulldown with GST and GST-WWE-tUBM acting as bait proteins. The pulldown was followed by Western blotting. Created with BioRender.com **B.** Left, Input - ubiquitinated proteins in the TCL. Top Right, ubiquitinated proteins pulled down by GST or GST-WWE-tUBM blotted using ubiquitin antibody (Cayman Chemistry #14220). **C** Left, Input - ADP-ribosylated proteins in the TCL. Top Right, ADP-ribosylated proteins pulled down by GST or GST-WWE-tUBM using MAR/PAR antibody (Cell Signaling Technology # 83732). In Both B and C, GAPDH was used as a loading control blotted using an antibody (Proteintech #60004-1). Ponceau S staining of the membranes shows GST and GST-WWE-tUBM proteins. *: the degradation band in the WWE-tUBM fusion protein lane matches the molecular weight of the GST-WWE.*

Previously, HUWE1 WWE domain has been shown to bind iso-ADPr (Figure 1.3 B); however, a new report has shown its ability to interact with ADPr biochemically, suggesting it could also bind both MAR and PAR (Münzker et al., 2024; Z. Wang et al., 2012). To further investigate the ability of HUWE1 in recognizing different forms of ADP-ribose modification, I reblotted the UV treated pulldown samples for specific MAR or PAR signals using their respective antibodies. Figure 3.9 B illustrates that the GST-WWE-tUBM pulls down both MAR and PAR. This is the first time that HUWE1 was shown to interact with both cellular mono- and poly-ADP-ribosylation.

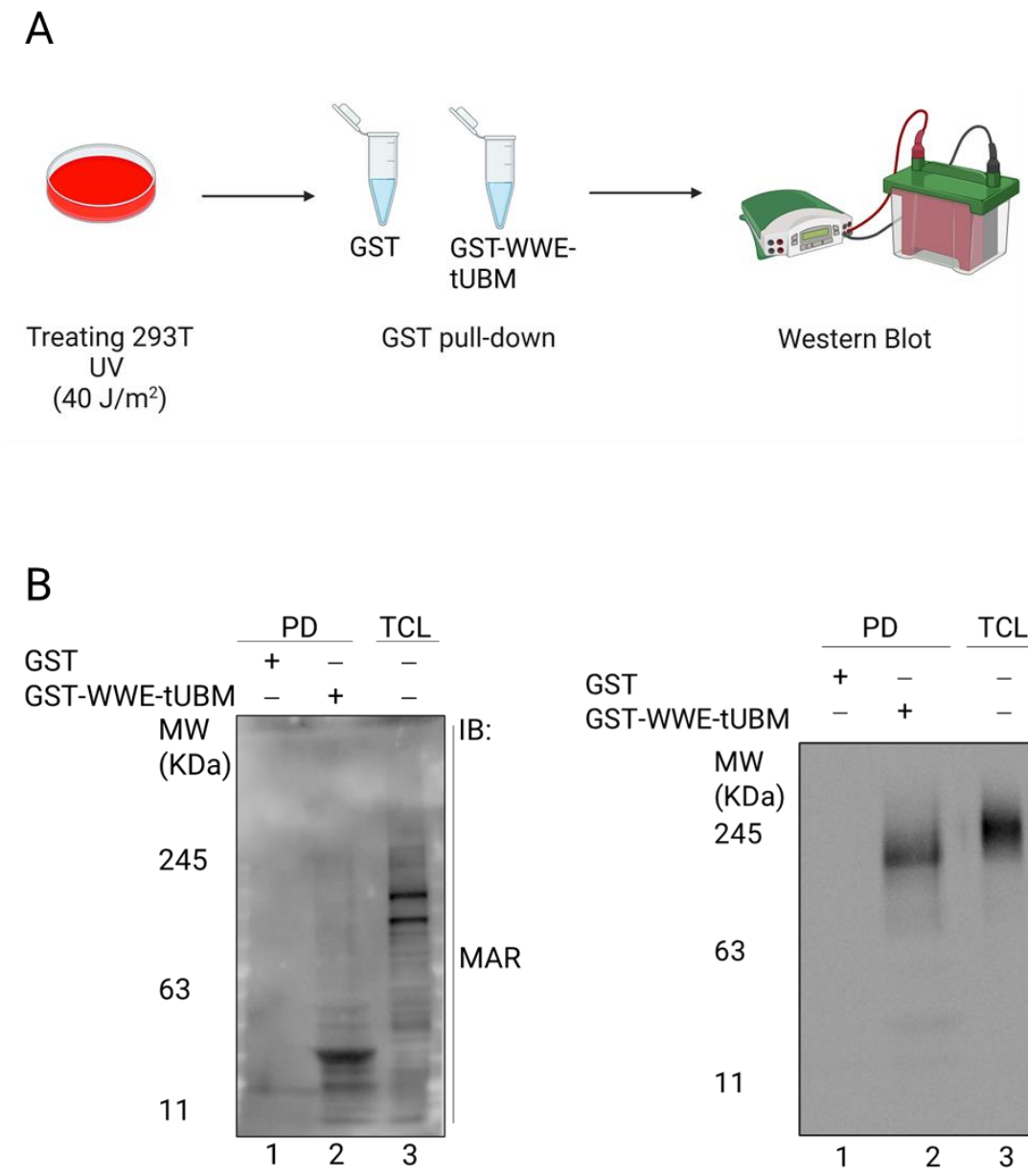

Figure 3.9. GST-WWE-tUBM pulls down MARylated and PARylated proteins. A. *Schematic of the GST pulldown assay. 293T cells were treated with 40 J/m^2 UV. TCL was used to perform GST pulldown with GST and GST-WWE-tUBM acting as bait proteins. The pulldown was followed by Western blotting. Created with BioRender.com* ***B.*** *Left blot for MARylated and Right blot for PARylated proteins pulled down by GST and GST fusion protein in UV treated cells blotted for using MAR (Sigma MABE #1076) and PAR (R&D Systems #4335-MC-100) antibodies, respectively.*

Moreover, to further examine the specificity of HUWE1 WWE and tUBM domains in binding respective ubiquitin and ADP-ribose signals, the GST-HUWE1 WWE domain was used as an additional control in the pulldown experiment. The 293T cells were also treated with Olaparib (50 μM) or vehicle control DMSO overnight and then subjected to UV treatment (40 J/m^2) (Figure 3.10 A) to generate TCL with varied amount of ADP-ribosylation signal. Moreover, I came across a report mentioning that sample preparation involved sonication would shear up the DNA and result in non-physiological ADP-ribosylation (Jungmichel et al., 2013), in the following experiments, the lysis IP buffer was supplemented with PARPi PJ34 (10 μM) to prevent sample processing induced non-physiological ADP-ribosylation.

As shown in Figure 3.10 B, ubiquitin was pulled down only by GST-WWE-tUBM, but not by GST-WWE or GST alone, supporting ubiquitin binding specificity of the tUBM domain. Moreover, inhibiting ADP-ribosylation did not affect the pulldown of ubiquitin (Figure 3.10 B).

As expected, Olaparib treatment reduced cellular ADP-ribose (MAR/PAR) in total cell lysate compared to the DMSO control (Figure 3.10 C). Figure 3.10 C showed that both GST-WWE-tUBM and GST-WWE efficiently bound cellular MAR/PAR and the amount of bound ADP-ribose reflected Olaparib induced decrease in ADP-ribose levels.

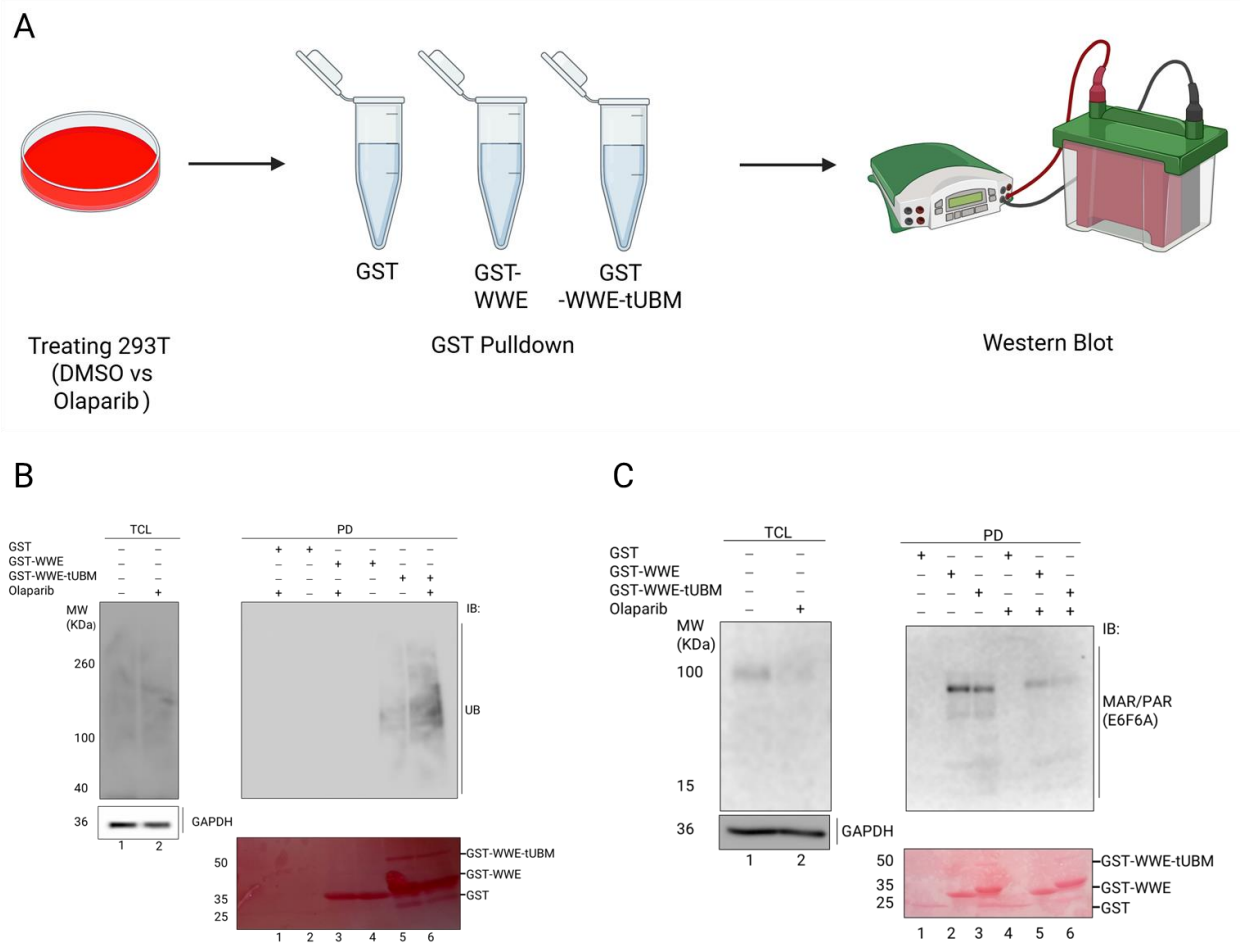

Figure 3.10. The specificity of tUBM and WWE binding to ubiquitin and ADP-ribose. ***A****. Schematic of the pulldown experiment. 293T cells were treated with Olaparib (50μM) or DMSO overnight. Cells were then treated with UV (40J/m^2) for 2h. The TCL was then added to the bait proteins GST, GST-WWE and GST-WWE-tUBM. Created with BioRender.com* ***B.*** *Left-input ubiquitinated proteins in the TCL. Right - ubiquitinated proteins pulled down by GST, GST-WWE, or GST-WWE-tUBM, blotted using ubiquitin antibody (Santa Cruz #sc-8017).* ***C.*** *Left-input ADP-ribosylated proteins in the TCL. Right-ADP-ribosylated proteins pulled down by GST, GST-WWE or GST-WWE-tUBM blotted using MAR/PAR antibody (Cell Signaling Technology #83732). In B and C, GAPDH was used as a loading control blotted using an antibody (Proteintech 60004-1). Ponceau S staining of the membranes shows GST, GST-WWE and GST-WWE-tUBM proteins.*

3.3 MS analysis of WWE-tUBM interactome

To investigate the cellular interacting proteins of the HUWE1 WWE and tUBM domain, GST pulldown assay was performed followed by mass spectrometry (Figure 3.5). 293 T cells were treated with UV (40 J/m^2) for 2h, and the lysates were subject to a GST pulldown using GST tagged WWE-tUBM fusion protein. The interacting proteins were then digested by trypsin and sent for MS analysis. The pulldown was performed in two biological replicates. The first biological replicate was run twice, designated as Run 1 with two injection replicates, and Run 2 with four injection replicates (rerun of the first biological replicate). The second biological replicate was designated as Run 3 with four injection replicates.

Table 3.1 B shows an overview of these three MS runs including (1) **the number of peptide spectral match (PSMs)**- the sum of matched spectral count found in each injection replicate; (2) **number of peptides**- the sum of the peptides being identified in each injection replicate; and (3) **number of proteins**- the sum of proteins inferred from the identified peptide sequences, in the GST and GST-WWE-tUBM across different injection replicates. The numbers depicted are the average of the injection replicates of each run.

A

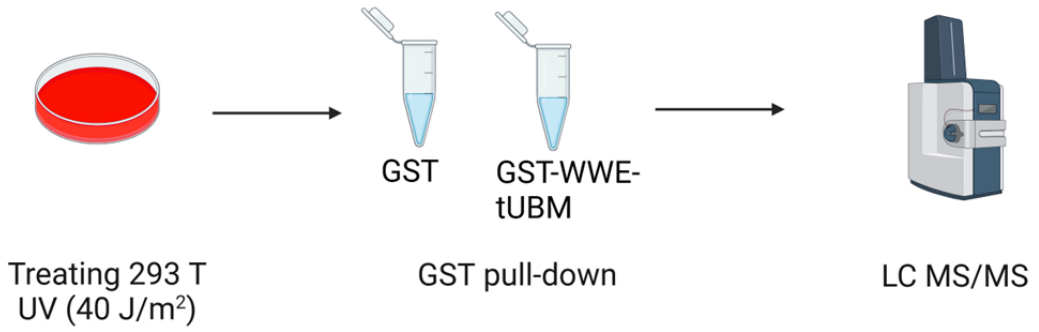

B

	Run 1		Run 2		Run 3	
	GST	**GST-WWE-tUBM**	**GST**	**GST-WWE-tUBM**	**GST**	**GST-WWE-tUBM**
# PSMs	2706	13346	4011	14777	5501	13866
# Peptides	2635	8985	4256	12172	5911	11777
# Proteins	755	2665	1048	2775	1816	3354

Table 3.1. Overview of different MS runs. ***A****. Schematic of the GST pulldown assay. 293T cells were treated with 40 J/m² UV. TCL was used to perform GST pulldown with GST and GST-WWE-tUBM acting as bait proteins. The pulldown was followed by MS.* ***Created with BioRender.com B****. The table depicts the average number of PSMs, peptides and proteins in GST and GST-WWE-tUBM between different runs of MS.*

3.3.1. MS detection of the ubiquitinated and/or ADP-Ribosylated peptides pulled down by HUWE1 WWE-tUBM

To gain an insight regarding the ability of the HUWE1 WWE and tUBM domains to pull down the ubiquitin and/or ADP-ribose modified proteins, I analyzed the MS results focusing on the modified peptides found in GST versus GST-WWE-tUBM.

It has been established that when trypsin digests ubiquitinated proteins, ubiquitin leaves a diglycine remnant (GG) on the modified peptides (Shi et al., 2011). The remnant has a mass shift of +114.0429Da that can be detected using the MS (Shi et al., 2011).

Similarly, the addition of MAR/PAR to peptides would lead to a distinct mass shift that the mass spectrometer would be able to detect. A MAR moiety will result in a +541.0611Da shift (Martello et al., 2016). To detect PARylation, the mass shifts of 2 and 3 MAR moieties are +1082.1222 and +1623.1833Da, respectively.

Figure 3.11 B compared the number of ubiquitinated and ADP-ribosylated peptides between GST and GST-WWE-tUBM. When looking at the number of ubiquitinated peptides containing K-GG, which is searched by +114.0429Da mass shift on a lysine, as expected, the GST-WWE-tUBM domain constantly pulled down more ubiquitinated peptides than the GST control (Figure 3.11 B). Moreover, GST-WWE-tUBM pulled down more ADP-ribosylated peptides as well as ADP-ribose and K-GG dual modifications, compared to the GST control (Figure 3.11 B). This supports the Western blot data in confirming the ability of WWE-tUBM to interact with ubiquitin and ADP-ribose.

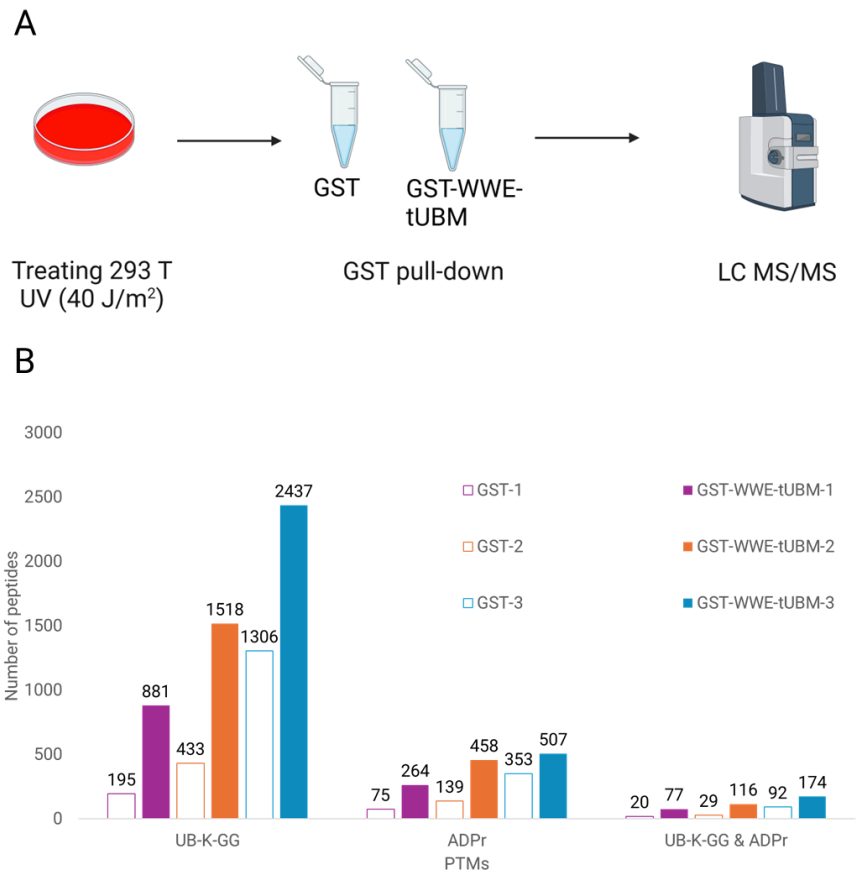

Figure 3.11. GST-WWE-tUBM pulls down modified peptides. ***A****. Schematic of the GST pulldown assay. 293T cells were treated with 40 J/m^2 UV. TCL was used to perform GST pulldown with GST and GST-WWE-tUBM acting as bait proteins. The pulldown was followed by trypsin digestion and MS analysis. Created with BioRender.com* ***B.*** *The graph depicts the number of modified peptides that are pulled down in the GST and GST-WWE-tUBM. UB-K-GG includes the peptides that harbor the diglycine ubiquitin remnant on their Lysine with the mass shift of +114.0429Da. ADP-ribose includes peptides modified with MAR/PAR with a mass shift of +541.0611Da, +1082.1222Da or +1623.1833Da. UB-K-GG & ADP-ribose contains peptides that contain both modifications.*

3.3.2. WWE-tUBM pulls down ubiquitin peptides and K48-linked chain

Since WWE-tUBM pulls down ubiquitinated proteins/peptides, I further investigated the type of ubiquitin modification being pulled down by WWE-tUBM. To achieve that, I used the intensity of the peptides, which are inferred from the area under the curve of the peptide intensity (W. Zhu et al., 2010) to calculate the peptide intensity of ubiquitin peptide and poly-ubiquitin from the GST control and GST-WWE-tUBM pulldown sample groups. Specifically, the ubiquitin peptide (unmodified) intensity was calculated based on the intensity of the peptide sequences that belong to ubiquitin with Uniprot ID P62979. For poly-ubiquitin chains, the intensity for ubiquitin peptides that are modified by +114.0429Da on their Lysine (i.e. Ub-lysine residues-linked GG) was calculated.

Despite the high background of ubiquitin peptides in the GST, the GST-WWE-tUBM showed higher intensity for these peptides (Figure 3.12 A). Importantly, poly-ubiquitin signals as indicated by the K-GG modified ubiquitin peptides were found only in GST-WWE-tUBM, not in the GST control (Figure 3.12 A), suggesting GST-WWE-tUBM has a more specific affinity for poly-ubiquitin chains.

Moreover, the fragmentation spectrum for the modified ubiquitin was extracted to investigate the ubiquitin linkage modification more closely. The linkage depicted in the spectrum is K48 since it happens at Lysine 48 of ubiquitin, which was the only linkage found to be pulled down by GST-WWE-tUBM (Figure 3.12 B). Moreover, the fragmentation spectrum of the modified ubiquitin peptide supports the presence of this modification. Figure 3.12 (B&C) depicts the fragmentation spectrum and ion table for fragment ions of K48-modified ubiquitin peptide. Moreover, the site of the modification can be inferred from the spectrum where a mass of 114.0429 Da resulting from the diglycine remnant is added to the mass of the modified Lysine

(Peng et al., 2003). This could be exemplified by looking at the b5 and b6 ions from the fragmentation spectrum of the ubiquitin peptide. The m/z for b5 (502.30) represents the mass of the LIFAG amino acid sequence of ubiquitin. The m/z for b6 (744.44) represents the mass of LIFAGK and the diglycine remnant on the modified Lysine.

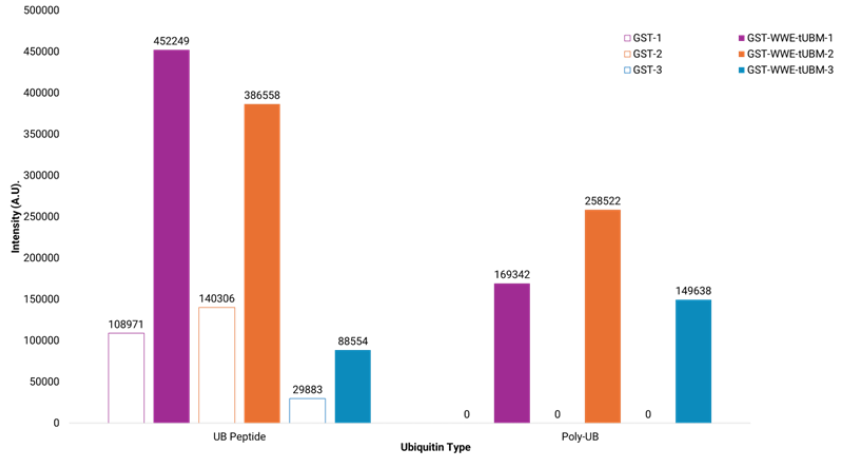

B

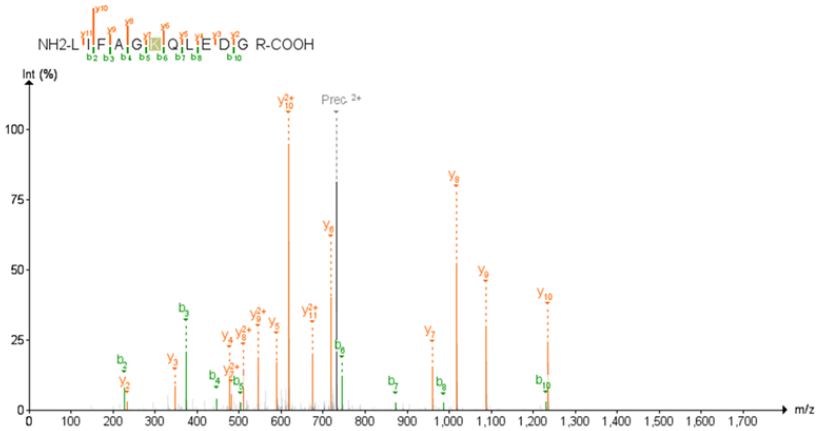

C

	b	b++	AA	y	y++	
1	114.09	57.55	L			12
2	227.18	114.09	I	1347.70	674.35	11
3	374.24	187.63	F	1234.62	617.81	10
4	445.28	223.14	A	1087.55	544.28	9
5	502.30	251.65	G	1016.51	508.76	8
6	744.44	372.72	K	959.49	480.25	7
7	872.50	436.75	Q	717.35	359.18	6
8	985.58	493.30	L	589.29	295.15	5
9	1114.63	557.82	E	476.21	238.61	4
10	1229.65	615.33	D	347.17	174.09	3
11	1286.67	643.84	G	232.14	116.57	2
12			R	175.12	88.06	1

Figure 3.12. WWE-tUBM pulls down ubiquitin peptides and K48 linked polyubiquitin. ***A****. Depiction of a comparison between the intensity of ubiquitin peptides and polyubiquitin between GST and GST-WWE-tUBM.* ***B****. Fragmentation spectrum of ubiquitin peptide extracted from the Fragpipe PDV viewer* (K. Li et al., 2019). ***C.*** *The ion table of the ubiquitin peptide. The colored cells contain the ions detected in the fragmentation spectrum.*

It is noted that although the +114.043 Da mass shift is highly characteristic of ubiquitination, it can sometimes arise from other modifications such as NEDD8 or ISG15, which both have the same C-terminal sequence as ubiquitin, or experimental artifacts to produce false positive results (Akimov et al., 2018; Vertegaal, 2011; G. Xu & Jaffrey, 2013). For example, it has been reported that the IAA alkylation as a part trypsin digestion process could introduce artificial modifications at 114 Da (Vertegaal, 2011; G. Xu & Jaffrey, 2013). To Increase confidence in ubiquitination identification of this study, I searched for presence of LRGG (+383.2281 Da) mass shift on the modified peptides in run 2. This is because during digestion with trypsin, ubiquitin can sometimes leave a longer remnant (LRGG) due to miscleavage resulting in the mass shift of +383.2 Da (Denis et al., 2007; Warren et al., 2005) (Figure 3.13 A). This LRGG remnant, despite being less common, is highly specific for ubiquitin, as it enables the differentiation between ubiquitin and many other modifications that do not generate the same mass shift.

One of the peptides that was shown to be modified by LRGG was the ubiquitin peptide. Figure 3.13 (B&C) illustrates the fragmentation spectrum and ion table for LRGG modified ubiquitin. The modification was found on K48 which further supports that WWE-tUBM pulls down K48 linked ubiquitin chains as was shown in Figure 3.12 (B&C)

A

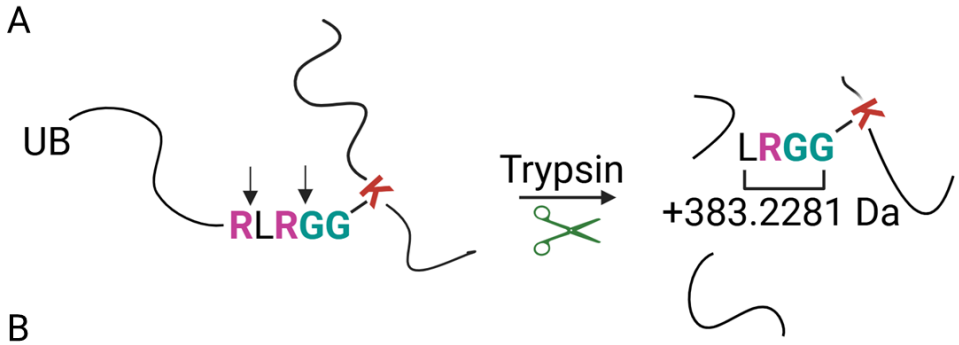

B

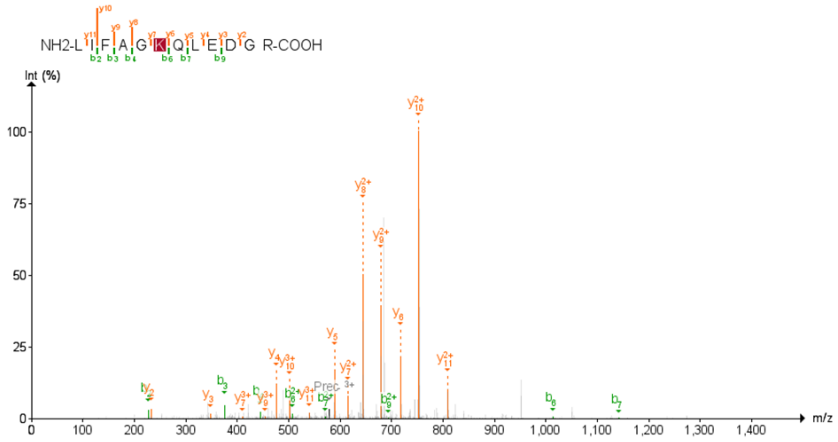

C

	b	b++	AA	Y	y++	
1	114.09	57.55	L			12
2	227.18	114.09	I	1616.89	808.95	11
3	374.24	187.63	F	1503.80	752.40	10
4	445.28	223.14	A	1356.73	678.87	9
5	502.30	251.65	G	1285.70	643.35	8
6	1013.63	507.32	K	1228.68	614.84	7
7	1141.68	571.35	Q	717.35	359.18	6
8	1254.77	627.89	L	589.29	295.15	5
9	1383.81	629.41	E	476.21	238.61	4
10	1498.84	749.92	D	347.17	174.09	3
11	1555.86	778.43	G	232.14	116.57	2
12			R	175.12	88.06	1

Figure 3.13. LRGG remnant confirms the ability of WWE-tUBM to interact with K48 linkage. ***A.*** *Schematic depicting trypsin digestion of proteins modified by ubiquitin which will lead to either GG or LRGG remnant (miscleavage). The arrows indicate the digestion sites for trypsin Created with BioRender.com* ***B.*** *Fragmentation spectrum of ubiquitin peptide extracted from the Fragpipe PDV viewer (K. Li et al., 2019).* ***C.*** *The ion table of the ubiquitin peptide. The colored cells contain the ions detected in the fragmentation spectrum.*

Interestingly, this study identified non-lysine modified peptides that were pulled down by WWE-tUBM. Figure 3.14 A and B showed Lysine and non-lysine linked ubiquitinated peptides pulled down by GST-WWE-tUBM identified by the GG or LRGG remnants. Specifically, when looking at the peptides modified by GG, it was shown that WWE-tUBM pulls down a total of 6830 modified peptides compared to 1495 peptides being pulled down by GST. These peptides were not only modified on their Lysine but also on their Serine, Threonine and Cysteine. Searching for LRGG remnant supported the conclusion that WWE-tUBM pulls down non-lysine ubiquitination. Specifically, GST-WWE-tUBM pulled down 582, 1592, 884, and 495 of K-LRGG, S-LRGG, T-LRGG and C-LRGG modified peptides, respectively, which was higher than the number of peptides being pulled down by GST for these modifications (Figure 3.14 B).

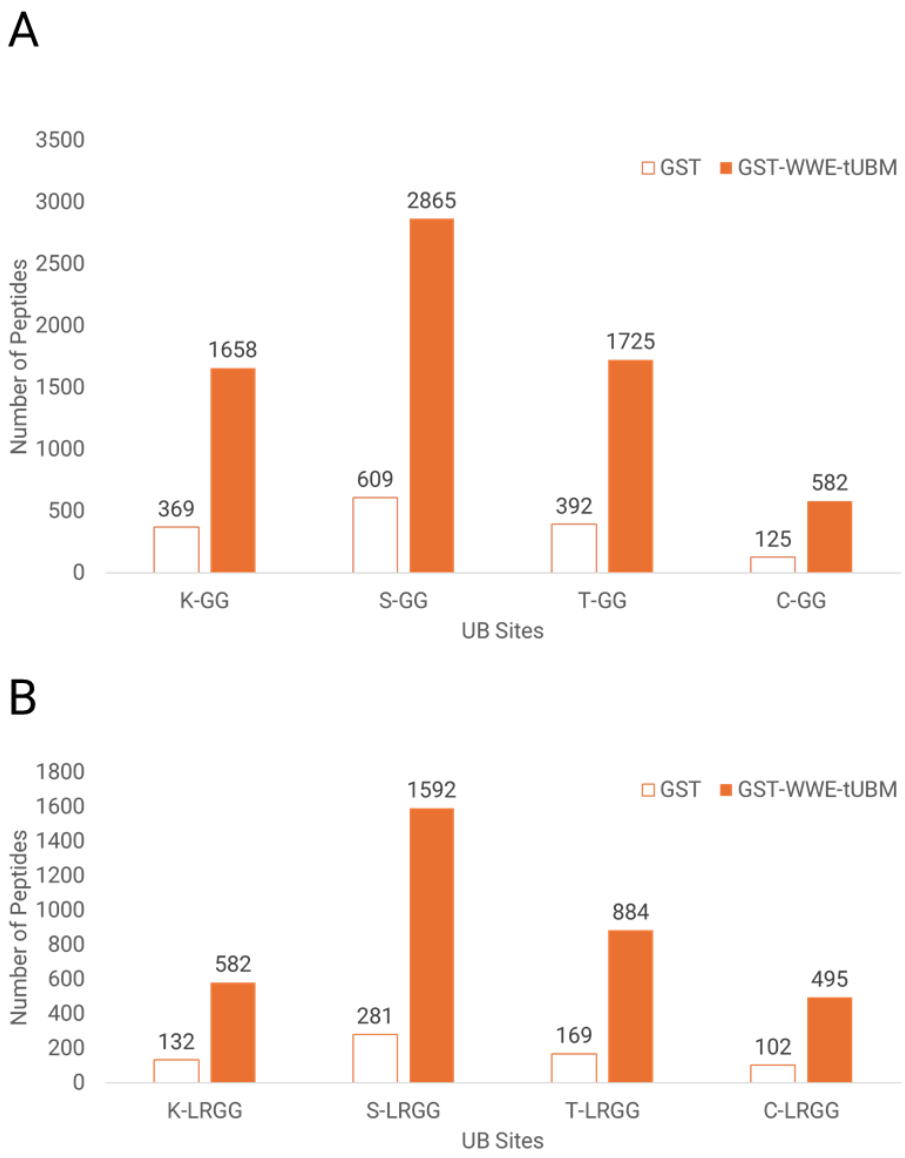

Figure 3.14. GST-WWE-tUBM pulls down Lysine and non-lysine linked ubiquitinated peptides. ***A.*** *The graph depicts the number of ubiquitinated peptides that contain the GG ubiquitin remnant pulled down by GST and GST-WWE-tUBM. K-GG, S-GG, T-GG, and C-GG refer to peptides that contain the GG remnant linked to Lysine, Serine, Threonine, and Cysteine, respectively.* ***B.*** *The graph depicts the number of ubiquitinated peptides that contain the LRGG ubiquitin remnant pulled down by GST and GST-WWE-tUBM. K-LRGG, S-LRGG, T-LRGG, and C-LRGG refer to peptides that contain the LRGG remnant linked to Lysine, Serine, Threonine, and Cysteine, respectively.*

3.2.3. MS identified WWE-tUBM domain interacting proteins

The interaction between HUWE1 WWE and tUBM domains with ADPr and ubiquitin, respectively (Khatun, 2017; Münzker et al., 2024) would enable it to interact with its targets by binding these PTMs using its reader domains. Therefore, the protein interactome of the WWE-tUBM domains might represent the potential target proteins of HUWE1.

To check the proteins modified by K-UB and/or ADP-ribose that interact with WWE-tUBM, I looked at the proteins that contain peptides that harbor these modifications that are being pulled down by WWE-tUBM. To enrich the proteins specifically interact with WWE-tUBM and not the GST tag, I calculated Log2 FD, which is the Log2 of average protein intensity in WWE-tUBM group over average intensity in the GST group. I included only the proteins with Log2FD≥2 (i.e. the intensity in the WWE-tUBM group is 4 or more folds than in GST group). Moreover, the proteins that were presented with FDR cutoff at 0.05 and each protein should at least contain two assigned peptides. By applying these criteria, 1314 proteins were reported from all runs (data not shown).

To get an insight into the processes, cellular components, and molecular function of the HUWE1 WWE-tUBM interacting proteins, Gene Ontology (GO) enrichment analysis was performed on K-UB and/or ADP-ribose modified proteins. The gene names of these proteins were entered to the enrichment tool at http://amp.pharm.mssm.edu/Enrichr (Chen et al., 2013; Kuleshov et al., 2016; Xie et al., 2021) and looked for the GO biological processes, cellular component and molecular function. The graphs in Figure 3.15 (A-C) illustrate the top ten enriched biological processes, cellular component and molecular function terms. All the presented terms are statistically significant with $P < 0.05$. There are many biological processes that are shown to be enriched in the WWE-tUBM interactome which reflects the involvement of

ubiquitination and ADP-ribosylation in many cellular processes. Cilium movement involved in cell motility and cilium dependent cell mobility biological processes contained proteins that are part of the dynein family of proteins (motor protein) such as dynein cytoplasmic 2 heavy chain 1 (Vaisberg et al., 1996) (Figure 3.15 A). Moreover, processes include ribosomal biogenesis and chromatin organization were also enriched (Figure 3.15 A). Moreover, when looking at cellular components, the terms for many nuclear compartments were shown to be enriched including nuclear lumen, nucleolus and the nucleus (Figure 3.15 B). Last, the molecular function where many of the enriched functions are related to RNA binding (mRNA, Single and double-strand RNA) (Figure 3.15 C).

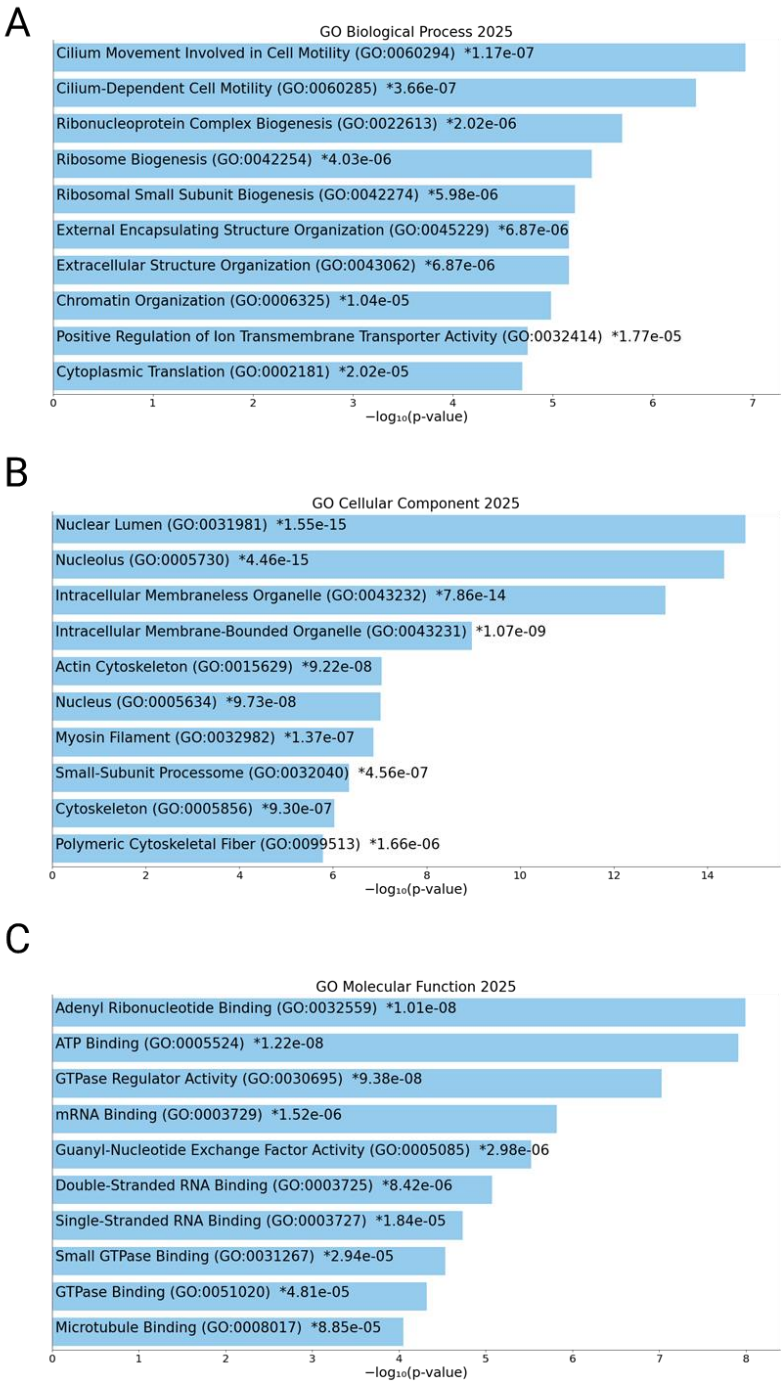

Figure 3.15. GO enrichment analysis of the WWE-tUBM interactome. Go analysis was performed for Lysine linked ubiquitinated and/or ADP-ribosylated proteins using Maayan lab tool (Chen et al., 2013; Kuleshov et al., 2016; Xie et al., 2021). **A-C** Top ten biological processes (A), cellular component (B) and molecular function (C) that are significantly enriched in WWE-tUBM interactome. The * indicates that the term has adjusted P value < 0.05.

Since the pulldown was done under DNA damaging treatment, I sought to highlight the proteins from the 1314-protein list that are involved in DNA damage. To achieve that, I highlighted the proteins that belong to biological processes terms related to DNA damage. Specifically, many DNA damage related processes were enriched in the GO analysis. For example, two of the biological processes that were enriched in the study were DNA repair (GO:0006281) and DNA damage response (GO:0006974) which had an overlap ratio of 29/302 and 38/421, respectively. DNA repair and DNA damage response had a P value of 0.01988 and 0.0215, respectively. Thus, since the GO analysis enables looking at the proteins contributing to each biological process, I highlighted all the proteins that are involved in DNA damage processes proteins in Table 3.2. The search for DNA damage related proteins resulted in 66 proteins. Although many of these proteins were shown in only one of the runs, some proteins showed in more than one run. These are proteins that could be investigated in the future as potential targets of HUWE1.

Table 3.2. Modified DNA damage proteins enriched in WWE-tUBM. *The table depicts DNA damage proteins that are enriched in the WWE-tUBM. The proteins are modified by K-UB and/or ADP-ribose. The proteins depicted contain at least 2 peptides mapped to them and log2 FD≥ 2.*

Protein Name	Run 1	Run 2	Run 3	Description
sp|P54277|PMS1_HUMAN	X	X		PMS1 protein homolog 1
sp|Q9HAY2|MAGF1_HUMAN	X			Melanoma-associated antigen F1
tr|E5RIC8|E5RIC8_HUMAN	X			MRN complex interacting protein
sp|Q5T890|ER6L2_HUMAN	X	X		DNA excision repair protein ERCC-6-like 2
sp|Q7Z333|SETX_HUMAN	X	X	X	Probable helicase senataxin
sp|Q7Z6E9|RBBP6_HUMAN	X			E3 ubiquitin-protein ligase RBBP6
sp|P38398|BRCA1_HUMAN	X			Breast cancer type 1 susceptibility protein
sp|Q86U86|PB1_HUMAN	X			Protein polybromo-1
sp|Q92499|DDX1_HUMAN		X		ATP-dependent RNA helicase DDX1
tr|H0Y4R8|H0Y4R8_HUMAN		X		SP100 nuclear antigen (Fragment)
sp|Q6NS38|ALKB2_HUMAN		X		DNA oxidative demethylase ALKBH2
sp|P06748|NPM_HUMAN		X		Nucleophosmin
sp|P46379|BAG6_HUMAN		X		Large proline-rich protein BAG6
sp|O94782|UBP1_HUMAN		X		Ubiquitin carboxyl-terminal hydrolase 1
sp|Q03468|ERCC6_HUMAN		X	X	DNA excision repair protein ERCC-6
sp|P13010|XRCC5_HUMAN		X		X-ray repair cross-complementing protein 5
sp|Q9NYF8|BCLF1_HUMAN		X		Bcl-2-associated transcription factor 1
sp|Q13573|SNW1_HUMAN		X		SNW domain-containing protein 1
sp|Q13018|PLA2R_HUMAN		X		Secretory phospholipase A2 receptor
sp|P51957|NEK4_HUMAN		X	X	Serine/threonine-protein kinase Nek4
sp|Q92900|RENT1_HUMAN		X		Regulator of nonsense transcripts 1
sp|Q96Q15|SMG1_HUMAN		X		Serine/threonine-protein kinase SMG1
sp|P46100|ATRX_HUMAN		X		Transcriptional regulator ATRX
sp|Q96QF7|GCNA_HUMAN		X		Germ cell nuclear acidic protein
sp|Q6WBX8|RAD9B_HUMAN		X		Cell cycle checkpoint control protein RAD9B
sp|Q96K58|ZN668_HUMAN		X		Zinc finger protein 668
sp|P42345|MTOR_HUMAN		X	X	Serine/threonine-protein kinase mTOR
sp|Q9C086|IN80B_HUMAN		X		INO80 complex subunit B
sp|Q14164|IKKE_HUMAN		X		Inhibitor of nuclear factor kappa-B kinase subunit epsilon
sp|Q96L91|EP400_HUMAN		X		E1A-binding protein p400
sp|P54132|BLM_HUMAN		X		RecQ-like DNA helicase BLM
sp|P51531|SMCA2_HUMAN		X		Probable global transcription activator SNF2L2
sp|Q7L590|MCM10_HUMAN			X	Protein MCM10 homolog
sp|Q68CP9|ARID2_HUMAN			X	AT-rich interactive domain-containing protein 2
sp|Q9Y3S1|WNK2_HUMAN			X	Serine/threonine-protein kinase WNK2
sp|Q16512|PKN1_HUMAN			X	Nuclear mitotic apparatus protein 1
sp|P07992|ERCC1_HUMAN			X	DNA excision repair protein ERCC-1
sp|P42285|MTREX_HUMAN			X	Exosome RNA helicase MTR4
sp|P46063|RECQ1_HUMAN			X	ATP-dependent DNA helicase Q1
sp|Q9Y620|RA54B_HUMAN			X	DNA repair and recombination protein RAD54B
sp|P78527|PRKDC_HUMAN			X	DNA-dependent protein kinase catalytic subunit
sp|Q08211|DHX9_HUMAN			X	ATP-dependent RNA helicase A
tr|A0A590UJ71|A0A590UJ71_HUMAN			X	RAD54 like (Fragment)
sp|Q14997|PSME4_HUMAN			X	Proteasome activator complex subunit 4
sp|Q14526|HIC1_HUMAN			X	Hypermethylated in cancer 1 protein
sp|Q7Z2Z1|TICRR_HUMAN			X	Treslin
sp|P23025|XPA_HUMAN			X	DNA repair protein complementing XP-A cells
sp|P45973|CBX5_HUMAN			X	Chromobox protein homolog 5
sp|Q08050|FOXM1_HUMAN			X	Forkhead box protein M1
sp|Q9BYP7|WNK3_HUMAN			X	Serine/threonine-protein kinase WNK3
sp|Q14566|MCM6_HUMAN			X	DNA replication licensing factor MCM6
tr|Q5QPE8|Q5QPE8_HUMAN			X	Mitochondrial genome maintenance exonuclease 1
sp|P52701|MSH6_HUMAN			X	DNA mismatch repair protein Msh6
sp|Q13574|DGKZ_HUMAN			X	Diacylglycerol kinase zeta
tr|B9ZVN9|B9ZVN9_HUMAN			X	DNA-directed RNA polymerase subunit
sp|Q15831|STK11_HUMAN			X	Serine/threonine-protein kinase STK11
sp|P23497|SP100_HUMAN			X	Nuclear autoantigen Sp-100
sp|O94763|RMP_HUMAN			X	Unconventional prefoldin RPB5 interactor 1
sp|Q13472|TOP3A_HUMAN			X	DNA topoisomerase 3-alpha
sp|Q6P4R8|NFRKB_HUMAN			X	Nuclear factor related to kappa-B-binding protein
sp|O60870|KIN17_HUMAN			X	DNA/RNA-binding protein KIN17
sp|Q15014|MO4L2_HUMAN			X	Mortality factor 4-like protein 2
sp|Q8N3C0|ASCC3_HUMAN			X	Activating signal cointegrator 1 complex subunit 3
sp|Q68E01|INT3_HUMAN			X	Integrator complex subunit 3
sp|P04053|TDT_HUMAN			X	DNA nucleotidylexotransferase
sp|P28340|DPOD1_HUMAN			X	DNA polymerase delta catalytic subunit

One of the proteins that were of special interest from Table 3.2 was X-ray repair cross-complementing protein 5 (XRCC 5). It is an interesting protein to investigate since it has been shown to be involved in DNA damage response to UV (Mao et al., 2022; Rastogi et al., 2010) which was the treatment used for the pulldowns. The MS analysis in run 2 where the modified XRCC5 was found (Table 3.2) showed 14 peptides mapped to XRCC5 in the pulldown and this protein has log 2-FD of 3.5 (data not shown). Among the identified XRCC5 peptides, there was one modified peptide that contained ubiquitin and ADP-ribose on lysine 283 and Threonine 284 of the peptide TWTVVDAKTLK, respectively.

To further investigate whether XRCC5 is being pulled down by WWE-tUBM and that the interaction is through ADP-ribosylation, I performed the pulldown in the presence or absence of PARPi Olaparib treatment. 293T cells were treated overnight with Olaparib (50 μM) (Figure 3.16 A). The cells were then treated with UV for 2h to induce DNA damage. The cells were then lysed and added to the immobilized proteins which consisted of GST, GST-WWE, and GST-WWE-tUBM. The samples were run on the gel and Western blot was performed to blot for XRCC5. Moreover, the inhibition of ADP-ribosylation was confirmed by using Western blot (Figure 3.10 C). Results in Figure 3.16 B showed that XRCC5 was pulled down by WWE and WWE-tUBM but not GST. Moreover, using Olaparib led to a decrease in XRCC5 being pulled down by WWE and WWE-tUBM which indicates that the interaction between these domains and XRCC5 is at least partly through ADP-ribose.

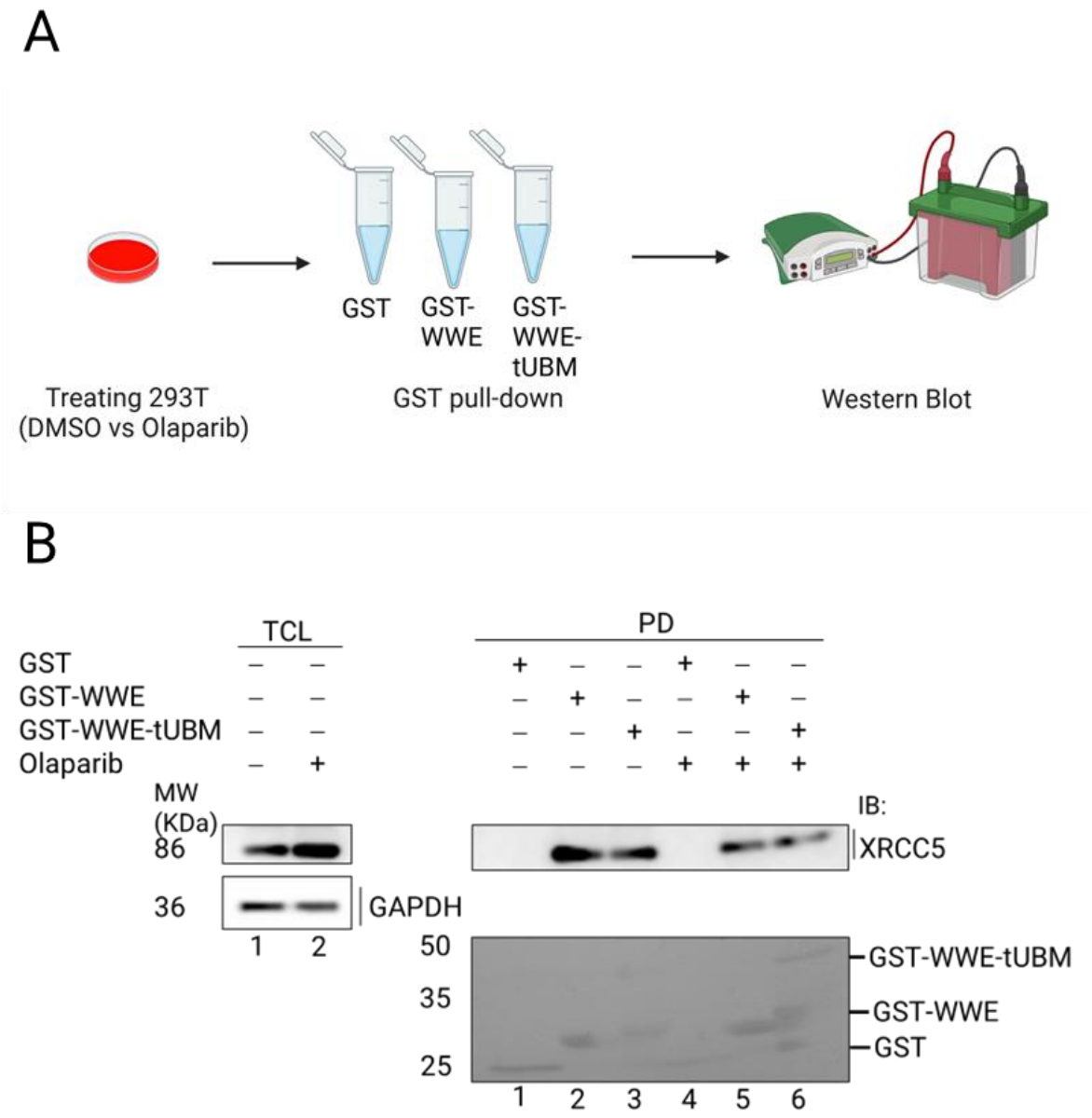

Figure 3.16. The interaction between WWE-tUBM and XRCC5. A. *Schematic of the pulldown experiment. 293T cells were treated with Olaparib (50μM) or DMSO overnight. Cells were then treated with UV (40J/m^2) for 2h. The TCL was then added to the bait proteins GST, GST-WWE and GST-WWE-tUBM.* ***B.*** *Left blot for XRCC5 in the TCL. GAPDH was used as a loading control and was blotted for using an antibody (Proteintech # 60004-1). Top right is blot for XRCC5 pulled down by GST, GST-WWE, or GST-WWE-tUBM, XRCC5 was blotted for using XRCC5 antibody (Cell Signaling Technology #2180). Bottom right is an image of the membrane showing GST, GST-WWE, and GST-WWE.*

Therefore, the data illustrated the interaction between WWE-tUBM with ubiquitinated and/or ADP-ribosylated cellular proteins. Moreover, the identity of these proteins was determined using MS. In the future, it would be of interest to investigate the E3 ligase activity of HUWE1 on these proteins by performing *in-vivo* ubiquitination assays.

Chapter 4: Discussion and Future Directions

HUWE1 is an important E3 ligase involved in many cellular processes through ligating ubiquitin onto various substrates (Kao et al., 2018). It contains specialized domains that mediate the interaction with its substrates such as the BH3 and PIP domains that have been shown to interact with Mcl1 and PCNA, respectively (Choe et al., 2016; Zhong et al., 2005). However, HUWE1 substrates outnumber the domains involved in substrate recognition (Hunkeler et al., 2021).

HUWE1 contains PTM reading domains for both ADP-ribose (WWE domain) and ubiquitin (tUBM domain) which potentiates it to be involved in PAR and ubiquitin-targeted ubiquitination (Hunkeler et al., 2021). However, the interaction between WWE-tUBM with cellular ADP-ribose and ubiquitin and their role in substrate recognition is not well investigated. Thus, this study aimed to further investigate the interaction between HUWE1 WWE-tUBM domains and cellular ADP-ribose and ubiquitin using GST pulldown assays followed by Western blot or LC-MS/MS.

The results from Western blots for the GST pulldown confirmed the ability of WWE-tUBM to interact with cellular ADP-ribosylated (MARylated and PARylated) and ubiquitinated proteins. The MS results further supported that WWE-tUBM pulldown ADP-ribosylated and ubiquitinated proteins by showing that WWE-tUBM pulled down more modified peptides compared to the GST control.

4.1. Investigating the differential response of DNA damaging agents on cellular ubiquitination and ADP-ribosylation

It is well known that ubiquitination and ADP-ribosylation, are involved in DNA damage response and there are reports that support the coordination between these PTMs in response to

DNA damage (H. C. Kang et al., 2011; Liu et al., 2013; Yan et al., 2013). Moreover, there are reports that support the differential regulation of these PTMs in response to different DNA damaging agents (Elia et al., 2015; Jungmichel et al., 2013). Different DNA damage conditions could lead to different types of DNA lesions which are repaired by different pathways (Fairbairn & O'Neill, 1994; Z. Li et al., 2014; Rastogi et al., 2010). Thus, I started by profiling the effect of different DNA damaging agents on the levels of cellular ubiquitination and ADP-ribosylation.

The increase in the levels of ubiquitination in the TCL upon DNA damage was not very pronounced, which could be attributed to ubiquitination being involved in almost all cellular processes (Elia et al., 2015). This could mask the increase in ubiquitination upon DNA damage. When looking at the nuclear extraction, the increase in the level of ubiquitination upon DNA damage was more pronounced. Moreover, the data from immunofluorescent confocal imaging supports the increase in the levels of ubiquitination in the nucleus upon treatment with UV DNA damage.

Looking at the levels of ADP-ribosylation, the results show that both etoposide and UV increased the levels of ADP-ribosylation in Total cell lysate, with etoposide showing a higher increase. The differential increase in ADP-ribosylation upon UV and etoposide treatment is in accordance with another report that illustrated that the level of PARylation is dependent on the type of genotoxic stress treatment (Jungmichel et al., 2013). When looking at the level of PARylation in the nucleus using Western blot both UV and etoposide led to an increase in the level of PARylation. Moreover, the immunofluorescent confocal images also supported the accumulation of PARylation in the nucleus upon DNA damage treatment. The increase in nuclear PARylation is in agreement with live cell imaging results using fluorescent PAR detector which illustrated the accumulation of PAR in the nucleus upon the treatment with different DNA

damaging agents (Koczor et al., 2022).

Ubiquitination and ADP-ribosylation have been shown to crosstalk with one another (H. C. Kang et al., 2011; Liu et al., 2013; Z. Wang et al., 2012; Yan et al., 2013). Thus, I sought to study the interplay between ubiquitination and ADP-ribosylation by inhibiting one or both of these modifications and investigating the effects it has on their levels. First, using the E1 inhibitor PYR41 led to an increase in the levels of ubiquitination, especially at higher molecular weight. When trouble-shooting this experiment, I found that E1 inhibitor PYR 41-induced accumulation of ubiquitination could be attributed to its inhibition of DUBs (Kapuria et al., 2011). PYR41 resulted in an increase in ADP-ribosylation. This increase could be attributed to the stress caused by the toxicity of PYR41.Thus, in the future, a different ubiquitination inhibitor should be used to explore the crosstalk effect of ubiquitin inhibition on cellular PARylation. As for the effect of PJ34 and Olaparib, both resulted in a decrease in the levels of ADP-ribosylation with Olaparib showing superior results, but they did not show any effect on cellular levels of ubiquitination. Overall, these data did not highlight the crosstalk between ubiquitination and ADP-ribosylation.

4.2. Investigating the interaction between WWE-tUBM and cellular ADP-ribosylation and ubiquitination

Previous reports demonstrated the ability of the HUWE1 WWE domain to interact with iso-ADPr; however; a new report illustrated that it has a preference for ADPr rather than iso-ADPr (Münzker et al., 2024; Z. Wang et al., 2012). Thus, in this study, I sought to investigate the interaction between WWE-tUBM and cellular ADP-ribose and ubiquitin. As expected, WWE-tUBM pulled down ubiquitin; however, WWE alone did not, which illustrates that ubiquitin is being pulled down by tUBM. Moreover, looking at ADP-ribosylation, WWE-tUBM was able to

pull down ADP-ribosylated proteins. When looking more closely at the ADP-ribosylated proteins, it was shown that WWE-tUBM pulled down both MAR and PAR. This data is in accordance with new reports that illustrate the ability of the HUWE1 WWE domain to interact with ADPr as opposed to the previous report that demonstrated that it interacts with iso-ADPr but not ADPr (Münzker et al., 2024; Z. Wang et al., 2012).

4.3. MS investigation of WWE-tUBM interactome

While many other proteomic studies investigated ubiquitination and ADP-ribosylation separately, there is a growing evidence that these PTMs crosstalk especially during DNA damage (Elia et al., 2015; Gagné et al., 2008; Jungmichel et al., 2013; H. C. Kang et al., 2011; Liu et al., 2013; Mandemaker et al., 2017; Martello et al., 2016; Peng et al., 2003; Shi et al., 2011; Z. Wang et al., 2012; Yan et al., 2013). Thus, our study investigated both of these PTMs. The MS results illustrated that WWE-tUBM pulled down ubiquitinated and ADP-ribosylated proteins, some of which contained dual modifications. The data further supports the idea of ubiquitin/ADP-ribose crosstalk and the possibility of HUWE1 playing a role in it.

Second, the results also shed light on the type of modification WWE-tUBM domains pull down. Specifically, it illustrated the ubiquitin linkage being pulled down by WWE-tUBM, where it showed that K48 is the only linkage being pulled down. Moreover, the ubiquitination sites were revealed where peptides were not only modified on Lysine residues but also atypical ubiquitination through Serine, Threonine and Cysteine was observed. While it is well accepted that ubiquitination could occur at amino acid residues other than Lysine. However, their labile nature is an obstacle facing their studies (Cadwell & Coscoy, 2005; Longarini & Matić, 2024).

Since many other E3 ligases are involved in targeting substrates with their ADP-ribose or UBDs reading domains (H. C. Kang et al., 2011; Liu et al., 2013; Thorslund et al., 2015), I

hypothesized that HUWE1 recognizes proteins that are pre-modified by ADP-ribose and/or ubiquitin using its WWE-tUBM. Thus, I investigated the interactome of WWE-tUBM which could aid in uncovering potential HUWE1 substrates. The results showed that HUWE1 WWE-tUBM pulls down proteins that are modified by ADP-ribose (MAR/PAR) and/or ubiquitin. Many of the proteins involved in DNA damage identified in this study were previously to be ADP-ribosylated or ubiquitinated. For example, XRCC5, PBRM1 and BCLAF1 were identified in other studies to be ADP-ribosylated (Jungmichel et al., 2013; Martello et al., 2016). However, interestingly, in my study, XRCC5 was also ubiquitinated on its Lysine residue. Moreover, other proteomic studies investigated the proteins that get ubiquitinated in response to UV treatment many of which were identified in this study (ASCC3, MSH6, PRKDC, XRCC5, DHX9, UPF1, CBX5) (Elia et al., 2015; Mandemaker et al., 2017).

The interaction with XRCC5 was further investigated since it was shown to play a role in cellular response to UV-induced DNA damage (Mao et al., 2022; Rastogi et al., 2010). Moreover, a previous report illustrated that XRCC5 is ADP-ribosylated in response to DNA damage (Jungmichel et al., 2013). Thus, I sought to further investigate the interaction between WWE-tUBM and XRCC5. Specifically, the cells were treated with PARPi Olaparib and DNA damage was induced using UV, then GST pulldown was performed followed by Western blotting. The results illustrated that the interaction between WWE-tUBM and XRCC5 was mediated, at least partly, by ADP-ribose. No previous reports established XRCC5 as a HUWE1 substrate. Thus, these results not only establish XRCC5 as a potential HUWE1 substrate but also shed a light regarding the means of its recognition by HUWE1. For future steps, it is of importance to do *in-vivo* experiments to further establish the role of HUWE1 in targeting the identified proteins.

4.4. Limitations and concluding remarks

While the current study establishes how HUWE1 engages post-translationally modified substrates via its WWE and tUBM domains, it addresses only the first part of the overall hypothesis. Specifically, it does not yet test whether HUWE1 directly ubiquitinates these pre-modified substrates or how this modification affects their stability and function. Understanding this downstream activity is critical for determining HUWE1's full regulatory role during the DNA damage response.

Future work will focus on functionally linking substrate recognition to ubiquitin transfer by HUWE1. Specifically, in-cell ubiquitination assays would be performed to investigate the role WWE-tUBM play in recognizing and targeting HUWE1's substrates. Since HUWE1 is frequently upregulated in ovarian cancer (D. Yang et al., 2017), the in-vivo ubiquitination assay will examine ubiquitination levels of the protein of interest in the ovarian cancer cells with either HUWE1 knock out or overexpression. Previously, I have generated HUWE1 knockout in the ovarian cancer cell line OVCAR3 using CRISPR. I will use the HUWE1 knockout cell line, in combination with HUWE1 overexpression using the HUWE1 wild-type plasmid or WWE-tUBM domain mutants. To assess substrate ubiquitination, I will immunopercipitate the substrate of interest using its specific antibody and detect substrate ubiquitination by Western blot using anti-ubiquitin antibody. If these proteins are targeted by HUWE1 through WWE-tUBM, overexpressing wild-type HUWE1 will increase the ubiquitination of the investigated proteins. Conversely, knocking HUWE1 out or overexpressing WWE-tUBM mutants will decrease the ubiquitination of the proteins.

Moreover, the functional role of HUWE1 in the regulation of these should be investigated. To examine whether HUWE1 regulates stability of the protein through ubiquitin-targeted proteasome degradation, I will examine the cellular levels of the protein of interest in the HUWE1 knockout cells, as well as the cells with HUWE1 overexpression using the HUWE1 wild-type plasmid or WWE-tUBM domain mutants. If HUWE1 targets the protein through ubiquitination, the overexpression of HUWE1 should destabilize these target proteins. In contrast, the protein will be stabilized in HUWE1 knockout cells or cells overexpressing mutant WWE-tUBM HUWE1. If the substrate is known to participate in additional cellular processes, specific functional assays should also be performed to evaluate whether HUWE1 influences these processes.

These studies will help uncover the biological consequences of HUWE1-mediated regulation and elucidate how HUWE1 interprets ADP-ribose and ubiquitin modifications to regulate substrate functions.

It is of note that HUWE1 WWE-tUBM interacting proteins were investigated using 293T cells in this study; however, for future functional assays, additional cell models including primary cells could be included to ensure the findings and identified potential substrates are biologically relevant.

Another caveat of this study is that, although the GST pulldown assay gives valuable insight into the interactome of WWE-tUBM; it is a non-physiological system, and not good at capturing weak interactors (Samavarchi-Tehrani et al., 2018). Thus, future work should be done to further investigate the interactome inside the cells. A way of studying the interaction between WWE-tUBM and cellular proteins is through the BioID system. BioID allows for studying protein-protein interaction by fusing the protein of interest with biotin ligase such as BirA

followed by expressing this protein in cells (Samavarchi-Tehrani et al., 2018). The fusion protein would then biotinylate proteins based on proximity which then is isolated using streptavidin beads (Samavarchi-Tehrani et al., 2018). Thus, this will further enable the identification of the WWE-tUBM interactome. To achieve this goal, I cloned NLS-WWE, NLS-tUBM and NLS-WWE-tUBM into a BioID plasmid to produce BirA fusion proteins. The BioID plasmid is a lentivirus plasmid that would be packaged to produce viral particles which would then be used to transduce the cells of interest (Samavarchi-Tehrani et al., 2018). Progress was made in incorporating the BioID system to perform the streptavidin pulldown for biotinylated protein followed by MS to investigate the WWE-tUBM *in-vivo* interactome. Specifically, I have completed cloning of the plasmids (S.1 A-C), they were intended to be used to produce virus particles which would then be used to transduce cells to express these plasmids. However, the attempt to implement the BioID system was halted due to time constraints within the MSc program.

Last, the MS data illustrated that HUWE1 WWE-tUBM interact with many DNA damage proteins. Moreover, the immunofluorescence-imaging data illustrated that ubiquitin and ADP-ribose respond to DNA damage. Thus, it would be of importance to investigate whether WWE-tUBM respond to DNA damage induction by interacting with ubiquitin and ADP-ribose. The ability of WWE-tUBM to respond and be recruited to the site of DNA damage would enable the recruitment of HUWE1 to damaged DNA. Thus, the recruitment of HUWE1 WWE-tUBM domains to the site of DNA damage could be investigated using microirradiation followed by immunofluorescence-imaging. Microirradiation is a method that have been used to study cellular interaction between ADP-ribose reading domains and UBDs with ADP-ribose and ubiquitin, respectively under DNA damage (H. C. Kang et al., 2011; Thorslund et al., 2015; M. Li et al.,

2013; Liu et al., 2013). Microirradiation induces localized DNA damage inside the cells and coupled with fluorescent microscopy, it would allow for visualizing the recruitment of DNA damage proteins to the site of the laser damage (J. J. Kim et al., 2019).

To investigate the recruitment of HUWE1 WWE-tUBM domains to the site of DNA damage, which would provide an insight about the potential mechanism by which HUWE1 gets recruited to and involved in DNA damage, laser microirradiation would be performed. The cellular investigation would involve the overexpression of fluorescently labelled WWE-tUBM in cells, then treating the cells with microirradiation and examining the recruitment of WWE-tUBM to DNA damage sites where ADP-ribose and ubiquitin are induced. To this end, I have generated mCherry WWE-tUBM plasmid. To investigate the interactions between these domains and nuclear ADP-ribose and ubiquitin, a NLS was fused to the domains along with the fluorescent proteins. I expect that fluorescently labelled WWE-tUBM will be recruited to the site of DNA damage in response to ADP-ribose and ubiquitin induction. The sequence alignment results for the fusion proteins along with the expression of NLS-WWE-tUBM in cells are shown in supplementary (S.2 A-D & S.3). The low expression levels of these domains were an obstacle in the way of investigating the interaction in the cells. Thus, to eliminate this obstacle future efforts aiming at increasing the transfection efficiency would allow the characterization of the *in-vivo* interaction between WWE-tUBM and cellular ubiquitin and ADP-ribose.

In conclusion, this research has contributed to a deeper understanding of HUWE1's role in recognizing multivalent PTMs, particularly through the dual WWE and tUBM domains. By investigating how HUWE1 coordinate ubiquitination and ADP-ribosylation and their associated protein networks, this study provides valuable insight into mechanisms of PTM signal transduction in cellular processes such as DNA damage responses.

References

Abplanalp, J., Leutert, M., Frugier, E., Nowak, K., Feurer, R., Kato, J., Kistemaker, H. V. A., Filippov, D. V., Moss, J., Caflisch, A., & Hottiger, M. O. (2017). Proteomic analyses identify ARH3 as a serine mono-ADP-ribosylhydrolase. *Nature Communications*, *8*(1), Article 1. https://doi.org/10.1038/s41467-017-02253-1

Akimov, V., Barrio-Hernandez, I., Hansen, S. V. F., Hallenborg, P., Pedersen, A.-K., Bekker-Jensen, D. B., Puglia, M., Christensen, S. D. K., Vanselow, J. T., Nielsen, M. M., Kratchmarova, I., Kelstrup, C. D., Olsen, J. V., & Blagoev, B. (2018). UbiSite approach for comprehensive mapping of lysine and N-terminal ubiquitination sites. *Nature Structural & Molecular Biology*, *25*(7), 631–640. https://doi.org/10.1038/s41594-018-0084-y

Al-Hakim, A., Escribano-Diaz, C., Landry, M.-C., O'Donnell, L., Panier, S., Szilard, R. K., & Durocher, D. (2010). The ubiquitous role of ubiquitin in the DNA damage response. *DNA Repair*, *9*(12), Article 12. https://doi.org/10.1016/j.dnarep.2010.09.011

Baker, R. T., & Board, P. G. (1987). The human ubiquitin gene family: Structure of a gene and pseudogenes from the Ub B subfamily. *Nucleic Acids Research*, *15*(2), 443–463. https://doi.org/10.1093/nar/15.2.443

Berndsen, C. E., & Wolberger, C. (2014). New insights into ubiquitin E3 ligase mechanism. *Nature Structural & Molecular Biology*, *21*(4), 301–307. https://doi.org/10.1038/nsmb.2780

Bonfiglio, J. J., Colby, T., & Matic, I. (2017). Mass spectrometry for serine ADP-ribosylation? Think o-glycosylation! *Nucleic Acids Research*, *45*(11), 6259–6264. https://doi.org/10.1093/nar/gkx446

Bonfiglio, J. J., Fontana, P., Zhang, Q., Colby, T., Gibbs-Seymour, I., Atanassov, I., Bartlett, E., Zaja, R., Ahel, I., & Matic, I. (2017). Serine ADP-Ribosylation Depends on HPF1. *Molecular Cell*, *65*(5), 932-940.e6. https://doi.org/10.1016/j.molcel.2017.01.003

Brzovic, P. S., Lissounov, A., Christensen, D. E., Hoyt, D. W., & Klevit, R. E. (2006). A UbcH5/ubiquitin noncovalent complex is required for processive BRCA1-directed ubiquitination. *Molecular Cell*, *21*(6), 873–880. https://doi.org/10.1016/j.molcel.2006.02.008

Burma, S., Chen, B. P., Murphy, M., Kurimasa, A., & Chen, D. J. (2001). ATM phosphorylates histone H2AX in response to DNA double-strand breaks. *The Journal of Biological Chemistry*, *276*(45), 42462–42467. https://doi.org/10.1074/jbc.C100466200

Bustos, D., Bakalarski, C. E., Yang, Y., Peng, J., & Kirkpatrick, D. S. (2012). Characterizing ubiquitination sites by peptide-based immunoaffinity enrichment. *Molecular & Cellular Proteomics: MCP*, *11*(12), 1529–1540. https://doi.org/10.1074/mcp.R112.019117

Cadwell, K., & Coscoy, L. (2005). Ubiquitination on nonlysine residues by a viral E3 ubiquitin ligase. *Science (New York, N.Y.)*, *309*(5731), 127–130. https://doi.org/10.1126/science.1110340

Chen, E. Y., Tan, C. M., Kou, Y., Duan, Q., Wang, Z., Meirelles, G. V., Clark, N. R., & Ma'ayan, A. (2013). Enrichr: Interactive and collaborative HTML5 gene list enrichment analysis tool. *BMC Bioinformatics*, *14*, 128. https://doi.org/10.1186/1471-2105-14-128

Choe, K. N., Nicolae, C. M., Constantin, D., Imamura Kawasawa, Y., Delgado-Diaz, M. R., De, S., Freire, R., Smits, V. A., & Moldovan, G.-L. (2016). HUWE1 interacts with PCNA to alleviate replication stress. *EMBO Reports*, *17*(6), 874–886. https://doi.org/10.15252/embr.201541685

Chua, N. K., Hart-Smith, G., & Brown, A. J. (2019). Non-canonical ubiquitination of the cholesterol-regulated degron of squalene monooxygenase. *The Journal of Biological Chemistry*, *294*(20), 8134–8147. https://doi.org/10.1074/jbc.RA119.007798

Ciechanover, A. (2009). Tracing the history of the ubiquitin proteolytic system: The pioneering article. *Biochemical and Biophysical Research Communications*, *387*(1), 1–10. https://doi.org/10.1016/j.bbrc.2009.06.065

Cohen, M. S., & Chang, P. (2018). Insights into the biogenesis, function, and regulation of ADP-ribosylation. *Nature Chemical Biology*, *14*(3), 236–243. https://doi.org/10.1038/nchembio.2568

Collier, R. J. (2001). Understanding the mode of action of diphtheria toxin: A perspective on progress during the 20th century. *Toxicon: Official Journal of the International Society on Toxinology*, *39*(11), 1793–1803. https://doi.org/10.1016/s0041-0101(01)00165-9

Cornilescu, G., Marquardt, J. L., Ottiger, M., & Bax, A. (1998). Validation of Protein Structure from Anisotropic Carbonyl Chemical Shifts in a Dilute Liquid Crystalline Phase. *Journal of the American Chemical Society*, *120*(27), 6836–6837. https://doi.org/10.1021/ja9812610

da Veiga Leprevost, F., Haynes, S. E., Avtonomov, D. M., Chang, H.-Y., Shanmugam, A. K., Mellacheruvu, D., Kong, A. T., & Nesvizhskii, A. I. (2020). Philosopher: A versatile toolkit for shotgun proteomics data analysis. *Nature Methods*, *17*(9), 869–870. https://doi.org/10.1038/s41592-020-0912-y

Daniels, C. M., Ong, S.-E., & Leung, A. K. L. (2015). The Promise of Proteomics for the Study of ADP-Ribosylation. *Molecular Cell*, *58*(6), Article 6. https://doi.org/10.1016/j.molcel.2015.06.012

Davis, M. W., & Jorgensen, E. M. (2022). ApE, A Plasmid Editor: A Freely Available DNA Manipulation and Visualization Program. *Frontiers in Bioinformatics*, *2*, 818619. https://doi.org/10.3389/fbinf.2022.818619

Denis, N. J., Vasilescu, J., Lambert, J.-P., Smith, J. C., & Figeys, D. (2007). Tryptic digestion of ubiquitin standards reveals an improved strategy for identifying ubiquitinated proteins by mass spectrometry. *Proteomics*, *7*(6), 868–874. https://doi.org/10.1002/pmic.200600410

Dikic, I., Wakatsuki, S., & Walters, K. J. (2009). Ubiquitin-binding domains—From structures to functions. *Nature Reviews. Molecular Cell Biology*, *10*(10), Article 10. https://doi.org/10.1038/nrm2767

Doil, C., Mailand, N., Bekker-Jensen, S., Menard, P., Larsen, D. H., Pepperkok, R., Ellenberg, J., Panier, S., Durocher, D., Bartek, J., Lukas, J., & Lukas, C. (2009). RNF168 binds and amplifies ubiquitin conjugates on damaged chromosomes to allow accumulation of repair proteins. *Cell*, *136*(3), Article 3. https://doi.org/10.1016/j.cell.2008.12.041

Dubois, M.-L., Meller, A., Samandi, S., Brunelle, M., Frion, J., Brunet, M. A., Toupin, A., Beaudoin, M. C., Jacques, J.-F., Lévesque, D., Scott, M. S., Lavigne, P., Roucou, X., & Boisvert, F.-M. (2020). UBB pseudogene 4 encodes functional ubiquitin variants. *Nature Communications*, *11*(1), Article 1. https://doi.org/10.1038/s41467-020-15090-6

Elia, A. E. H., Boardman, A. P., Wang, D. C., Huttlin, E. L., Everley, R. A., Dephoure, N., Zhou, C., Koren, I., Gygi, S. P., & Elledge, S. J. (2015). Quantitative Proteomic Atlas of Ubiquitination and Acetylation in the DNA Damage Response. *Molecular Cell*, *59*(5), 867–881. https://doi.org/10.1016/j.molcel.2015.05.006

Fairbairn, D. W., & O'Neill, K. L. (1994). DNA Strand Break Repair Involvement in Hydrogen Peroxide Induced Damage. *Molecules and Cells*, *4*(3), 343–348. https://doi.org/10.1016/S1016-8478(23)17247-5

French, M. E., Koehler, C. F., & Hunter, T. (2021). Emerging functions of branched ubiquitin chains. *Cell Discovery*, *7*(1), 6. https://doi.org/10.1038/s41421-020-00237-y

Gagné, J.-P., Isabelle, M., Lo, K. S., Bourassa, S., Hendzel, M. J., Dawson, V. L., Dawson, T. M., & Poirier, G. G. (2008). Proteome-wide identification of poly(ADP-ribose) binding proteins and poly(ADP-ribose)-associated protein complexes. *Nucleic Acids Research*, *36*(22), 6959–6976. https://doi.org/10.1093/nar/gkn771

Gatti, M., Imhof, R., Huang, Q., Baudis, M., & Altmeyer, M. (2020). The Ubiquitin Ligase TRIP12 Limits PARP1 Trapping and Constrains PARP Inhibitor Efficiency. *Cell Reports*, *32*(5), 107985. https://doi.org/10.1016/j.celrep.2020.107985

Gehrig, P. M., Nowak, K., Panse, C., Leutert, M., Grossmann, J., Schlapbach, R., & Hottiger, M. O. (2021). Gas-Phase Fragmentation of ADP-Ribosylated Peptides: Arginine-Specific Side-Chain Losses and Their Implication in Database Searches. *Journal of the American Society for Mass Spectrometry*, *32*(1), 157–168. https://doi.org/10.1021/jasms.0c00040

Gibson, D. G., Young, L., Chuang, R.-Y., Venter, J. C., Hutchison, C. A., & Smith, H. O. (2009). Enzymatic assembly of DNA molecules up to several hundred kilobases. *Nature Methods*, *6*(5), 343–345. https://doi.org/10.1038/nmeth.1318

Haglund, K., Sigismund, S., Polo, S., Szymkiewicz, I., Di Fiore, P. P., & Dikic, I. (2003). Multiple monoubiquitination of RTKs is sufficient for their endocytosis and degradation. *Nature Cell Biology*, *5*(5), 461–466. https://doi.org/10.1038/ncb983

Hershko, A., & Ciechanover, A. (1998). The ubiquitin system. *Annual Review of Biochemistry*, *67*, 425–479. https://doi.org/10.1146/annurev.biochem.67.1.425

Hicke, L., Schubert, H. L., & Hill, C. P. (2005). Ubiquitin-binding domains. *Nature Reviews. Molecular Cell Biology*, *6*(8), Article 8. https://doi.org/10.1038/nrm1701

Hjerpe, R., Aillet, F., Lopitz-Otsoa, F., Lang, V., England, P., & Rodriguez, M. S. (2009). Efficient protection and isolation of ubiquitylated proteins using tandem ubiquitin-binding entities. *EMBO Reports*, *10*(11), Article 11. https://doi.org/10.1038/embor.2009.192

Hu, Y., Scully, R., Sobhian, B., Xie, A., Shestakova, E., & Livingston, D. M. (2011). RAP80-directed tuning of BRCA1 homologous recombination function at ionizing radiation-induced nuclear foci. *Genes & Development*, *25*(7), 685–700. https://doi.org/10.1101/gad.2011011

Huang, S. (2021). *Characterization of the Functional Roles of the E3 Ligase HUWE1 in the Regulation of Poly [ADP-ribose] Polymerase 1 (PARP-1) under DNA Damage*.

Hunkeler, M., Jin, C. Y., Ma, M. W., Monda, J. K., Overwijn, D., Bennett, E. J., & Fischer, E. S. (2021). Solenoid architecture of HUWE1 contributes to ligase activity and substrate recognition. *Molecular Cell*, *81*(17), Article 17. https://doi.org/10.1016/j.molcel.2021.06.032

Hurley, J. H., Lee, S., & Prag, G. (2006). Ubiquitin-binding domains. *The Biochemical Journal*, *399*(3), Article 3. https://doi.org/10.1042/BJ20061138

Husnjak, K., & Dikic, I. (2012). Ubiquitin-binding proteins: Decoders of ubiquitin-mediated cellular functions. *Annual Review of Biochemistry*, *81*, 291–322. https://doi.org/10.1146/annurev-biochem-051810-094654

Jeram, S. M., Srikumar, T., Pedrioli, P. G. A., & Raught, B. (2009). Using mass spectrometry to identify ubiquitin and ubiquitin-like protein conjugation sites. *Proteomics*, *9*(4), 922–934. https://doi.org/10.1002/pmic.200800666

Jungmichel, S., Rosenthal, F., Altmeyer, M., Lukas, J., Hottiger, M. O., & Nielsen, M. L. (2013). Proteome-wide identification of poly(ADP-Ribosyl)ation targets in different genotoxic stress responses. *Molecular Cell*, *52*(2), 272–285. https://doi.org/10.1016/j.molcel.2013.08.026

Kalisch, T., Amé, J.-C., Dantzer, F., & Schreiber, V. (2012). New readers and interpretations of poly(ADP-ribosyl)ation. *Trends in Biochemical Sciences*, *37*(9), Article 9. https://doi.org/10.1016/j.tibs.2012.06.001

Käll, L., Canterbury, J. D., Weston, J., Noble, W. S., & MacCoss, M. J. (2007). Semi-supervised learning for peptide identification from shotgun proteomics datasets. *Nature Methods*, *4*(11), 923–925. https://doi.org/10.1038/nmeth1113

Kang, H. C., Lee, Y.-I., Shin, J.-H., Andrabi, S. A., Chi, Z., Gagné, J.-P., Lee, Y., Ko, H. S., Lee, B. D., Poirier, G. G., Dawson, V. L., & Dawson, T. M. (2011). Iduna is a poly(ADP-ribose) (PAR)-dependent E3 ubiquitin ligase that regulates DNA damage. *Proceedings of the National Academy of Sciences of the United States of America*, *108*(34), Article 34. https://doi.org/10.1073/pnas.1108799108

Kang, R. S., Daniels, C. M., Francis, S. A., Shih, S. C., Salerno, W. J., Hicke, L., & Radhakrishnan, I. (2003). Solution structure of a CUE-ubiquitin complex reveals a conserved mode of ubiquitin binding. *Cell*, *113*(5), 621–630. https://doi.org/10.1016/s0092-8674(03)00362-3

Kao, S.-H., Wu, H.-T., & Wu, K.-J. (2018). Ubiquitination by HUWE1 in tumorigenesis and beyond. *Journal of Biomedical Science*, *25*(1), Article 1. https://doi.org/10.1186/s12929-018-0470-0

Kapuria, V., Peterson, L. F., Showalter, H. D. H., Kirchhoff, P. D., Talpaz, M., & Donato, N. J. (2011). Protein cross-linking as a novel mechanism of action of a ubiquitin-activating enzyme inhibitor with anti-tumor activity. *Biochemical Pharmacology*, *82*(4), 341–349. https://doi.org/10.1016/j.bcp.2011.05.012

Karras, G. I., Kustatscher, G., Buhecha, H. R., Allen, M. D., Pugieux, C., Sait, F., Bycroft, M., & Ladurner, A. G. (2005). The macro domain is an ADP-ribose binding module. *The EMBO Journal*, *24*(11), 1911–1920. https://doi.org/10.1038/sj.emboj.7600664

Karve, T. M., & Cheema, A. K. (2011). Small changes huge impact: The role of protein posttranslational modifications in cellular homeostasis and disease. *Journal of Amino Acids*, *2011*, 207691. https://doi.org/10.4061/2011/207691

Kelsall, I. R. (2022). Non-lysine ubiquitylation: Doing things differently. *Frontiers in Molecular Biosciences*, *9*, 1008175. https://doi.org/10.3389/fmolb.2022.1008175

Khatun, R. (2017). *STRUCTURAL AND FUNCTIONAL STUDIES OF HUMAN UBIQUITIN E3 LIGASE HUWE1*.

Kim, H., Chen, J., & Yu, X. (2007). Ubiquitin-binding protein RAP80 mediates BRCA1-dependent DNA damage response. *Science (New York, N.Y.)*, *316*(5828), 1202–1205. https://doi.org/10.1126/science.1139621

Kim, J. J., Kumbhar, R., Gong, F., & Miller, K. M. (2019). In Time and Space: Laser Microirradiation and the DNA Damage Response. *Methods in Molecular Biology (Clifton, N.J.)*, *1999*, 61–74. https://doi.org/10.1007/978-1-4939-9500-4_3

Kim, M. Y., Zhang, T., & Kraus, W. L. (2005). Poly(ADP-ribosyl)ation by PARP-1: "PAR-laying" NAD+ into a nuclear signal. *Genes & Development*, *19*(17), 1951–1967. https://doi.org/10.1101/gad.1331805

Kirisako, T., Kamei, K., Murata, S., Kato, M., Fukumoto, H., Kanie, M., Sano, S., Tokunaga, F., Tanaka, K., & Iwai, K. (2006). A ubiquitin ligase complex assembles linear polyubiquitin chains. *The EMBO Journal*, *25*(20), 4877–4887. https://doi.org/10.1038/sj.emboj.7601360

Kirkpatrick, D. S., Denison, C., & Gygi, S. P. (2005). Weighing in on ubiquitin: The expanding role of mass-spectrometry-based proteomics. *Nature Cell Biology*, *7*(8), 750–757. https://doi.org/10.1038/ncb0805-750

Kirschner, L. S., & Stratakis, C. A. (2000). Structure of the human ubiquitin fusion gene Uba80 (RPS27a) and one of its pseudogenes. *Biochemical and Biophysical Research Communications*, *270*(3), 1106–1110. https://doi.org/10.1006/bbrc.2000.2568

Koczor, C. A., Haider, A. J., Saville, K. M., Li, J., Andrews, J. F., Beiser, A. V., & Sobol, R. W. (2022). Live Cell Detection of Poly(ADP-Ribose) for Use in Genetic and Genotoxic Compound Screens. *Cancers*, *14*(15), 3676. https://doi.org/10.3390/cancers14153676

Komander, D., & Rape, M. (2012). The ubiquitin code. *Annual Review of Biochemistry*, *81*, 203–229. https://doi.org/10.1146/annurev-biochem-060310-170328

Kong, A. T., Leprevost, F. V., Avtonomov, D. M., Mellacheruvu, D., & Nesvizhskii, A. I. (2017). MSFragger: Ultrafast and comprehensive peptide identification in mass spectrometry-based proteomics. *Nature Methods*, *14*(5), 513–520. https://doi.org/10.1038/nmeth.4256

Kuleshov, M. V., Jones, M. R., Rouillard, A. D., Fernandez, N. F., Duan, Q., Wang, Z., Koplev, S., Jenkins, S. L., Jagodnik, K. M., Lachmann, A., McDermott, M. G., Monteiro, C. D., Gundersen, G. W., & Ma'ayan, A. (2016). Enrichr: A comprehensive gene set enrichment analysis web server 2016 update. *Nucleic Acids Research*, *44*(W1), W90-97. https://doi.org/10.1093/nar/gkw377

Larsen, S. C., Hendriks, I. A., Lyon, D., Jensen, L. J., & Nielsen, M. L. (2018). Systems-wide Analysis of Serine ADP-Ribosylation Reveals Widespread Occurrence and Site-Specific Overlap with Phosphorylation. *Cell Reports*, *24*(9), Article 9. https://doi.org/10.1016/j.celrep.2018.07.083

Lee, S., Tsai, Y. C., Mattera, R., Smith, W. J., Kostelansky, M. S., Weissman, A. M., Bonifacino, J. S., & Hurley, J. H. (2006). Structural basis for ubiquitin recognition and autoubiquitination by Rabex-5. *Nature Structural & Molecular Biology*, *13*(3), 264–271. https://doi.org/10.1038/nsmb1064

Li, K., Vaudel, M., Zhang, B., Ren, Y., & Wen, B. (2019). PDV: An integrative proteomics data viewer. *Bioinformatics (Oxford, England)*, *35*(7), 1249–1251. https://doi.org/10.1093/bioinformatics/bty770

Li, M., Lu, L.-Y., Yang, C.-Y., Wang, S., & Yu, X. (2013). The FHA and BRCT domains recognize ADP-ribosylation during DNA damage response. *Genes & Development*, *27*(16), 1752–1768. https://doi.org/10.1101/gad.226357.113

Li, M., & Yu, X. (2015). The role of poly(ADP-ribosyl)ation in DNA damage response and cancer chemotherapy. *Oncogene*, *34*(26), Article 26. https://doi.org/10.1038/onc.2014.295

Li, Z., Sun, B., Clewell, R. A., Adeleye, Y., Andersen, M. E., & Zhang, Q. (2014). Dose-response modeling of etoposide-induced DNA damage response. *Toxicological Sciences:*

An Official Journal of the Society of Toxicology, *137*(2), 371–384. https://doi.org/10.1093/toxsci/kft259

Liu, C., Vyas, A., Kassab, M. A., Singh, A. K., & Yu, X. (2017). The role of poly ADP-ribosylation in the first wave of DNA damage response. *Nucleic Acids Research*, *45*(14), Article 14. https://doi.org/10.1093/nar/gkx565

Liu, C., Wu, J., Paudyal, S. C., You, Z., & Yu, X. (2013). CHFR is important for the first wave of ubiquitination at DNA damage sites. *Nucleic Acids Research*, *41*(3), 1698–1710. https://doi.org/10.1093/nar/gks1278

Longarini, E. J., Dauben, H., Locatelli, C., Wondisford, A. R., Smith, R., Muench, C., Kolvenbach, A., Lynskey, M. L., Pope, A., Bonfiglio, J. J., Jurado, E. P., Fajka-Boja, R., Colby, T., Schuller, M., Ahel, I., Timinszky, G., O'Sullivan, R. J., Huet, S., & Matic, I. (2023). Modular antibodies reveal DNA damage-induced mono-ADP-ribosylation as a second wave of PARP1 signaling. *Molecular Cell*, *83*(10), Article 10. https://doi.org/10.1016/j.molcel.2023.03.027

Longarini, E. J., & Matić, I. (2024). Preserving ester-linked modifications reveals glutamate and aspartate mono-ADP-ribosylation by PARP1 and its reversal by PARG. *Nature Communications*, *15*(1), 4239. https://doi.org/10.1038/s41467-024-48314-0

Luo, X., & Kraus, W. L. (2012). On PAR with PARP: Cellular stress signaling through poly(ADP-ribose) and PARP-1. *Genes & Development*, *26*(5), 417–432. https://doi.org/10.1101/gad.183509.111

Lüscher, B., Ahel, I., Altmeyer, M., Ashworth, A., Bai, P., Chang, P., Cohen, M., Corda, D., Dantzer, F., Daugherty, M. D., Dawson, T. M., Dawson, V. L., Deindl, S., Fehr, A. R., Feijs, K. L. H., Filippov, D. V., Gagné, J.-P., Grimaldi, G., Guettler, S., … Ziegler, M. (2022). ADP-ribosyltransferases, an update on function and nomenclature. *The FEBS Journal*, *289*(23), Article 23. https://doi.org/10.1111/febs.16142

Lüscher, B., Bütepage, M., Eckei, L., Krieg, S., Verheugd, P., & Shilton, B. H. (2018). ADP-Ribosylation, a Multifaceted Posttranslational Modification Involved in the Control of Cell Physiology in Health and Disease. *Chemical Reviews*, *118*(3), 1092–1136. https://doi.org/10.1021/acs.chemrev.7b00122

MacLean, B., Tomazela, D. M., Shulman, N., Chambers, M., Finney, G. L., Frewen, B., Kern, R., Tabb, D. L., Liebler, D. C., & MacCoss, M. J. (2010). Skyline: An open source document editor for creating and analyzing targeted proteomics experiments. *Bioinformatics (Oxford, England)*, *26*(7), 966–968. https://doi.org/10.1093/bioinformatics/btq054

Malanga, M., Czubaty, A., Girstun, A., Staron, K., & Althaus, F. R. (2008). Poly(ADP-ribose) binds to the splicing factor ASF/SF2 and regulates its phosphorylation by DNA topoisomerase I. *The Journal of Biological Chemistry*, *283*(29), 19991–19998. https://doi.org/10.1074/jbc.M709495200

Mandemaker, I. K., van Cuijk, L., Janssens, R. C., Lans, H., Bezstarosti, K., Hoeijmakers, J. H., Demmers, J. A., Vermeulen, W., & Marteijn, J. A. (2017). DNA damage-induced histone H1 ubiquitylation is mediated by HUWE1 and stimulates the RNF8-RNF168 pathway. *Scientific Reports*, *7*(1), Article 1. https://doi.org/10.1038/s41598-017-15194-y

Mao, X., Ji, M., Kang, L., Qin, B., Luo, J., Zhang, W., Wu, A., Yuan, Y., Zhang, G., & Guan, H. (2022). XRCC5 downregulated by TRIM25 is susceptible for lens epithelial cell apoptosis. *Cellular Signalling*, *94*, 110314. https://doi.org/10.1016/j.cellsig.2022.110314

Marsh, D. J., Ma, Y., & Dickson, K.-A. (2020). Histone Monoubiquitination in Chromatin Remodelling: Focus on the Histone H2B Interactome and Cancer. *Cancers*, *12*(11), 3462. https://doi.org/10.3390/cancers12113462

Martello, R., Leutert, M., Jungmichel, S., Bilan, V., Larsen, S. C., Young, C., Hottiger, M. O., & Nielsen, M. L. (2016). Proteome-wide identification of the endogenous ADP-ribosylome of mammalian cells and tissue. *Nature Communications*, *7*, 12917. https://doi.org/10.1038/ncomms12917

Martinho, D. (2023). *INVESTIGATING THE ROLE OF HUWE1 IN DNA REPAIR: IMPLICATIONS IN CANCER THERAPY*.

Moortgat, S., Berland, S., Aukrust, I., Maystadt, I., Baker, L., Benoit, V., Caro-Llopis, A., Cooper, N. S., Debray, F.-G., Faivre, L., Gardeitchik, T., Haukanes, B. I., Houge, G., Kivuva, E., Martinez, F., Mehta, S. G., Nassogne, M.-C., Powell-Hamilton, N., Pfundt, R., … Newbury-Ecob, R. A. (2018). HUWE1 variants cause dominant X-linked intellectual disability: A clinical study of 21 patients. *European Journal of Human Genetics: EJHG*, *26*(1), 64–74. https://doi.org/10.1038/s41431-017-0038-6

Münzker, L., Kimani, S. W., Fowkes, M. M., Dong, A., Zheng, H., Li, Y., Dasovich, M., Zak, K. M., Leung, A. K. L., Elkins, J. M., Kessler, D., Arrowsmith, C. H., Halabelian, L., & Böttcher, J. (2024). A ligand discovery toolbox for the WWE domain family of human E3 ligases. *Communications Biology*, *7*(1), 901. https://doi.org/10.1038/s42003-024-06584-w

Nesvizhskii, A. I., Keller, A., Kolker, E., & Aebersold, R. (2003). A statistical model for identifying proteins by tandem mass spectrometry. *Analytical Chemistry*, *75*(17), 4646–4658. https://doi.org/10.1021/ac0341261

Oberoi, J., Richards, M. W., Crumpler, S., Brown, N., Blagg, J., & Bayliss, R. (2010). Structural basis of poly(ADP-ribose) recognition by the multizinc binding domain of checkpoint with forkhead-associated and RING Domains (CHFR). *The Journal of Biological Chemistry*, *285*(50), 39348–39358. https://doi.org/10.1074/jbc.M110.159855

Ohtake, F., Saeki, Y., Ishido, S., Kanno, J., & Tanaka, K. (2016). The K48-K63 Branched Ubiquitin Chain Regulates NF-κB Signaling. *Molecular Cell*, *64*(2), 251–266. https://doi.org/10.1016/j.molcel.2016.09.014

O'Sullivan, J., Tedim Ferreira, M., Gagné, J.-P., Sharma, A. K., Hendzel, M. J., Masson, J.-Y., & Poirier, G. G. (2019). Emerging roles of eraser enzymes in the dynamic control of protein ADP-ribosylation. *Nature Communications*, *10*(1), 1182. https://doi.org/10.1038/s41467-019-08859-x

Pandya, R. K., Partridge, J. R., Love, K. R., Schwartz, T. U., & Ploegh, H. L. (2010). A structural element within the HUWE1 HECT domain modulates self-ubiquitination and substrate ubiquitination activities. *The Journal of Biological Chemistry*, *285*(8), 5664–5673. https://doi.org/10.1074/jbc.M109.051805

Panier, S., Ichijima, Y., Fradet-Turcotte, A., Leung, C. C. Y., Kaustov, L., Arrowsmith, C. H., & Durocher, D. (2012). Tandem protein interaction modules organize the ubiquitin-dependent response to DNA double-strand breaks. *Molecular Cell*, *47*(3), Article 3. https://doi.org/10.1016/j.molcel.2012.05.045

Park, C.-W., & Ryu, K.-Y. (2014). Cellular ubiquitin pool dynamics and homeostasis. *BMB Reports*, *47*(9), 475–482. https://doi.org/10.5483/bmbrep.2014.47.9.128

Penengo, L., Mapelli, M., Murachelli, A. G., Confalonieri, S., Magri, L., Musacchio, A., Di Fiore, P. P., Polo, S., & Schneider, T. R. (2006). Crystal structure of the ubiquitin binding

domains of rabex-5 reveals two modes of interaction with ubiquitin. *Cell*, *124*(6), 1183–1195. https://doi.org/10.1016/j.cell.2006.02.020

Peng, J., Schwartz, D., Elias, J. E., Thoreen, C. C., Cheng, D., Marsischky, G., Roelofs, J., Finley, D., & Gygi, S. P. (2003). A proteomics approach to understanding protein ubiquitination. *Nature Biotechnology*, *21*(8), 921–926. https://doi.org/10.1038/nbt849

Pickart, C. M., & Eddins, M. J. (2004). Ubiquitin: Structures, functions, mechanisms. *Biochimica Et Biophysica Acta*, *1695*(1–3), 55–72. https://doi.org/10.1016/j.bbamcr.2004.09.019

Polasky, D. A., Geiszler, D. J., Yu, F., Li, K., Teo, G. C., & Nesvizhskii, A. I. (2023). MSFragger-Labile: A Flexible Method to Improve Labile PTM Analysis in Proteomics. *Molecular & Cellular Proteomics: MCP*, *22*(5), 100538. https://doi.org/10.1016/j.mcpro.2023.100538

Rahighi, S., Ikeda, F., Kawasaki, M., Akutsu, M., Suzuki, N., Kato, R., Kensche, T., Uejima, T., Bloor, S., Komander, D., Randow, F., Wakatsuki, S., & Dikic, I. (2009). Specific recognition of linear ubiquitin chains by NEMO is important for NF-kappaB activation. *Cell*, *136*(6), 1098–1109. https://doi.org/10.1016/j.cell.2009.03.007

Rastogi, R. P., Richa, null, Kumar, A., Tyagi, M. B., & Sinha, R. P. (2010). Molecular mechanisms of ultraviolet radiation-induced DNA damage and repair. *Journal of Nucleic Acids*, *2010*, 592980. https://doi.org/10.4061/2010/592980

Reber, J. M., & Mangerich, A. (2021). Why structure and chain length matter: On the biological significance underlying the structural heterogeneity of poly(ADP-ribose). *Nucleic Acids Research*, *49*(15), 8432–8448. https://doi.org/10.1093/nar/gkab618

Redman, K. L., & Rechsteiner, M. (1989). Identification of the long ubiquitin extension as ribosomal protein S27a. *Nature*, *338*(6214), 438–440. https://doi.org/10.1038/338438a0

Reyes-Turcu, F. E., Horton, J. R., Mullally, J. E., Heroux, A., Cheng, X., & Wilkinson, K. D. (2006). The ubiquitin binding domain ZnF UBP recognizes the C-terminal diglycine motif of unanchored ubiquitin. *Cell*, *124*(6), 1197–1208. https://doi.org/10.1016/j.cell.2006.02.038

Rosenthal, F., Feijs, K. L. H., Frugier, E., Bonalli, M., Forst, A. H., Imhof, R., Winkler, H. C., Fischer, D., Caflisch, A., Hassa, P. O., Lüscher, B., & Hottiger, M. O. (2013). Macrodomain-containing proteins are new mono-ADP-ribosylhydrolases. *Nature Structural & Molecular Biology*, *20*(4), 502–507. https://doi.org/10.1038/nsmb.2521

Samavarchi-Tehrani, P., Abdouni, H., Samson, R., & Gingras, A.-C. (2018). A Versatile Lentiviral Delivery Toolkit for Proximity-dependent Biotinylation in Diverse Cell Types. *Molecular & Cellular Proteomics*, *17*(11), 2256–2269. https://doi.org/10.1074/mcp.TIR118.000902

Sato, Y., Yoshikawa, A., Mimura, H., Yamashita, M., Yamagata, A., & Fukai, S. (2009). Structural basis for specific recognition of Lys 63-linked polyubiquitin chains by tandem UIMs of RAP80. *The EMBO Journal*, *28*(16), 2461–2468. https://doi.org/10.1038/emboj.2009.160

Sharma, A., Singh, K., & Almasan, A. (2012). Histone H2AX phosphorylation: A marker for DNA damage. *Methods in Molecular Biology (Clifton, N.J.)*, *920*, 613–626. https://doi.org/10.1007/978-1-61779-998-3_40

Sheng, X., Xia, Z., Yang, H., & Hu, R. (2024). The ubiquitin codes in cellular stress responses. *Protein & Cell*, *15*(3), 157–190. https://doi.org/10.1093/procel/pwad045

Shi, Y., Chan, D. W., Jung, S. Y., Malovannaya, A., Wang, Y., & Qin, J. (2011). A data set of human endogenous protein ubiquitination sites. *Molecular & Cellular Proteomics: MCP*, *10*(5), M110.002089. https://doi.org/10.1074/mcp.M110.002089

Shiba, Y., Katoh, Y., Shiba, T., Yoshino, K., Takatsu, H., Kobayashi, H., Shin, H.-W., Wakatsuki, S., & Nakayama, K. (2004). GAT (GGA and Tom1) domain responsible for ubiquitin binding and ubiquitination. *The Journal of Biological Chemistry*, *279*(8), 7105–7111. https://doi.org/10.1074/jbc.M311702200

Sims, J. J., & Cohen, R. E. (2009). Linkage-specific avidity defines the lysine 63-linked polyubiquitin-binding preference of rap80. *Molecular Cell*, *33*(6), 775–783. https://doi.org/10.1016/j.molcel.2009.02.011

Šlechtová, T., Gilar, M., Kalíková, K., & Tesařová, E. (2015). Insight into Trypsin Miscleavage: Comparison of Kinetic Constants of Problematic Peptide Sequences. *Analytical Chemistry*, *87*(15), 7636–7643. https://doi.org/10.1021/acs.analchem.5b00866

Smith, D. B., & Johnson, K. S. (1988). Single-step purification of polypeptides expressed in Escherichia coli as fusions with glutathione S-transferase. *Gene*, *67*(1), 31–40. https://doi.org/10.1016/0378-1119(88)90005-4

Stewart, M. D., Ritterhoff, T., Klevit, R. E., & Brzovic, P. S. (2016). E2 enzymes: More than just middle men. *Cell Research*, *26*(4), 423–440. https://doi.org/10.1038/cr.2016.35

Suskiewicz, M. J., Prokhorova, E., Rack, J. G. M., & Ahel, I. (2023). ADP-ribosylation from molecular mechanisms to therapeutic implications. *Cell*, *186*(21), 4475–4495. https://doi.org/10.1016/j.cell.2023.08.030

Suskiewicz, M. J., Zobel, F., Ogden, T. E. H., Fontana, P., Ariza, A., Yang, J.-C., Zhu, K., Bracken, L., Hawthorne, W. J., Ahel, D., Neuhaus, D., & Ahel, I. (2020). HPF1 completes the PARP active site for DNA damage-induced ADP-ribosylation. *Nature*, *579*(7800), 598–602. https://doi.org/10.1038/s41586-020-2013-6

Swanson, K. A., Hicke, L., & Radhakrishnan, I. (2006). Structural basis for monoubiquitin recognition by the Ede1 UBA domain. *Journal of Molecular Biology*, *358*(3), 713–724. https://doi.org/10.1016/j.jmb.2006.02.059

Swanson, K. A., Kang, R. S., Stamenova, S. D., Hicke, L., & Radhakrishnan, I. (2003). Solution structure of Vps27 UIM-ubiquitin complex important for endosomal sorting and receptor downregulation. *The EMBO Journal*, *22*(18), 4597–4606. https://doi.org/10.1093/emboj/cdg471

Takeda, K., Flechsig, H., Muro, I., Amyot, R., Kobayashi, F., Kodera, N., Ando, T., & Konno, H. (2023). Structural Dynamics of E6AP E3 Ligase HECT Domain and Involvement of a Flexible Hinge Loop in the Ubiquitin Chain Synthesis Mechanism. *Nano Letters*, *23*(24), 11940–11948. https://doi.org/10.1021/acs.nanolett.3c04150

Tan, F., Lu, L., Cai, Y., Wang, J., Xie, Y., Wang, L., Gong, Y., Xu, B.-E., Wu, J., Luo, Y., Qiang, B., Yuan, J., Sun, X., & Peng, X. (2008). Proteomic analysis of ubiquitinated proteins in normal hepatocyte cell line Chang liver cells. *Proteomics*, *8*(14), 2885–2896. https://doi.org/10.1002/pmic.200700887

Teloni, F., & Altmeyer, M. (2016). Readers of poly(ADP-ribose): Designed to be fit for purpose. *Nucleic Acids Research*, *44*(3), 993–1006. https://doi.org/10.1093/nar/gkv1383

Teo, G. C., Polasky, D. A., Yu, F., & Nesvizhskii, A. I. (2021). Fast Deisotoping Algorithm and Its Implementation in the MSFragger Search Engine. *Journal of Proteome Research*, *20*(1), 498–505. https://doi.org/10.1021/acs.jproteome.0c00544

Thorslund, T., Ripplinger, A., Hoffmann, S., Wild, T., Uckelmann, M., Villumsen, B., Narita, T., Sixma, T. K., Choudhary, C., Bekker-Jensen, S., & Mailand, N. (2015). Histone H1 couples initiation and amplification of ubiquitin signalling after DNA damage. *Nature*, *527*(7578), Article 7578. https://doi.org/10.1038/nature15401

Timinszky, G., Till, S., Hassa, P. O., Hothorn, M., Kustatscher, G., Nijmeijer, B., Colombelli, J., Altmeyer, M., Stelzer, E. H. K., Scheffzek, K., Hottiger, M. O., & Ladurner, A. G. (2009). A macrodomain-containing histone rearranges chromatin upon sensing PARP1 activation. *Nature Structural & Molecular Biology*, *16*(9), 923–929. https://doi.org/10.1038/nsmb.1664

Vaisberg, E. A., Grissom, P. M., & McIntosh, J. R. (1996). Mammalian cells express three distinct dynein heavy chains that are localized to different cytoplasmic organelles. *The Journal of Cell Biology*, *133*(4), 831–842. https://doi.org/10.1083/jcb.133.4.831

Varadan, R., Assfalg, M., Raasi, S., Pickart, C., & Fushman, D. (2005). Structural determinants for selective recognition of a Lys48-linked polyubiquitin chain by a UBA domain. *Molecular Cell*, *18*(6), 687–698. https://doi.org/10.1016/j.molcel.2005.05.013

Vertegaal, A. C. O. (2011). Uncovering ubiquitin and ubiquitin-like signaling networks. *Chemical Reviews*, *111*(12), Article 12. https://doi.org/10.1021/cr200187e

Vivelo, C. A., & Leung, A. K. L. (2015). Proteomics approaches to identify mono-(ADP-ribosyl)ated and poly(ADP-ribosyl)ated proteins. *Proteomics*, *15*(2–3), Article 2–3. https://doi.org/10.1002/pmic.201400217

Walsh, C. T., Garneau-Tsodikova, S., & Gatto, G. J. (2005). Protein posttranslational modifications: The chemistry of proteome diversifications. *Angewandte Chemie (International Ed. in English)*, *44*(45), Article 45. https://doi.org/10.1002/anie.200501023

Wang, H., Yang, L., Liu, M., & Luo, J. (2023). Protein post-translational modifications in the regulation of cancer hallmarks. *Cancer Gene Therapy*, *30*(4), 529–547. https://doi.org/10.1038/s41417-022-00464-3

Wang, X., Herr, R. A., Chua, W.-J., Lybarger, L., Wiertz, E. J. H. J., & Hansen, T. H. (2007). Ubiquitination of serine, threonine, or lysine residues on the cytoplasmic tail can induce ERAD of MHC-I by viral E3 ligase mK3. *The Journal of Cell Biology*, *177*(4), 613–624. https://doi.org/10.1083/jcb.200611063

Wang, Z., Michaud, G. A., Cheng, Z., Zhang, Y., Hinds, T. R., Fan, E., Cong, F., & Xu, W. (2012). Recognition of the iso-ADP-ribose moiety in poly(ADP-ribose) by WWE domains suggests a general mechanism for poly(ADP-ribosyl)ation-dependent ubiquitination. *Genes & Development*, *26*(3), Article 3. https://doi.org/10.1101/gad.182618.111

Warren, M. R. E., Parker, C. E., Mocanu, V., Klapper, D., & Borchers, C. H. (2005). Electrospray ionization tandem mass spectrometry of model peptides reveals diagnostic fragment ions for protein ubiquitination. *Rapid Communications in Mass Spectrometry: RCM*, *19*(4), 429–437. https://doi.org/10.1002/rcm.1798

Webb, G. C., Baker, R. T., Coggan, M., & Board, P. G. (1994). Localization of the human UBA52 ubiquitin fusion gene to chromosome band 19p13.1-p12. *Genomics*, *19*(3), 567–569. https://doi.org/10.1006/geno.1994.1108

Wiborg, O., Pedersen, M. S., Wind, A., Berglund, L. E., Marcker, K. A., & Vuust, J. (1985). The human ubiquitin multigene family: Some genes contain multiple directly repeated ubiquitin coding sequences. *The EMBO Journal*, *4*(3), 755–759. https://doi.org/10.1002/j.1460-2075.1985.tb03693.x

Xie, Z., Bailey, A., Kuleshov, M. V., Clarke, D. J. B., Evangelista, J. E., Jenkins, S. L., Lachmann, A., Wojciechowicz, M. L., Kropiwnicki, E., Jagodnik, K. M., Jeon, M., & Ma'ayan, A. (2021). Gene Set Knowledge Discovery with Enrichr. *Current Protocols*, *1*(3), e90. https://doi.org/10.1002/cpz1.90

Xu, G., & Jaffrey, S. R. (2013). Proteomic identification of protein ubiquitination events. *Biotechnology & Genetic Engineering Reviews*, *29*(1), 73–109. https://doi.org/10.1080/02648725.2013.801232

Xu, G. W., Ali, M., Wood, T. E., Wong, D., Maclean, N., Wang, X., Gronda, M., Skrtic, M., Li, X., Hurren, R., Mao, X., Venkatesan, M., Beheshti Zavareh, R., Ketela, T., Reed, J. C., Rose, D., Moffat, J., Batey, R. A., Dhe-Paganon, S., & Schimmer, A. D. (2010). The ubiquitin-activating enzyme E1 as a therapeutic target for the treatment of leukemia and multiple myeloma. *Blood*, *115*(11), 2251–2259. https://doi.org/10.1182/blood-2009-07-231191

Xu, P., & Peng, J. (2006). Dissecting the ubiquitin pathway by mass spectrometry. *Biochimica Et Biophysica Acta*, *1764*(12), 1940–1947. https://doi.org/10.1016/j.bbapap.2006.09.004

Yan, Q., Xu, R., Zhu, L., Cheng, X., Wang, Z., Manis, J., & Shipp, M. A. (2013). BAL1 and its partner E3 ligase, BBAP, link Poly(ADP-ribose) activation, ubiquitylation, and double-strand DNA repair independent of ATM, MDC1, and RNF8. *Molecular and Cellular Biology*, *33*(4), Article 4. https://doi.org/10.1128/MCB.00990-12

Yang, D., Sun, B., Zhang, X., Cheng, D., Yu, X., Yan, L., Li, L., An, S., Jiang, H., Lasorella, A., Iavarone, A., Zhang, S., Zou, F., & Zhao, X. (2017). Huwe1 Sustains Normal Ovarian Epithelial Cell Transformation and Tumor Growth through the Histone H1.3- *H19* Cascade. *Cancer Research*, *77*(18), 4773–4784. https://doi.org/10.1158/0008-5472.CAN-16-2597

Yang, K. L., Yu, F., Teo, G. C., Li, K., Demichev, V., Ralser, M., & Nesvizhskii, A. I. (2023). MSBooster: Improving peptide identification rates using deep learning-based features. *Nature Communications*, *14*(1), 4539. https://doi.org/10.1038/s41467-023-40129-9

Yang, Y., Kitagaki, J., Dai, R.-M., Tsai, Y. C., Lorick, K. L., Ludwig, R. L., Pierre, S. A., Jensen, J. P., Davydov, I. V., Oberoi, P., Li, C.-C. H., Kenten, J. H., Beutler, J. A., Vousden, K. H., & Weissman, A. M. (2007). Inhibitors of ubiquitin-activating enzyme (E1), a new class of potential cancer therapeutics. *Cancer Research*, *67*(19), 9472–9481. https://doi.org/10.1158/0008-5472.CAN-07-0568

Yu, F., Haynes, S. E., & Nesvizhskii, A. I. (2021). IonQuant Enables Accurate and Sensitive Label-Free Quantification With FDR-Controlled Match-Between-Runs. *Molecular & Cellular Proteomics: MCP*, *20*, 100077. https://doi.org/10.1016/j.mcpro.2021.100077

Yu, F., Haynes, S. E., Teo, G. C., Avtonomov, D. M., Polasky, D. A., & Nesvizhskii, A. I. (2020). Fast Quantitative Analysis of timsTOF PASEF Data with MSFragger and IonQuant. *Molecular & Cellular Proteomics: MCP*, *19*(9), 1575–1585. https://doi.org/10.1074/mcp.TIR120.002048

Yu, F., Teo, G. C., Kong, A. T., Haynes, S. E., Avtonomov, D. M., Geiszler, D. J., & Nesvizhskii, A. I. (2020). Identification of modified peptides using localization-aware open search. *Nature Communications*, *11*(1), 4065. https://doi.org/10.1038/s41467-020-17921-y

Zheng, N., & Shabek, N. (2017). Ubiquitin Ligases: Structure, Function, and Regulation. *Annual Review of Biochemistry*, *86*, 129–157. https://doi.org/10.1146/annurev-biochem-060815-014922

Zhong, Q., Gao, W., Du, F., & Wang, X. (2005). Mule/ARF-BP1, a BH3-only E3 ubiquitin ligase, catalyzes the polyubiquitination of Mcl-1 and regulates apoptosis. *Cell*, *121*(7), Article 7. https://doi.org/10.1016/j.cell.2005.06.009

Zhu, K., Suskiewicz, M. J., Hloušek-Kasun, A., Meudal, H., Mikoč, A., Aucagne, V., Ahel, D., & Ahel, I. (2022). DELTEX E3 ligases ubiquitylate ADP-ribosyl modification on protein substrates. *Science Advances*, *8*(40), eadd4253. https://doi.org/10.1126/sciadv.add4253

Zhu, W., Smith, J. W., & Huang, C.-M. (2010). Mass spectrometry-based label-free quantitative proteomics. *Journal of Biomedicine & Biotechnology*, *2010*, 840518. https://doi.org/10.1155/2010/840518

Appendix A: Supplementary Figures

Contribution: Angelo Vivona contributed to transfection of U2OS cells in Figure S.3

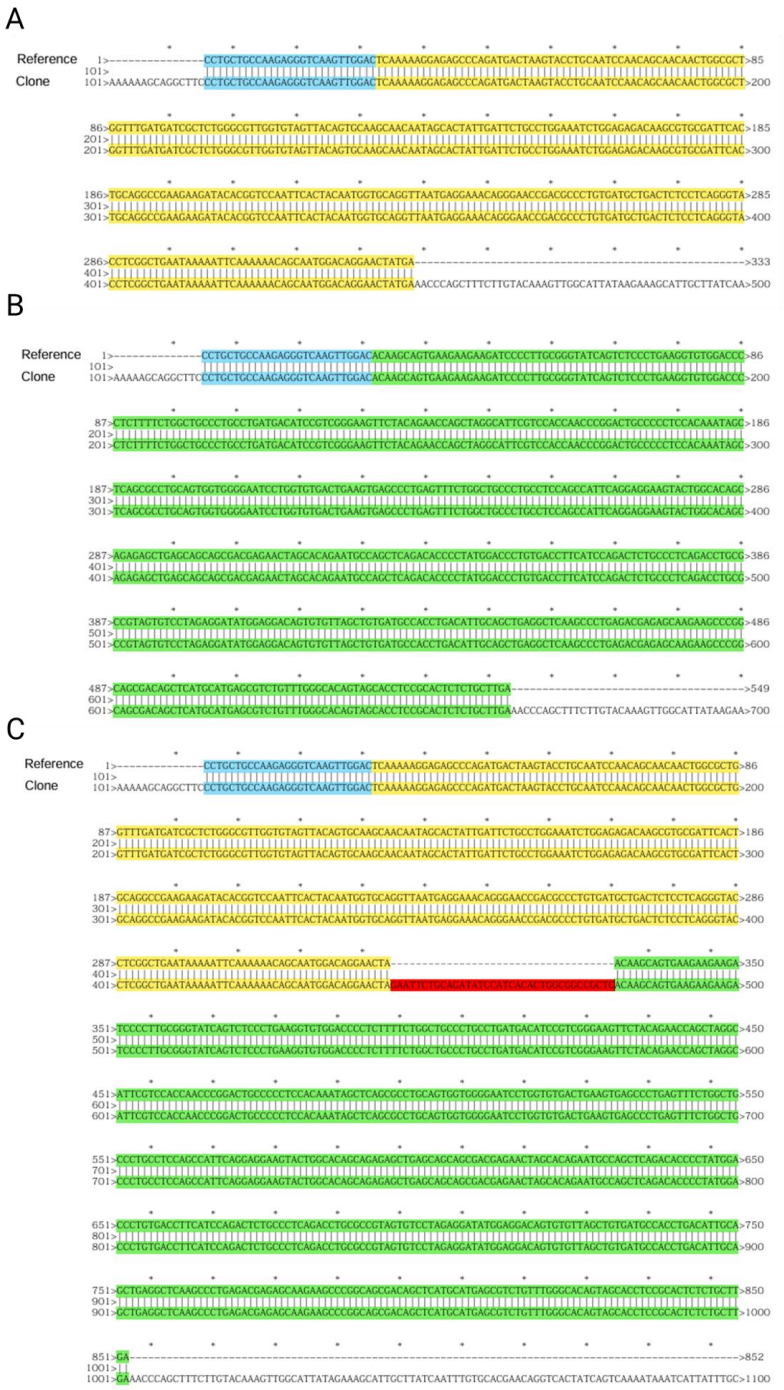

Figure S.1. Cloning of NLS-WWE, NLS-tUBM and NLS-WWE-tUBM into DONR 221 plasmid. A. *Sequence alignment between the reference sequence of HUWE1 WWE domain and the cloned sequence for WWE where the WWE is colored in yellow.* ***B****. Sequence alignment between reference sequence of HUWE1 tUBM domain and the cloned sequence for tUBM which is colored in green.* ***C****. Sequence alignment between the reference sequence of HUWE1 WWE-tUBM domain and the cloned sequence for WWE-tUBM. The inserts were sequenced using M13 forward primer. Blue highlights the sequence of NLS sequence. The ApE software was used for sequence alignment (Davis & Jorgensen, 2022).*

A

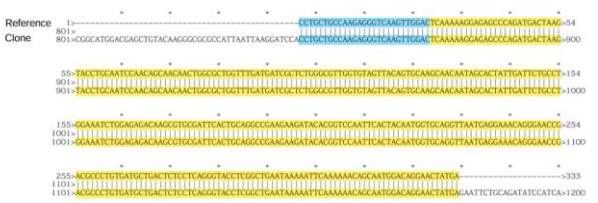

B

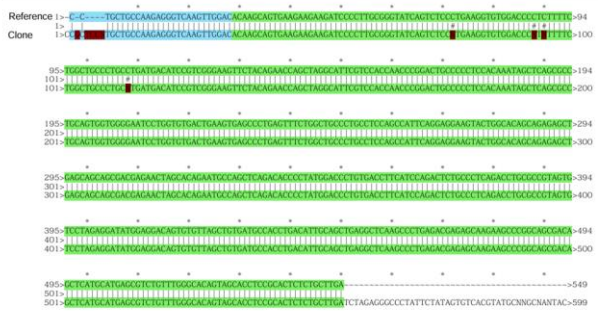

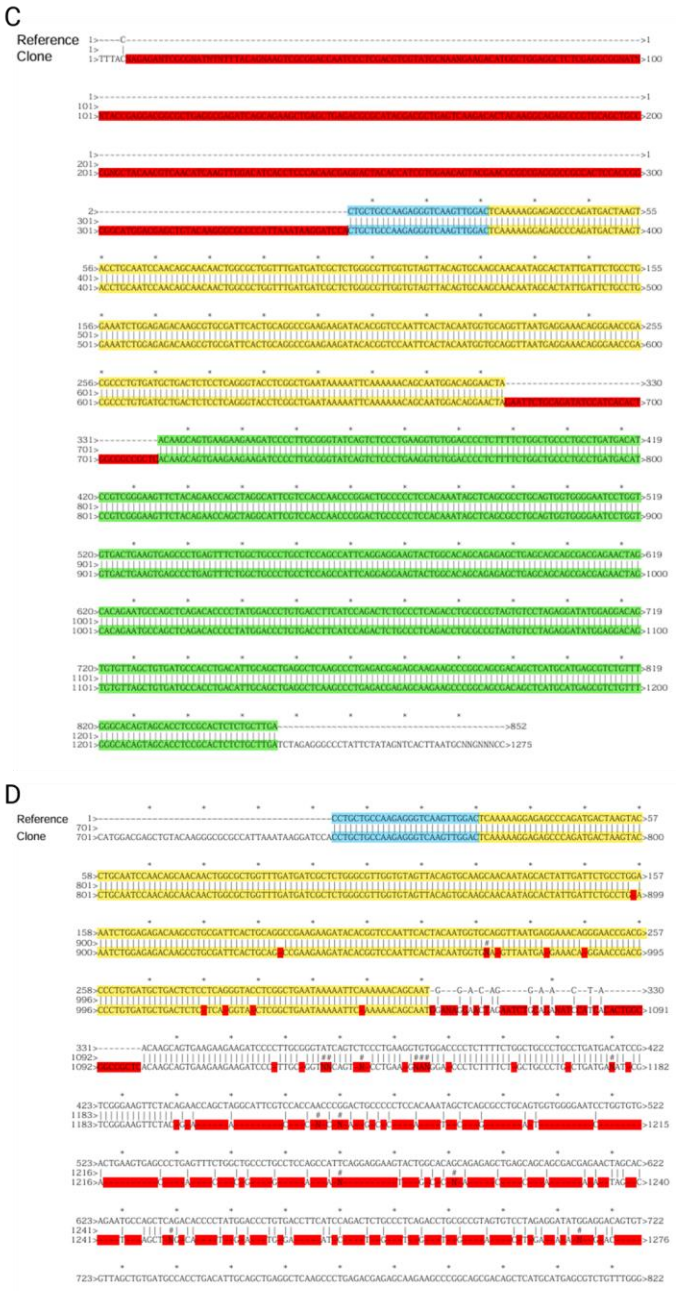

Figure S.2. Cloning of NLS-WWE, NLS-tUBM and NLS-WWE-tUBM into pcDNA 3.1. A*. Sequence alignment between the reference sequence of HUWE1 WWE domain and the cloned sequence for WWE (cloned into pcDNA3.1 mCherry) where the WWE is colored in yellow. The insert was sequenced using the reverse primer BGHR* ***B.*** *Sequence alignment between reference sequence of HUWE1 tUBM domain and the cloned sequence (Cloned into pcDNA 3.1 Venus) for tUBM which is colored in green.* ***C-D****. Sequence alignment between the reference sequence of HUWE1 WWE-tUBM domain and the cloned sequence for WWE-tUBM (cloned into pcDNA3.1 mCherry) sequenced using the reverse primer BGHR (C) and the forward primer (D). Blue highlights the sequence for NLS. The ApE software was used for sequence alignment (Davis & Jorgensen, 2022).*

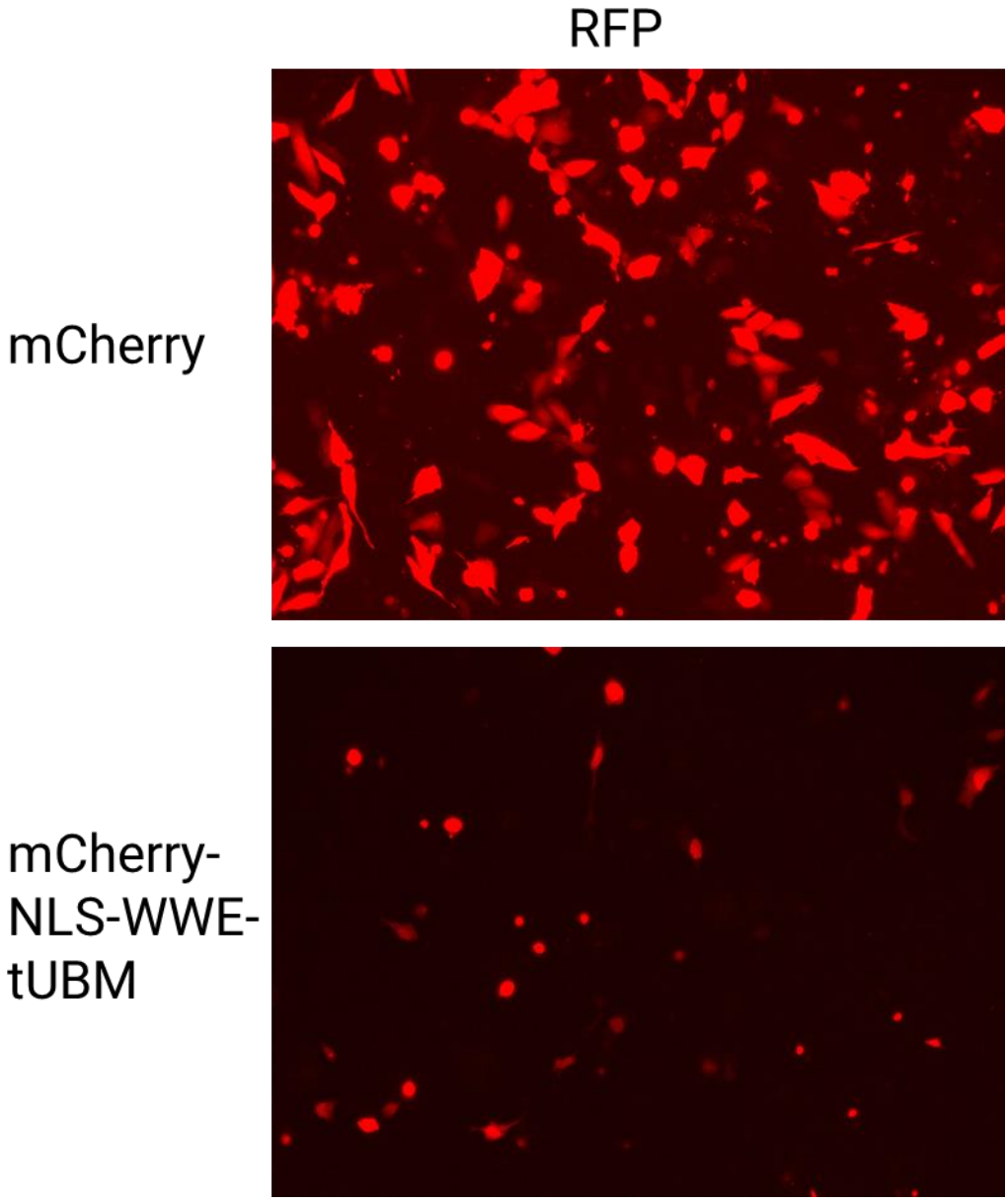

Figure S.3. Cellular expression of NLS-WWE-tUBM. *U2OS cells were transfected with mCherry (RFP) or mCherry NLS WWE tUBM (RFP-NLS WWE tUBM). The images were taken 47 hours post-transfection with 10x objective.*